STUDIES ON ORGANOPHOSPHORUS CATALYZED C(SP^3)–H AMINATION FOR THE SYNTHESIS OF BENZIMIDAZOLES

By

Gisselle Pombar

B.S. Chemistry
University of Central Florida, 2019

SUBMITTED TO THE DEPARTMENT OF CHEMISTRY IN PARTIAL FUILFILLMENT OF THE REQUIREMENTS FOR THE DEGREE OF

MASTER OF SCIENCE IN CHEMISTRY
AT THE
MASSACHUSETTS INSTITUTE OF TECHNOLOGY

September 2022

Signature of Author: _____
Department of Chemistry
August 12, 2022

Certified by: _____
Alexander T. Radosevich
Associate Professor of Chemistry
Thesis Supervisor

Accepted by:_____
Adam Willard
Associate Professor
Graduate Officer

STUDIES ON ORGANOPHOSPHORUS CATALYZED C(SP^3)–H AMINATION FOR THE SYNTHESIS OF BENZIMIDAZOLES

By

Gisselle Pombar

Submitted to the Department of Chemistry on August 12, 2022 in Partial Fulfillment of the Requirements for the Degree of Master of Science in Chemistry

ABSTRACT

A P^{III}/P^{V}=O-catalyzed C(sp^3)–H amination has been realized for (dihydro)benzimidazole synthesis. This work reports: (1) optimization of organophosphorus-catalyzed C(sp^3)–H functionalization; (2) scope studies to benzimidazoles by in situ oxidation of the corresponding dihydrobenzimidazole; and (3) insight into the reaction mechanism through in situ spectroscopic monitoring under catalytic conditions and Hammett linear free energy relationship studies. The synthetic method and mechanistic information provide insight into design principles for the expansion of C(sp^3)–H functionalization reactions through P^{III}/P^{V}=O *O*-atom transfer reactivity.

Thesis Supervisor: Alexander T. Radosevich

Title: Associate Professor of Chemistry

TABLE OF CONTENTS

LIST OF FIGURES....5

LIST OF TABLES....7

ACKNOWLEDGEMENTS....8

Chapter 1. The Advancement of P^{III}/P^{V}=O Redox Cycling....11

1.1.An Introduction to Organophosphorus-Based Redox Catalysis....11

1.2.Geometric Tuning approach towards Catalytic Phosphine-Mediated Transformations....12

1.3.Phosphetane-Catalyzed Deoxygenation Reactions....14

1.4.Summary and Looking Ahead....15

1.5.References....16

Chapter 2. The Development of an Organophosphorus Catalyzed C(sp^3)–H Amination Method....18

2.1.Previous Work....18

2.2.Importance and Relevance....19

2.3.Developing a Catalytic Protocol to C(sp^3)-H Amination....20

2.4.Substrate Scope....23

2.5.Summary and Outlook....26

2.6.References....26

Chapter 3. Mechanistic Investigations into C(sp^3)–H Amination....33

3.1.Probing Catalyst Resting State....33

3.2.Mechanistic Discussion Supported by Computational Studies....33

3.3.Hammett Study Probing C–N Bond Forming Event....34

3.4.Intramolecular Competition KIE Study....35

3.5.Possible Alternative Mechanism....37

3.6.Summary....39

3.7.References....40

Chapter 4. Experimental Section....41

I. General Notes....41

II. Optimization of Reaction Conditions....41

A. Optimization with *N,N*-dibenzyl *o*-nitroaniline (**2.1**)....41

III. Procedures for the Preparation of Starting Materials....45

A. Preparation of Phosphorus Compounds....45
B. Preparation of Benzimidazole Precursors....45
C. Substrates used for Mechanistic Studies....50
IV. Synthetic Examples....53
A. General Procedure....53
B. Analytical Data....54
C. X-ray Data for N-Tosyl-benzimidazolines....60
V. Mechanistic Experiments....62
A. In situ NMR experiments....62
B. Computational Studies....62
C. Hammett Correlation Experiments....64
D. Intramolecular Competition KIE Study....66
VI. Spectral Data....67
VII. References....94

LIST OF FIGURES

Figure 1.1 A) First example of a catalytic P^{III}/P^{V}=O transformation enabled by a cyclic phospholane oxide and chemoselective hydrosilane reductant. B) An illustration of how geometric constraint of phosphine oxides facilitates reduction. 12

Figure 1.2 Walsh diagram for PR_3 electronic structure. 13

Figure 1.2. Frontier molecular orbital energies for phosphacycloalkanes computed at B3LYP/6-311++G** level. Energies in eV. 14

Figure 1.4. A biphilic phosphetane enables deoxygenative condensation of α-ketoesters and carboxylic acids. 14

Figure 1.5. Deoxygenation of nitroarenes enabled by a biphilic phosphetane. 15

Figure 2.1. A) Previous work in C(sp^2)–H amination. B) Formation of nitrenoid intermediate. 18

Figure 3.2. Common redox methods for benzimidazole synthesis. 20

Figure 2.3. Substrate Scope of the catalytic reductive C(sp^3)–H amination. [a]^{1}H NMR Yield determined with the aid of 1,3,5-trimethoxy benzene as an internal standard. 24

Figure 2.4. In Situ Protection of Dihydrobenzimidazole Intermediates. 25

Figure 2.5. Future Directions Synthesis of oxazoles and thiazoles. [a] ^{1}H NMR Yield determined with the aid of 1,3,5-trimethoxy benzene as an internal standard. 26

Figure 3.1. Monitored cyclization of nitroaniline **3.1** to dihydrobenzimidazole A) Time-stacked in situ ^{31}P NMR spectra (T = 100 °C, toluene-d_8) at t = 0 min, 10 min, 30 min, and 60 min. Chemical shifts: P1•[O], δ 55.5 ppm (blue); *anti*-**P1**, δ 31.7 (orange) and *syn*-**P1** δ 28.5 ppm. ..34

Figure 3.2. Proposed mechanism for benzimidazole formation through a nitrenoid intermediate supported by DFT calculations. 35

Figure 3.3. Hammett plot of log(X/Y) for benzimidazole formation according to the reaction depicted against the σ_p- parameter. Equation: y = 0.2136x + 0.0575; R^2= 0.88. 37

Figure 3.4. KIE of 2.24 k_H/k_D from intramolecular competition. 38

Figure 3.5. Alternative mechanism for benzimidazole formation through *o*-nitrosoaniline pathway. 39

Figure 4.4. Representative ^{1}H NMR spectrum for yield determination for optimization of reductive C–N cyclization of *N,N*-dibenzyl *o*-nitroaniline (**2.1**) by **P1**•[O] (optimal conditions, 88% **2.3**) 43

Figure 4.2. Computed reaction profiles from nitroso intermediate **Int-3.5**. 63

Figure 5.3. Representative ^{1}H NMR spectrum for ratio determination for Hammett correlation experiments of N-benzyl-N-(4-methoxybenzyl)-2-nitroaniline by P1•[O]. 66
Figure 4.6. Representative ^{1}H NMR spectrum for k_H/k_X ratio determination for Intramolecular Competition KIE experiments of Hammett correlation experiments of *N*-benzyl-2-nitro-*N*-(phenylmethyl-d_2)aniline by **P1**•[O]. 67

LIST OF TABLES

Table 2.1. Solvent screen for reduction of *o*-N,N-dibenzyl nitroaniline. 21
Table 2.2. Additive Screen. 21
Table 2.3. Catalyst Screen. 22
Table 2.4. Conditions Optimization. 23
Table 4.1. Complete Optimization Table. 44
Table 4.2: Experimental Hammett Values. 65

ACKNOWLEDGEMENTS

Firstly, I would like to greatly thank Professor Alexander T. Radosevich for all the guidance and advice I received during my graduate career. Thank you for the opportunity to join your group and for your faith in my ability to pass second-year exams and succeed at MIT. I will cherish our thought provoking and stimulating discussions about science during group meetings and I will carry your words of wisdom with me as I continue forward. I also want to thank my committee chair, Professor Tim Jamison, for your encouragement, support, and aid in my research and future endeavors. I would also like to thank Elizabeth Guttenberg from GradSupport and Jennifer Weisman for all their words of support, resources, and financial assistance.

I would like to thank all of my undergraduate research advisors for cultivating my skills as a scientist and allowing me to be a member of their research group: Professors Karin Chumbimuni-Torres, Fernando Uribe-Romo, Paul Chirik, and Song Lin.

None of this would have been possible without the Ronald E. McNair Program. Special thanks to Michael Aldarondo-Jeffries for all your work and effort in making the program what it is. Your work behind the scenes creates the impossible a reality for us scholars. As well as to Dr. Natalia Toro for being my mom away from home during my undergraduate career. Thank you for your constant empowering motivation, always seeing the greatness in me, and reminding me that I am enough. You are an inspiration and role model to Hispanic women. Your work through us will continue to impact future generations.

Additionally, I would like to thank my McNair cohort for all the memories and sleepless nights. As we prepared for our GREs, NSF proposals, graduate school applications, and graduate school visits, all while taking a full course load and working. I couldn't imagine spending my last year at UCF any other way. I wish you all luck as you all continue onto your academic careers.

While my time at MIT has been challenging, to say the least, I would not have made it this far without the help of these individuals. I thank Dr. Emily Zygiel for assisting me as I transitioned into a new group. Her kind words and emotional support were greatly appreciated as I went through a difficult time in my life. I would like to thank Dr. Krysta Dummit for her honest advice and moral support as I navigated graduate school. I am fortunate to have worked alongside Dr. Colet te Grotenhuis on this project and for her continuous aid and contributions with DFT studies and overall guidance. I especially would like to thank Dr. Jeff Lipshultz for being my unofficial mentor during my time in the Radosevich group. Since day one, you went above and beyond in making

me feel welcomed in the group. You took the time to show me around the lab, reached out to me if I needed help, and always were available to talk about science. You helped me prepare for my 2nd-year exam by filling gaps of knowledge and providing insight into the field during our practice sessions. If it were not for all of your guidance, I truly believe I would not have lasted in the program as long as I did. I cherish all your efforts in making me into the scientist I am today. I wish you the best as you embark on your journey to Stony Brook University. I look forward to reading about your accomplishments and seeing you become tenured one day.

To my fellow current and past Radosevich group members, you are the brightest group of individuals I have come across. I appreciate you all for the warm welcome upon joining the group and the mentorship I received. I will especially cherish all the fun memories during our group outings and shenanigans: former and current group members Drs. Connor Gilhula, Gregory Cleveland, Hye Won Moon, Akira Tanushi and Gen Li; Drs. Ayan Maity, Yuzuru Kanda, Seung Youn Hong; Drs. Myles Drance, Quinton Bruch, John Andjaba; Soohyun Lim, Nichakan "Gear" Khuichad, and Shicheng Hu. I look forward to seeing all your accomplishments and wish you all the best in your endeavors.

Friendships I have been so fortunate to have outside of the lab: Valerie Lensch, Janet Peet, Leticia Cardoso, Hadiqa Zafar, Kathleen Wang, Carolyn Suh, Corshai Williams as well as my childhood friends: Maria Fonseca, Daniela Bocanegra, Lianne Brito, Lili Navarro. Thank you for the immense emotional support and memorable experiences that enriched my time at MIT. I am incredibly fortunate to have met Alan Carter at MIT. You motivate me to be the best version of myself while also reminding me to take care of myself. You inspire me with your brilliance, and I expect nothing but a successful future in science for you. Thank you for your love and continued support inside and out of academia, and I look forward to where our future will take us.

Lastly, I would like to thank my biggest supporter: my family. I would like to thank my sister, Sylvia Machado, for always having my back in any situation and standing up for me when I can't. Thank you for always being my role model. I want to thank my dad for instilling my work ethic and always providing for the family. Lastly, I would like to thank my mother, the strongest and wisest person I know. You have taught me how to be the strong, independent woman I am today. You taught me to never give up on my dreams, but that failure is okay. You taught me to constantly push myself to be the best, but you also reminded me that I am enough. You are an amazing mother, an inspiring leader, an empathetic caretaker, and beautiful inside and out. I hope

I have made you proud and want to thank you for your unconditional love, support, and belief in me. This is all a daughter could ever ask for. Te quiero mucho mami.

Gisselle Pombar

August 12, 2022

Chapter 1

Advancements in P^{III}/P^{V}=O Redox Cycling

The ability of phosphorus to access several oxidation states has enabled its use in redox reactivity. Most commonly observed in the organic literature are trivalent phosphorus compounds, which can act as *O*-atom acceptors due to their oxophilic nature.[1] The driving force of P^{III} to P^{V}=O is attributed to the formation of the strong P=O bond (128-139 kcal/mol)[1] and the stability of phosphorus in its +5-oxidation state.[2] This reactivity is the foundation and driving force of several established synthetic transformations such as the Wittig, Appel, and Mitsunobu reactions.[3] To overcome the undesired generation of stoichiometric quantities of phosphine oxide waste in these powerful reactions, catalytic cycling in the P^{III}/P^{V}=O process is desirable.[4] Furthermore, any advancements in organophosphorus-based redox catalysis could enable development of novel organocatalytic transformations.

A central challenge in P^{III}/P^{V}=O redox cycling, as alluded to earlier, is the high thermodynamic barrier of reducing strong P=O bonds, which can require harsh conditions and reagents such as metal hydrides that are not chemoselective.[4] One key approach that has enabled the feasibility of P^{III}/P^{V}=O redox cycling is the implementation of hydrosilanes as safer and more practical alternative reductant for their ability to selectively reduce P=O in the presence of sensitive functional groups.[5]

1.1 – An Introduction to Organophosphorus-Based Redox Catalysis

The first report of P^{III}/P^{V}=O redox cycling was described by O'Brien in 2009, achieving a catalytic Witting reaction using a phospholane oxide catalyst (Figure 1.1).[6] By using a strained cyclic organophosphine oxide **1.4•[O]** with C-P-C angle close to 90°, reduction of phosphine oxide by diphenylsilane is facilitated due to a ground-state destabilization resulting in a lower penalty associated with the formation of a pentacoordinate phosphorane intermediate (Figure 1B) prior to elimination of silanol and P^{III} product **1.7**. In fact, the effects on ring strain of the organophosphine oxide and improved kinetics were studied and further supported this conclusion that the closer the C-P-C angle is to the ideal 90° intermediate, the faster the reduction.[7] In that same vein, a larger angle is associated with greater geometry distortion in order to accommodate the addition of the hydride from silane. Minimizing the kinetic barrier of P^{III}/P^{V}=O redox cycling by utilizing cyclic

organophosphine oxides has led to advancements in catalytic Appel[7] and Staudinger[8] reactions, as well as other reductive *O*-atom transfer reactions,[9] which will be the focus of this report.

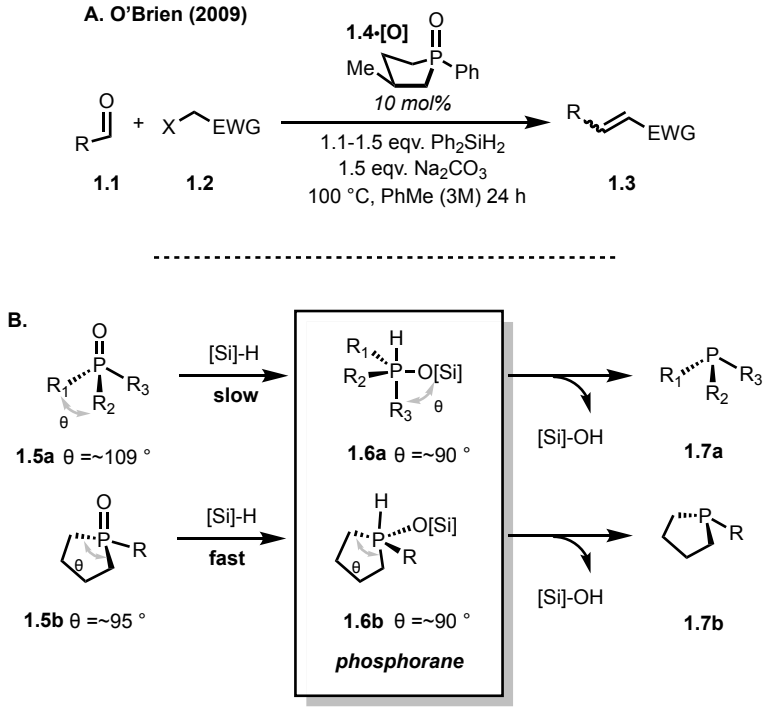

Figure 7.1 A) First example of a catalytic P^{III}/P^{V}=O transformation enabled by a cyclic phospholane oxide and chemoselective hydrosilane reductant. B) An illustration of how geometric constraint of phosphine oxides facilitates reduction.

1.2 – Geometric Tuning approach towards Catalytic Phosphine-Mediated Transformations

Interested in the potential of organophosphorus compounds as catalysts, the Radosevich group has investigated the interrelationship between molecular geometry, electronic structure, and reactivity. Tricoordinate phosphorus species with C_{3v} geometry predominantly react as archetypal nucleophiles by nature of their highest occupied molecular orbital (HOMO) manifested as a non-bonding electron lone pair residing primarily on phosphorus. A degenerate pair of lowest unoccupied molecular orbitals (LUMOs) of antibonding character are high in energy and not readily accessible for chemistry. Distorting the local geometry from a trigonal environment by contraction of the angle between phosphorus substituents results in the removal of degeneracy of the two LUMOs (Figure 1.2). These molecular orbitals experience either increased or decreased destructive orbital overlap, resulting in higher or lower energy levels, respectively. In contrast, the phosphorus-localized HOMO would be relatively unchanged due to the high nonbonding character

in that lone pair.[10] The overall result is a drastically contracted HOMO-LUMO energy gap allowing phosphorus to react in both a nucleophilic and electrophilic (*i.e.* biphilic) manner. Constraining the molecular geometry of phosphorus molecules would thereby tune their electronic structure to channel biphilic reactivity.

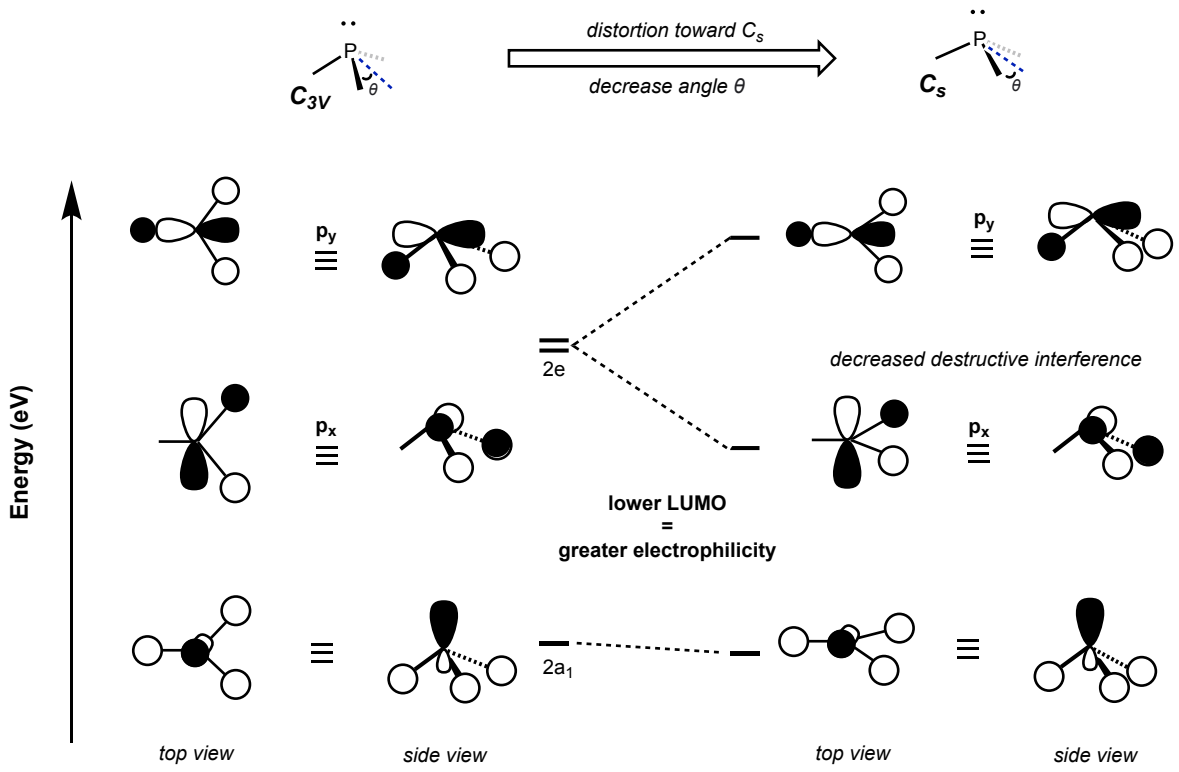

Figure 1.2 Walsh diagram for PR_3 electronic structure.

This geometric tuning hypothesis is supported computationally (Figure 1.3), as a series of cyclic phosphines and their calculated energy gaps demonstrate that four-membered ring phosphetane has a remarkably narrow HOMO-LUMO energy gap relative to other phosphacycles,[12] and is thus predicted to have the greatest biphilic reactivity of the series. Critically, a similar LUMO-lowering effect in the *P*-oxide can be invoked to explain the dramatic rate enhancement of small-ring cyclic phosphine *P*-oxide reduction, in synergy with the ground state destabilization argument invoked earlier.

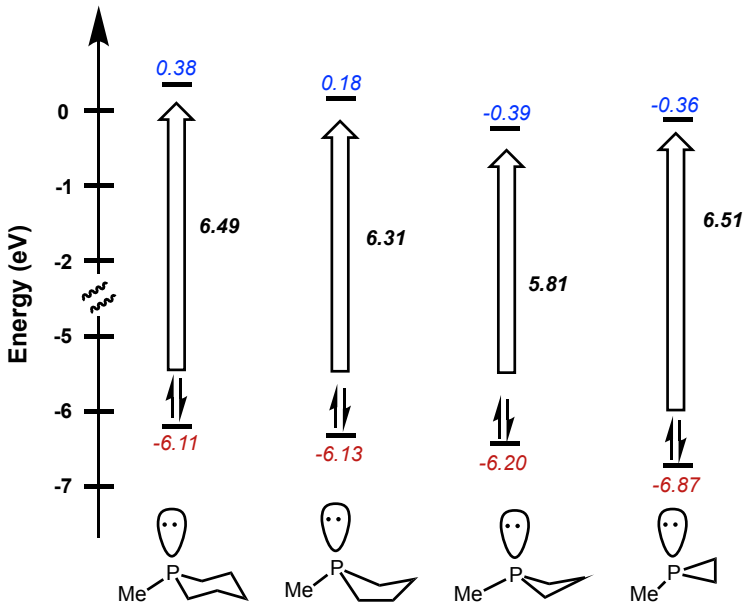

1.3 – Phosphetane-Catalyzed Deoxygenation Reactions

Figure 1.8. Frontier molecular orbital energies for phosphacycloalkanes computed at B3LYP/6-311++G** level. Energies in eV.

The Radosevich lab has experimentally validated this biphilic hypothesis through the development of various phosphetane-catalyzed deoxygenation reactions. First, phosphetane oxide

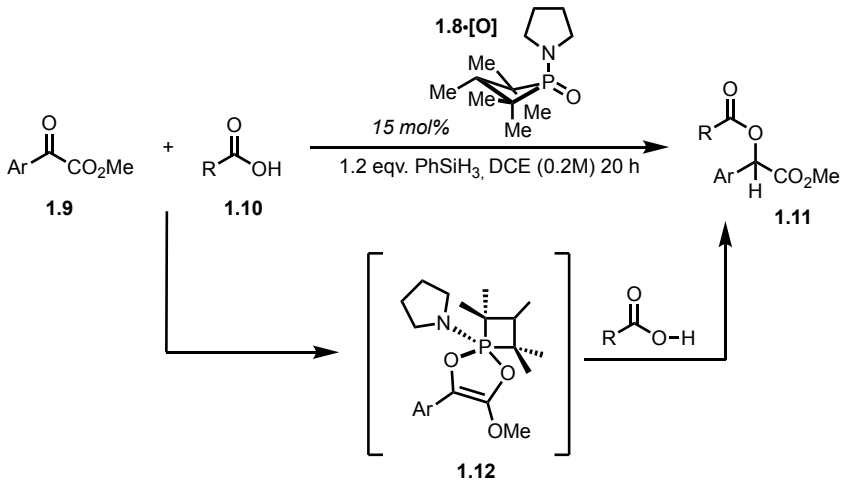

Figure 1.4. A biphilic phosphetane enables deoxygenative condensation of α-ketoesters and carboxylic acids.

1.8•[O] was demonstrated to be highly effective in the deoxygenative condensation reaction of carboxylic acids and α-keto esters.[13] Upon reduction with phenyl silane, the phosphorus species underwent formation to a 5-membered dioxaphospholene, a Kukhtin Ramirez adduct,[14] through

its ability to accept electron density. Protonation of this intermediate allowed for substitution by the deprotonated benzoic acid, providing the final product and expelling the phosphetane *P*-oxide as a leaving group.

Expansion of this organophosphorus redox cycling for *O*-atom transfer has been developed for substrates containing nitro functional groups. Catalytic N–N bond forming Cadogan heterocyclization was promoted by sequential reduction of *o*-substituted nitroarenes using the more electron-rich and kinetically stable catalyst **1.13**.[13]Critical to this reaction is the co-localized nucleophilic and electrophilic nature of the catalyst that engages the nitro group in an initial deoxygenation event to a nitroso intermediate, which can subsequently be further deoxygenated. The rate limiting [3+1] cycloaddition to form intermediate **Int-1.1** is supported by DFT studies and by virtue of the P^{III} resting state of the catalyst. These studies highlight the biphilic nature of **1.13** by virtue of a lower energy LUMO that allows for the cooperative interaction of electron density donation from the P^{III} HOMO to the NO_2 moiety LUMO while simultaneous donation of the NO_2 moiety HOMO to the P^{III} LUMO in a concerted process.

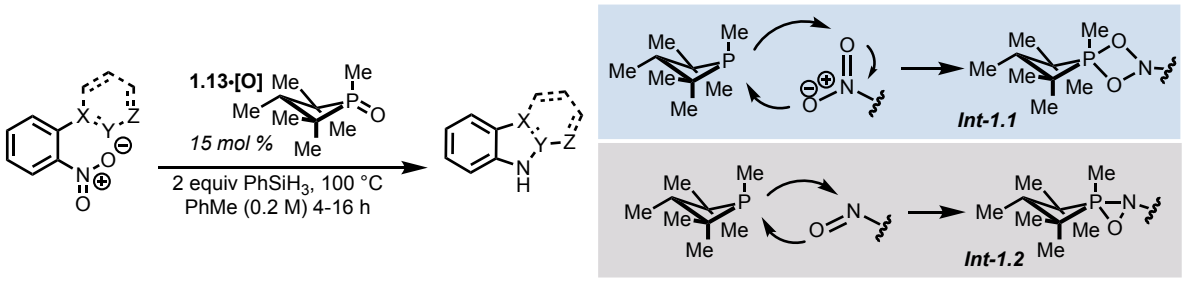

Figure 1.5. Deoxygenation of nitroarenes enabled by a biphilic phosphetane.

In a follow up study, expansion of this reactivity for catalytic C–N bond forming, an oxazaphosphirane nitrenoid intermediate was able to be identified at low temperature by ^{31}P and ^{15}N NMR.[14] In a similar sequential deoxygenation event, the P^{III} species would form an adduct with the nitroso to form **Int-1.2** in a [2+1] process. Decomposition of this intermediate results in the loss of phosphine oxide and generation of a nitrene intermediate that undergoes C–H insertion for the synthesis of indole and carbazole products. This P^{III}/P^{V}=O redox method was successful in the implementation to a catalytic intramolecular Csp^2-H amination.

1.4 – Summary and Looking Ahead

This thesis describes the development of a catalytic P^{III}/P^{V}=O redox method for C(sp^3)-H amination, building on the above-described work of leveraging nitro groups for aryl amination reaction. The results shown here will tie in aspects of previous reactivity with these systems and

new divergent reactivity in order to enhance our mechanistic understanding of P^{III}/P^{V}=O cycling, thereby elucidating fundamental design principles for novel reactivity.

1.5 – References

[1]Quin, L. D. *A Guide to Organophosphorus Chemistry*; John Wiley & Sons: New York, 2000; pp 95.

[2](a) Cahours, A.; Hofmann, A. W. Untersuchungen Über Die Phosphorbasen. *Ann. der Chemie und Pharm.* **1857**, *104*, 1−39. (b) Cadogan, J. I. G.; Mackie, R. K. Tervalent Phosphorus Compounds in Organic Synthesis. *Chem. Soc. Rev.* **1974**, *3*, 87−137.

[3](a) Maryanoff, B. E.; Reitz, A. B. The Wittig Olefination Reaction and Modifications Involving Phosphoryl-Stabilized Carbanions. Stereochemistry, Mechanism, and Selected Synthetic Aspects. *Chem. Rev.* **1989**, *89*, 863. (b) Swamy, K. C. K; Kumar, N. N. B.; Balaraman, E.; Kumar, K. V. P. P. Mitsunobu and Related Reactions: Advances and Applications. *Chem. Rev.* **2009**, *109*, 2551.

[4]Krenske, E. H. Theoretical Investigation of the Mechanisms and Stereoselectivities of Reductions of Acyclic Phosphine Oxides and Sulfides by Chlorosilanes. *J. Am. Chem. Soc.* **2012**, *77*, 3969-3977

[5]Hérault, D.; Nguyen, D. H.; Nuel, D.; Buono, G. Reduction of Secondary and Tertiary Phosphine Oxides to Phosphines. *Chem. Soc. Rev.* **2015**, *44*, 2508–2528.

[6]O'Brien, C. J.; Tellez, J. L.; Nixon, Z. S.; Kang, L. J.; Carter, A. L.; Kunkel, S. R.; Przeworski, K. C.; Chass, G. A. Recycling the Waste: The Development of a Catalytic Wittig Reaction. *Angew. Chem. Intl. Ed.* **2009**, *48*, 6836–6839.

[7]van Kalkeren, H. A.; Leenders, S. H. A. M.; Hommersom, C. R. A.; Rutjes, F. P. J. T.; van Delft, F. L. In Situ Phosphine Oxide Reduction: A Catalytic Appel Reaction. *Chem. Eur. J.* **2011**, *17*, 11290.

[8]van Kalkeren, H. A.; Bruins, J. J. Rutjes F. P. J. T.; van Delft, F. L. Organophosphorus-Catalyzed Staudinger Reduction. *Adv. Synth. Catal.* **2012**, *354*, 1417.

[9]Osman, F. H.; El-Samahy, F. A. Reactions of α-Diketones and o-Quinones with Phosphorus Compounds. *Chem. Rev.* **2002**, *102*, 629.

[10]Lee, K.; Blake, A. Tanushi, A.; McCarthy, S.; Kim, D.; Loria, S.; Donahue, C.; Spielvogel, K.; Keith, J.; Daly, S.; Radosevich, A. T. Validating the Biphilic Hypothesis of Nontrigonal P(III) Compounds. *Angew. Chem. Int. Ed.* **2019**, *58*, 6993.

[11]Zhao, W.; Yan, P. K.; Radosevich, A. T. A Phosphetane Catalyzes Deoxygenative Condensation of α-Keto Esters and Carboxylic Acids via P^{III}/P^{V}=O Redox Cycling. *J. Am. Chem. Soc.* **2015**, *137*, 616−619.

[12]Osman, F. H.; El-Samahy, F. A. Reactions of α-Diketones and o-Quinones with Phosphorus Compounds. *Chem. Rev*. **2002**, *102*, 629−678.

[13]Nykaza, T. V.; Harrison, T. S.; Ghosh, A.; Putnik, R. A.; Radosevich, A. T. A Biphilic Phosphetane Catalyzes N-N Bond Forming Cadogan Heterocyclization via P^{III}/P^{V}=O Redox Cycling. *J. Am. Chem. Soc.* **2017**, *139*, 6839−6842

[14]Nykaza, T. V.; Ramirez, A.; Harrison, T. S.; Luzung, M. R.; Radosevich, A. T. Biphilic Organophosphorus-Catalyzed Intramolecular Csp^2−H Amination: Evidence for a Nitrenoid in Catalytic Cadogan Cyclizations. *J. Am. Chem. Soc.* **2018**, *140*, 3103−3113.

Chapter 2

The Development of an Organophosphorus Catalyzed C(sp^3)–H Amination Method

With the aim of expanding catalytic phosphine/phosphine oxide (P^{III}/P^{V}=O) redox cycling into C(sp^3)–H functionalization, this chapter describes a main group catalyzed C(sp^3)–H amination method for dihydrobenzimidazoles and the corresponding oxidized benzimidazoles.

2.1 – Previous Work

The ubiquitous presence of nitrogen-containing molecules in materials, agrochemicals, and pharmaceuticals has led to several developments in catalytic C–N bond-forming reactions.[1, 2] Amination by direct C(sp^3)–H insertion has emerged as an efficient, step-economical method for C–N bond formation.[2b-c, 3] Traditionally, nitrenes serve as the reactive intermediate that will insert into the C–H bond.[4] Thermolysis or photolysis of azides[5] form these reactive intermediates that undergo C–H amination, albeit unselectively. Alternative methods such as transition metal nitrenoids[6, 7] and organonitrenoids[8] have also been demonstrated to undergo direct C–H amination. Drawbacks to these methods arise from the use of precious metals such as Ru,[9] Rh,[10] Ir[11] in addition to directing groups[12] that are difficult to remove. Hence, the development of sustainable, mild, and metal-free catalytic amination reactions is highly attractive from both an economic and environmental standpoint.

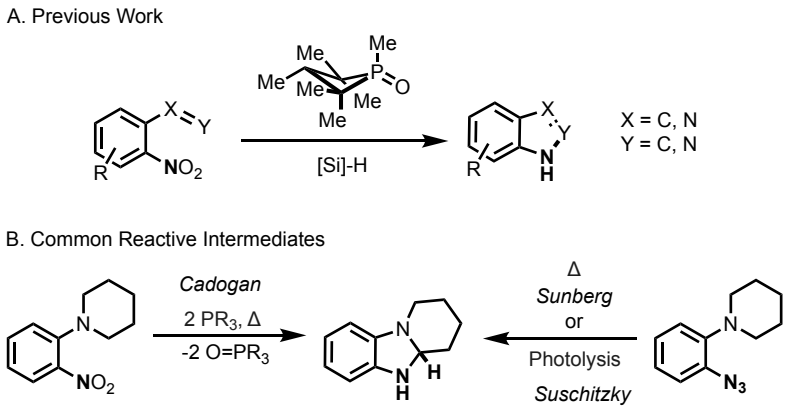

Figure 2.1. A) Previous work in C(sp^2)–H amination. B) Formation of nitrenoid intermediate.

Prior work for catalytic C–N bond forming reactivity is the deoxygenation of nitroarenes by P^{III}/P^{V}=O cycling, enabling novel C(sp^2)–H aminative reactivity (Figure 2.1A.) [13] The key C–N bond-forming step is realized through a nitrene insertion into the corresponding C–H bond. This step is preceded by the formation of an oxazaphosphirane intermediate – observed at low

temperatures by ^{31}P and ^{15}N NMR– a novel non-metal nitrenoid. [13] Decomposition of this intermediate results in the loss of phosphine oxide and liberation of a nitrene intermediate that underwent C–H insertion. In a similar vein, previous reports by Cadogen[14] and Suschitzky[15] demonstrate deoxygenation of o-*N*-alkyl nitroanilines in superstoichiometric trimethyl phosphite produced dihydrobenzimidazoles (Figure 2.1B.) analogous to photolysis[15] and thermolysis[16] of the similar *o*-azido anilines. This suggests that nitrene stemming from deoxygenation of the nitro group can undergo C(sp^3)–H amination.

2.2 –Importance and Relevance

With literature precedent for 1) P^{III}-catalyzed nitro-reduction through nitrenoids leading to C(sp^2)–H nitrene insertion,[13] and 2) the synthesis of dihydrobenzimidazoles through nitrenoid intermediates,[14] we investigated organophosphorus-catalyzed deoxygenation as an entry into nitrenoid reactivity to aminate proximal C(sp^3)–H bonds in an intramolecular fashion.

A regiodefined synthesis of *N1*-substituted benzimidazoles via a direct and atom economical method is desirable. Due to their bioactive properties, benzimidazoles and their derivatives have found several uses in the pharmaceutical industry for their antifungal[17] and antiviral[18] properties showing potential activity against influenza and HIV[19]. Their success as proton pump inhibitors is also well recognized as shown in the billion-dollar industry of esomeprazole (Nexium)[20] and lansoprazole which contain the benzimidazole motif. Furthermore, benzimidazoles are widely utilized in chemical industry as dyes,[21] optics,[22] and protective membranes for fuel cells.[23]

The most common method for the synthesis of simple benzimidazoles is the condensation of 1,2-diaminobenzene with carbonyl derivatives,[24] but is quite limited in scope. For 1,2-disubstituted or polycyclic benzimidazole synthesis, oxidative and reductive cyclization methods are utilized, which require an oxidant or reductant. Examples of conditions for oxidative cyclization of the commonly used *o*-phenylenediamine have employed hydrogen peroxide,[25] oxone[26] (in conjunction with mineral acids), and TEMPO.[27] Drawbacks to these methods stem from starting material availability where the electron-rich and oxidatively unstable *o*-phenylenediamine is often synthesized from the parent *o*-nitroaniline, with severe limitations with respect to functional groups that are stable under these strong oxidizing conditions.[28] Methods focused on reductive cyclizations of the parent *o*-nitro aniline substrate offer a direct method to these complex benzimidazole structures. Hydrogenative methods are ideal but require heavy

metals such as Pd.[29] Methods without the use of heavy metals such as $TiCl_3$,[30] Cu,[31] Na_2SO_3,[32] and pyrolytic[33] are prominent alternatives but often at the cost of requiring harsh conditions. Other C–H amination methods exist through metal-mediated nitrene/nitrenoid reactivity but often require either azides as precursors[34] that are dangerous to work with on scale[35] or the use of heavy metals Rh,[36] Ru,[37] and Pd.[38] In this chapter, I describe a reductive C–H aminative method for the synthesis of benzimidazoles, by aerobic oxidation of dihydrobenzimiazole intermediates, through a P^{III}/P^{V}=O redox catalytic cycle.

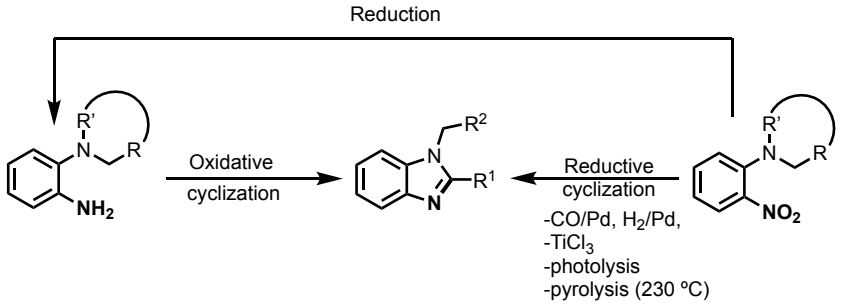

Figure 9.2. Common redox methods for benzimidazole synthesis.

2.3 – Developing a Catalytic Protocol to C(sp^3)-H Amination

In our initial investigations, *N*,*N*-dibenzyl *o*-nitroaniline **2.1** was chosen as the substrate to evaluate the desired C(sp^3)–H amination reaction. Similar conditions, as reported for the Cadogan cyclization,[13] provided a promising initial result of the desired benzimidazole with a 40% yield (Table 2.1, entry 1). The unstable dihydrobenzimidazole, putatively formed thru C(sp^3)–H amination, is presumably oxidized upon exposure to air. Vigorous bubbling with air at 100 °C is performed for complete conversion to the benzimidazole **2.3**. Various high boiling solvents were tested, displaying a preference for polar and aromatic solvents, specifically benzonitrile (64%) (Table 2.1, entry 5). In contrast, ethereal or polar solvents with high dielectric constants eroded yield, which is in alignment with a previous investigation reporting these solvents inhibit Cadogan cyclization.[39]

Table 2.1. Solvent screen for reduction of *o*-N,N-dibenzyl nitroaniline.[a]

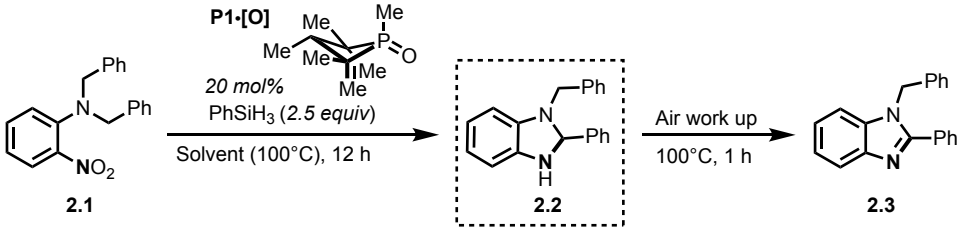

Entry	Solvent	Yield (%)
1	Toluene	40%
2	Dioxane	27%
3	$PhCF_3$	24%
4	DMF	51%
5	Benzonitrile	64%

[a]Yield determined by ^{1}H NMR analysis of crude reaction mixture with 1,3,5-trimethoxybenzene added as internal standard.

The effect of added base was evaluated to diminish side product formation, leading to the identification of DBU as an optimal additive resulting in a notable increase in yield (88%) (Table 2.2, entry 6).

Table 2.2. Additive Screen[a]

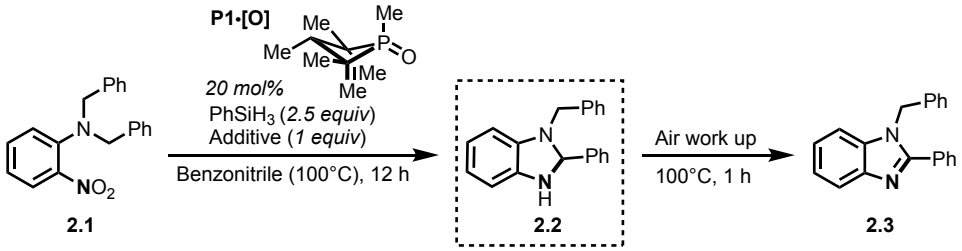

Entry	Additives	Yield (%)
1	Water	72%
2	MeOH	61%
3	NEt_3	60%
4	DIPEA	49%
5	Pyridine	65%
6	DBU	88%

[a]Yield determined by ^{1}H NMR analysis of crude reaction mixture with 1,3,5-trimethoxybenzene added as internal standard.

Other phosphorus catalysts used in other P^{III}/P^{V}=O cycling reactions were evaluated. Superior biphillic activity was displayed by the 1,2,2,3,4,4-hexamethylphosphetane oxide over other phosphetane oxides, 5-membered cyclic phosphine oxides and acyclic phosphine oxides by its ability to turn over and effectively engage the NO_2 moiety (Table 2.3, entries 2-6).

Table 2.3. Catalyst Screen[a]

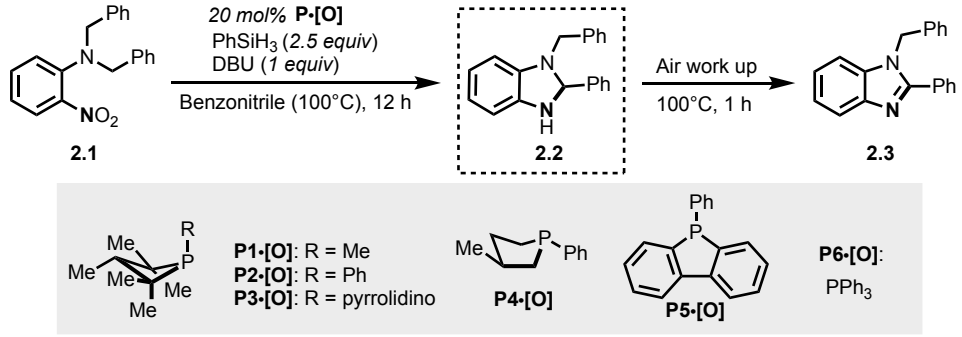

Entry	Conditions	Yield (%)
1	**P1**•[O]	88%
2	**P2**•[O]	33%
3	**P3**•[O]	42%
4	**P4**•[O]	47%
5	**P5**•[O]	5%
6	**P6**•[O]	4%

[a]Yield determined by ^{1}H NMR analysis of crude reaction mixture with 1,3,5-trimethoxybenzene added as internal standard.

Control experiments – excluding $PhSiH_3$ or catalyst – show no product formation (Table 2.4, entry 4-5), with full recovery of starting material. Other hydrosilanes such as Ph_2SiH_2 showed comparable results (77%) for this reaction, but a mild hydrosilane reductant (PMHS) demonstrated decreased reactivity (Table 2.4, entry 7). Varying concentration, temperature, catalyst loadings, and reaction time converged on optimal conditions of 0.5 M in benzonitrile, 100° C, 20 mol% catalyst for 12 h, yielding 88% yield (Table 2.4, entry 3).

Table 2.4. Conditions Optimization[a]

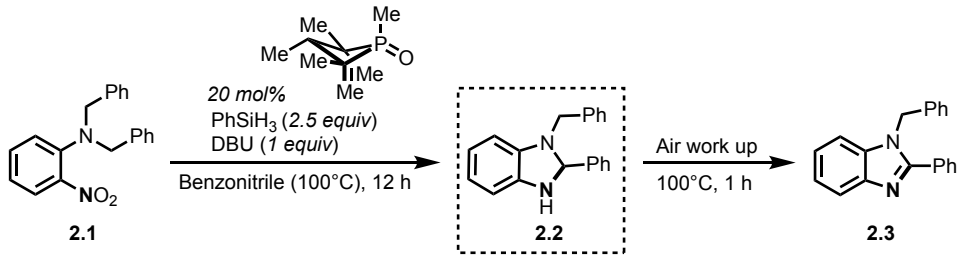

Entry	Conditions	Yield (%)
1	0.1 M	62%
2	0.5 M	97% (87%[b])
3	1.0 M	88%
4	No catalyst	0%
5	No silane	0%
6	Ph_2SiH_2	77%
7	PMHS	29%
8	0.67 eq $PhSiH_3$	34%
9	2% cat. 12h	35%
10	5% cat. 12h	50%
11	10% cat. 24h	82%
12	60 °C	19%
13	80 °C 48h	64%
14	DBU 0.5 eq	86%
15	DBU 2.5 eq	82%

[a]Yield determined by ^{1}H NMR analysis of crude reaction mixture with 1,3,5-trimethoxybenzene added as internal standard. [b]Isolated Yield

2.4 – Substrate Scope

With these optimized conditions at hand, the scope and limitations with respect to substrate was determined to delineate the contours of synthetic utility (Figure 2.3). This organophosphorus-catalyzed method for nitroarene reduction illustrates a complementary approach to existing methods for the synthesis of benzimidazoles with relatively mild conditions. Various *N*-benzyl *o*-nitro anilines are readily transformed into their corresponding benzimidazoles, with yields ranging from 87%-95% (**2.4-2.9**) with shorter reaction times (12 h). Other alkylated substituted *o*-nitro anilines substrates are also amenable to these conditions, with complete conversion seen in 1.5-2 days. These substrates display modest to excellent yields for cyclic and acyclic variants with no clear trend in increasing either alkyl chain length or ring size (**2.10-2.17**).

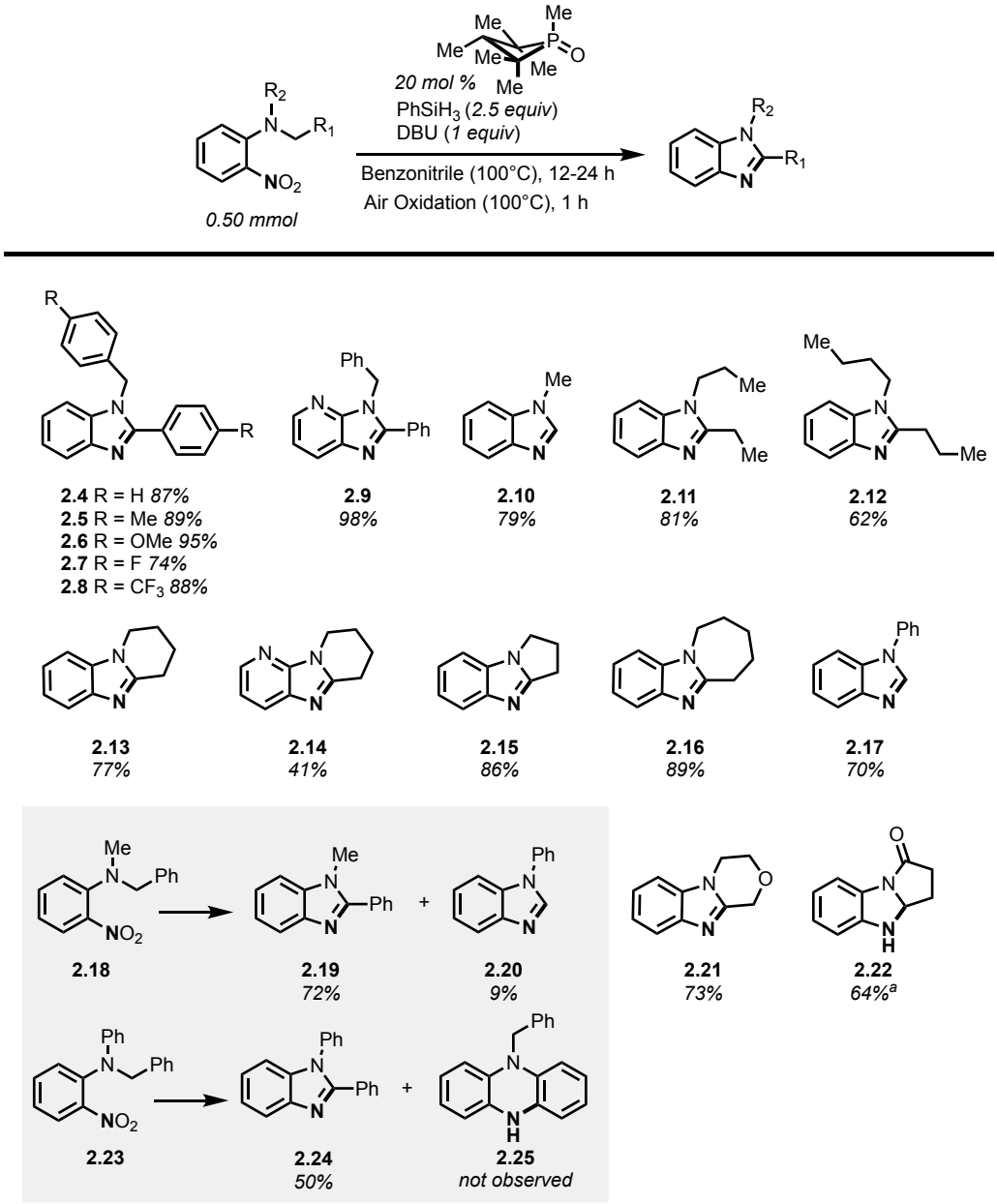

Figure 2.3. Substrate Scope of the catalytic reductive C(sp^3)–H amination. [a]^{1}H NMR Yield determined with the aid of 1,3,5-trimethoxy benzene as an internal standard.

To probe chemoselectivity for alkyl versus benzylic functionalization, substrate **2.18** was submitted to the catalytic reaction, and a ratio of ~9:1 was found for products **2.19** and **2.20** favoring functionalization at the benzylic position. Furthermore, sp^3 amination to make a 5-membered ring (**2.24**) completely dominates over sp^2 amination to make a 6-membered ring (**2.25**). Additionally. when 1-(2-nitrophenyl)pyrrolidin-2-one was used as a substrate, incomplete oxidation product **2.22** was observed post air work up with a yield of 64%, illustrating the extreme

stability of this dihydrobenzimidazole[40] and an opportunity to derivatize this intermediate into complex natural products.

The dihydrobenzimidazole product **2.27** is observed more readily with the *N*-alkyl *o*-nitro aniline substrates, which is fully converted to benzimidazole product **2.28** by air oxidation conditions as mentioned previously. This prompted us to investigate the possibility of trapping this dihydrobenzimidazole intermediate **2.29** with a protecting group to enable isolation of the immediate C(sp^3)–H aminated scaffold. Additionally, these intermediates would also serve as interesting structural motifs as they are relatively unknown in the literature. A brief optimization for this in situ protection using p-toluenesulfonic chloride (TsCl) in neat 2,6-lutidine N-oxide[41] provided a promising yield of 64%. A crystal structure of the tosylated dihydrobenzimidazole was accquired, confirming the sp^3-hybridized nature of the central C atom. Ongoing work is being

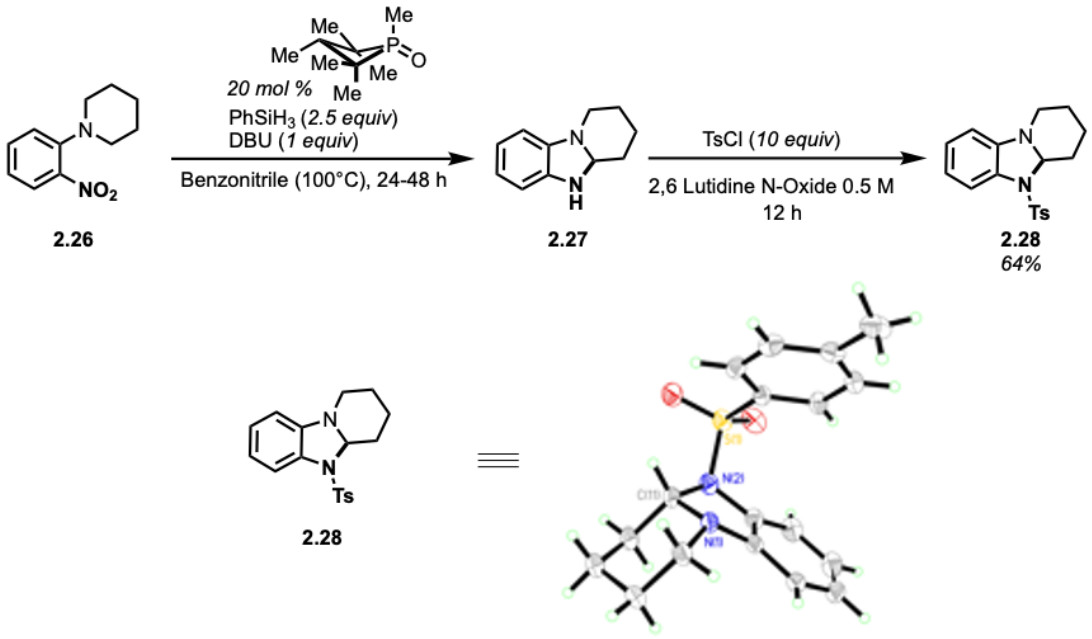

Figure 2.4. In Situ Protection of Dihydrobenzimidazole Intermediates.

developed to expand the scope of these unique tosylated benzimidazole products.

2.5 – Summary and Outlook

This chapter demonstrated the development and reaction scope of a biphillic organophosphorus catalyzed nitroarene deoxygenation reaction for C(sp^3)–H amination. An efficient new method for the preparation of benzimidazoles that parallels other synthetic methods due to the ability to functionalize both benzylic and alkyl *o*-nitro aniline substrates and the ability

to trap the highly elusive dihydrobenzimidazoles was discussed. The 1,2,2,3,4,4-hexamethylphosphetane oxide played a crucial role in displaying superior biphillic activity for the cyclization event over other main group catalysts. Additionally, the use of DBU as an additive also greatly improved the yield, which could most likely be attributed to interfering with possible Buchner ring expansion side product formation.[42] New directions of this work will focus on broadening the scope to include other heteroatom variants to the aniline moiety, such as thiazoles oxazoles. Preliminary data for C-H amination of benzyl(2-nitrophenyl)sulfane and 1-ethoxy-2-nitrobenzene provided a promising 31% of **2.29** and 34% of **2.30**, respectively, illustrating the feasibility of this proposal. The next chapter will investigate the reaction mechanism through a series of experiments supported by DFT computational studies.

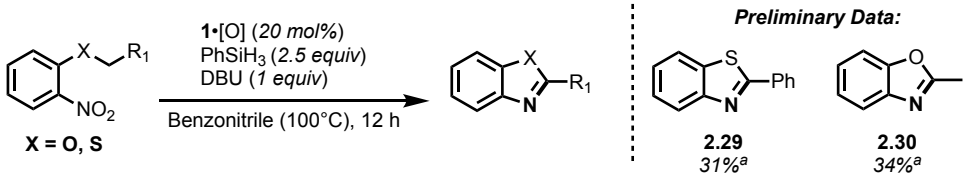

Figure 2.5. Future Directions Synthesis of oxazoles and thiazoles. [a] ^{1}H NMR Yield determined with the aid of 1,3,5-trimethoxy benzene as an internal standard.

2.6 – References

[1](a) Catarzi, D.; Colotta, V.; Varano, F. Competitive AMPA Receptor Antagonists. *Med. Res. Rev.* **2007**, *27*, 239–278. (b) Keri, R. S.; Hiremathad, A.; Budagumpi, S.; Nagaraja, B. M. Comprehensive Review in Current Developments of Benzimidazole-Based Medicinal Chemistry. *Chem. Biol. Drug Des.* **2015**, *86*, 19–65. (c) Taylor, A. P.; Robinson, R. P.; Fobian, Y. M.; Blakemore, D. C.; Jones, L. H.; Fadeyi, O. Modern Advances in Heterocyclic Chemistry in Drug Discovery. *Org. Biomol. Chem.* **2016**, *14*, 6611–6637. (d) Nautiyal, O. H. Synthesis of Oxindoles, Spirooxindoles, and Isatins with Prominent Bioactive Probes: Review. *OMCIJ* **2018**, *5*, 555671. (e) Pallesen, J.; Møllerud, S.; Frydenvang, K.; Pickering, D. S.; Bornholdt, J.; Nielsen, B.; Pasini, D.; Han, L.; Marconi, L.; Kastrup, J. S.; et al. N1-Substituted Quinoxaline-2,3-Diones as Kainate Receptor Antagonists: X-Ray Crystallography, Structure–Affinity Relationships, and in Vitro Pharmacology. *ACS Chem. Neurosci.* **2019**, *10*, 1841–1853.

[2](a) Asensio, J. A.; Sánchez, E. M.; Gómez-Romero, P. Proton-Conducting Membranes Based on Benzimidazole Polymers for High-Temperature PEM Fuel Cells. A Chemical Quest. *Chem. Soc. Rev.* **2010**, *39*, 3210–3239. (b) Molina, P.; Tárraga, A.; Otón, F. Imidazole Derivatives: A

Comprehensive Survey of Their Recognition Properties. *Org. Biomol. Chem.* **2012**, *10*, 1711–1724. (c) Rabbani, M. G.; El-Kaderi, H. M. Synthesis and Characterization of Porous Benzimidazole-Linked Polymers and Their Performance in Small Gas Storage and Selective Uptake. *Chem. Mater.* **2012**, *24*, 1511–1517.

[3](a) Jeffrey, J. L.; Sarpong, R. Intramolecular C(sp^3)–H amination. *Chem. Sci.* **2013**, *11*, 4092-4106. (b) Lescot, C.; Darses, B.; Collet, F.; Retailleau, P.; Dauban, P. *J. Org. Chem*. **2012**, *77*, 7232. (c) Park, Y.; Kim, Y.; Chang, S. Transition metal-catalyzed C–H amination: scope, mechanism, and applications. *Chem. Rev.* **2017**, *13*, 9247-9301.

[4] (a) Reichl, K. D.; Dunn, N. L.; Fastuca, N. J.; Radosevich, A. T. Biphilic Organophosphorus Catalysis: Regioselective Reductive Transposition of Allylic Bromides via PIII/PV Redox Cycling. *J. Am. Chem. Soc.* **2015**, *137*, 5292–5295. (b) Zhao, W.; Yan, P. K.; Radosevich, A. T. A Phosphetane Catalyzes Deoxygenative Condensation of α-Keto Esters and Carboxylic Acids via P III/PV═O Redox Cycling. *J. Am. Chem. Soc.* **2015**, *137*, 616–619. (c) Lin, Y.-C.; Hatzakis, E.; McCarthy, S. M.; Reichl, K. D.; Lai, T.-Y.; Yennawar, H. P.; Radosevich, A. T. P–N Cooperative Borane Activation and Catalytic Hydroboration by a Distorted Phosphorous Triamide Platform. *J. Am. Chem. Soc.* **2017**, *139*, 6008–6016. (d) Nykaza, T. V.; Harrison, T. S.; Ghosh, A.; Putnik, R. A.; Radosevich, A. T. A Biphilic Phosphetane Catalyzes N–N Bond-Forming Cadogan Heterocyclization via PIII/PV═O Redox Cycling. *J. Am. Chem. Soc.* **2017**, *139*, 6839–6842. (e) Nykaza, T. V.; Ramirez, A.; Harrison, T. S.; Luzung, M. R.; Radosevich, A. T. Biphilic Organophosphorus-Catalyzed Intramolecular Csp2–H Amination: Evidence for a Nitrenoid in Catalytic Cadogan Cyclizations. *J. Am. Chem. Soc.* **2018**, *140*, 3103–3113. (f) Ghosh, A.; Lecomte, M.; Kim-Lee, S.-H.; Radosevich, A. T. Organophosphorus-Catalyzed Deoxygenation of Sulfonyl Chlorides: Electrophilic (Fluoroalkyl)Sulfenylation by PIII/PV=O Redox Cycling. *Angew. Chem. Int. Ed*. **2019**, *58*, 2864–2869. (g) Lecomte, M.; Lipshultz, J. M.; Kim-Lee, S.-H.; Li, G.; Radosevich, A. T. Driving Recursive Dehydration by PIII/PV Catalysis: Annulation of Amines and Carboxylic Acids by Sequential C–N and C–C Bond Formation. *J. Am. Chem. Soc.* **2019**, *141*, 12507–12512.

[5]L'abbe, G. Decomposition and addition reactions of organic azides. *Chem. Rev.* **1969**, *69*, 345-363.

[6]Shin, K.; Kim, H.; Chang, S. Transition-metal-catalyzed C–N bond forming reactions using organic azides as the nitrogen source: a journey for the mild and versatile C–H amination. *Acc. Chem. Res.* **2015**, *4*, 1040-1052.

[7]Hinman, A.; Du Bois, J. *J. Chem. Soc.* **2003***, 125*, 11510-11511.

[8]Ochiai, M.; Miyamoto, K.; Kaneaki, T.; Hayashi, S.; Nakanishi, W. *Science*, **2011**, *332*, 448-451.

[9](a) Chan, S. L.-F.; Kan, Y.-H.; Yip, K.-L.; Huang, J.-S.; Che, C.-M. Ruthenium Complexes of 1,4,7-Trimethyl-1,4,7-triazacyclononane for Atom and Group Transfer Reactions. *Coord. Chem. Rev.* **2011**, *255*, 899−919. (b) Cenini, S.; Tollari, S.; Penoni, A.; Cereda, C. Catalytic Amination of Unsaturated Hydrocarbons: Reactions of p-Nitrophenylazide with Alkenes Catalysed by phenylazide with Alkenes Catalysed by Metallo-Porphyrins. *J. Mol. Catal. A: Chem.* **1999**, *137*, 135−146. (c) Yu, X.-Q.; Huang, J.-S.; Zhou, X.-G.; Che, C.-M. Amidation of Saturated C−H Bonds Catalyzed by Electron-Deficient Ruthenium and Manganese Porphyrins. A Highly Catalytic Nitrogen Atom Transfer Process. *Org. Lett.* **2000**, *2*, 2233−2236. (d) Intrieri, D.; Caselli, A.; Ragaini, F.; Macchi, P.; Casati, N.; Gallo, E. Insights into the Mechanism of the Ruthenium−PorphyrinCatalysed Allylic Amination of Olefins by Aryl Azides. *Eur. J. Inorg. Chem.* **2012**, *2012*, 569−580. (e) Harvey, M. E.; Musaev, D. G.; Du Bois, J. A Diruthenium Catalyst for Selective, Intramolecular Allylic C−H Amination: Reaction Development and Mechanistic Insight Gained through Experiment and Theory. *J. Am. Chem. Soc.* **2011**, *133*, 17207−17216. (f) Nishioka, Y.; Uchida, T.; Katsuki, T. Enantio- and Regioselective Intermolecular Benzylic and Allylic C−H Bond Amination. *Angew. Chem., Int. Ed.* **2013**, *52*, 1739−1742.

[10](a) Du Bois, J. Rhodium-Catalyzed C−H Amination - An Enabling Method for Chemical Synthesis. *Org. Process Res. Dev.* **2011**, *15*, 758− 762. (b) Davies, H. M. L.; Manning, J. R. Catalytic C−H Functionalization by Metal Carbenoid and Nitrenoid Insertion. *Nature* **2008**, *451*, 417−424. (c) Quyen, N.; Sun, K.; Driver, T. G. Rh_2(II)-Catalyzed Intramolecular Aliphatic C−H Bond Amination Reactions Using Aryl Azides as the N-Atom Source. *J. Am. Chem. Soc.* **2012***, 134*, 7262− 7265. (d) Xu, H.; Zhang, X.; Ke, Z.; Zhao, C. A Theoretical Study of Dirhodium-Catalyzed Intramolecular Aliphatic C−H bond Amination of Aryl Azides. *RSC Adv.* **2016***, 6,* 29045−29053. (e) Roizen, J. L.; Zalatan, D. N.; Du Bois, J. Selective Intermolecular Amination of C−H Bonds at Tertiary Carbon Centers. *Angew. Chem., Int. Ed.* **2013***, 52,* 11343−11346.

[11](a) Sun, K.; Sachwani, R.; Richert, K. J.; Driver, T. G. Intramolecular Ir(I)-Catalyzed Benzylic C−H Bond Amination of ortho-Substituted Aryl Azides. *Org. Lett.* **2009***, 11*, 3598−3601. (b) Ichinose, M.; Suematsu, H.; Yasutomi, Y.; Nishioka, Y.; Uchida, T.; Katsuki, T. Enantioselective Intramolecular Benzylic C−H Bond Amination: Efficient Synthesis of Optically Active Benzosultams. *Angew. Chem., Int. Ed.* **2011***, 50*, 9884−9887. (c) Nishioka, Y.; Uchida, T.; Katsuki, T. Enantio- and Regioselective Intermolecular Benzylic and Allylic C−H Bond Amination. *Angew. Chem., Int. Ed.* **2013***, 52*, 1739−1742.

[12](a) Thansandote, P.; Lautens, M. Construction of NitrogenContaining Heterocycles by C−H Bond Functionalization. Chem. - Eur. J. 2009, 15, 5874−5883. (71) Mei, T.-S.; Kou, L.; Ma, S.; Engle, K. M.; Yu, J.-Q. Heterocycle Formation via Palladium-Catalyzed C−H Functionalization. *Synthesis* **2012***, 44*, 1778−1791. (b) Nack, W. A.; Chen, G. Syntheses of Nitrogen-Containing Heterocycles via Palladium-Catalyzed Intramolecular Dehydrogenative C−H Amination. *Synlett* **2015***, 26*, 2505−2511. (c) Wang, C.; Han, J.; Zhao, Y. Recent Development in NAuxilixary-Assisted Intramolecular Amination for Amine Substrates. *Synlett* **2015***, 26*, 997−1002. (d) Yuan, J.; Liu, C.; Lei, A. Construction of N-Containing Heterocycles via Oxidative Intramolecular N−H/X−H Coupling. *Chem. Commun.* **2015***, 51*, 1394−1409. (e) Subramanian, P.; Rudolf, G. C.; Kaliappan, K. P. Recent Trends in Copper-Catalyzed C−H Amination Routes To Biologically Important Nitrogen Scaffolds. *Chem. - Asian J.* **2016***, 11*, 168−192. (f) Brasche, G.; Buchwald, S. L. C−H Functionalization/C−N Bond Formation: Copper-Catalyzed Synthesis of Benzimidazoles from Amidines. *Angew. Chem., Int. Ed.* **2008***, 47*, 1932−1934.

[13]Nykaza, T. V.; Ramirez, A.; Harrison, T. S.; Luzung, M. R.; Radosevich, A. T. Biphilic Organophosphorus-Catalyzed Intramolecular Csp^2−H Amination: Evidence for a Nitrenoid in Catalytic Cadogan Cyclizations. *J. Am. Chem. Soc.* **2018**, *140*, 3103−3113.

[14]Cadogan, J. I. G. Reduction of nitro-and nitroso-compounds by tervalent phosphorus reagents. *Quart. Rev.* **1968**, *2*, 222-251.

[15]Garner, R.; Garner, G. V.; Suschitzky, H. Heterocyclic syntheses. Part XXIII. Synthesis and reactions of 2, 3-dihydrobenzimidazoles. *J. Am. Chem. Soc.* **1970**, *6*, 825-829.

[16]Sundberg, R. J.; Russell, H. F.; Ligon, W. V.; Lin, L.- S. *J. Org. Chem.* **1972**, *37*, 719.

[17]Morstyn, G. L. L. N. J. M. J.; Keech, W.; Sheridan, L.; Campbell, M.; Green, D.; Metcalf, R.; Fox, L. M.; Souza N.; Alton, K. Effect of granulocyte colony stimulating factor on neutropenia induced by cytotoxic chemotherapy. *Lancet*. **1988**, *331*, 667-672. (b) Tahara, S.; Matsukura, Y.;

Katsuta, H.; Mizutani, J.; Naturforsch, Z. Naturally occurring antidotes against benzimidazole fungicides. *Z. Naturforsch. C.* **1993***, 48,* 757–765

[18](a) Kazimierczuk, Z.; Upcroft, J. A.; Upcroft, P.; Górska, A.; Starościak, B.; Laudy, A. Synthesis, antiprotozoal and antibacterial activity of nitro- and halogeno-substituted benzimidazole derivatives. *Acta Biochim. Pol.* **2002**, *49*, 185 (b) Ansari, K. F.; Lal, C. Synthesis and evaluation of some new benzimidazole derivatives as potential antimicrobial agents. *Eur. J. Med. Che.* **2009**, *44*, 2294 (c) Prajapat, P.; Kumawat, M.; Talesara, G. L.; Kalal, P.; Agarwal, S.; Kapoor, C. S. J; Benzimidazole scaffold as a versatile biophore in drug discovery: A review. *Chem. Biol. Interfaces.* **2018**, *8*, 1–10.

[19]Srivastava, V.; Srivastava, A. M.; Tiwari, A. K.; Srivastava, R.; Sharma, R.; Sharma, H.; Singh, V. K. Disubstituted 4 (3H) quinazolones: A novel class of antitumor agents. *Chem. Biol. Drug Des*. **2009**, *74*, 297-301.

[20]Srinivasulu, R.; Kumar, K. R.; Satyanarayana, P. V. V. Facile and efficient method for synthesis of benzimidazole derivatives catalyzed by zinc triflate. *Green Sustain. Chem.* **2014**, *4*, 3.

[21]Fritsch, P. *In Dermatologie und Venerologie*; Springer Verlag: Berlin, 2004; pp 171.

[22]Smith, H. M. *High Performance Pigments*; Wiley: Weinheim, Germany, 2002; pp 135−158.

[23](a) Meuthen, B.; Jandel, A. S. *Coil Coating*; Vieweg & Sohn Verlag: Wiesbaden, Germany, 2008; pp 65. (d) Scherer, G. G. *Fuel Cells II*; Springer Verlag: Berlin, 2008; pp 65−120

[24](a) Elder, M. S.; Melsonand, G. A.; Busch, D. H.; Reactions of Coordinated Ligands. XII. The Synthesis of o-Benzylene-2,1-benzimidazole in the Presence of Nickel(II) Ions, and a Study of Some of Its Metal Complexes. *Inorg. Chem*. **1966**, *5*, 74; (b) Chen, J.; Qu, J.; Zhang, Y.; Chen, Y.; Liu, N.; Chen, B. Metal-free construction of tricyclic or tetracyclic compounds—acid-promoted synthesis of benzo[4,5]imidazo[2,1-a]isoindole and 1,2-dialkyl-2,3-dihydrobenzimidazoles. *Tetrahedron* **2013**, *69*, 316.

[25]Suleman, A.; Skibo, E. B.; A Comprehensive Study of the Active Site Residues of DT-Diaphorase: Rational Design of Benzimidazolediones as DT-Diaphorase Substrates. *J. Med. Chem*. **2002**, *45*, 1211.

[26]Fagan, V.; Bonham, S.; McArdle, P.; Carty, M. P.; Aldabbagh, F.; Synthesis and Toxicity of New Ring-Fused Imidazo[5,4-f]benzimidazolequinones and Mechanism Using Amine N-Oxide Cyclizations. *Eur. J. Org. Chem.* **2012**, 1967.

[27]Xue, D; Long, Y. Metal-Free TEMPO-Promoted C(sp^3)–H Amination To Afford Multisubstituted Benzimidazoles. *J. Org. Chem.* **2014**, *79*, 4727.

[28]Gurry, M.; Sweeney, M.; McArdle, P.; Aldabbagh, F. One-Pot Hydrogen Peroxide and Hydrohalic Acid Induced Ring Closure and Selective Aromatic Halogenation To Give New Ring-Fused Benzimidazoles. *Org. Lett*. **2015**, *17*, 2856

[29]Joardar, S.; Bhattacharyya, A.; Das, S. A Palladium on Carbon Catalyzed One-Pot Synthesis of Substituted Benzimidazoles. *Synthesis*, **2014**, *46*, 3121-3132.

[30](a) Suschitzky, H.; Sutton, M. E. Reductive cyclization of aromatic nitro compounds to benzimidazoles with titanous chloride. *Tetrahedron* **1968**, *24*, 4581; (b) Shawcross, A. P.; Stanforth, S. P. Reaction of N-nitroaryl-1, 2, 3, 4-tetrahydroisoquinoline derivatives with oxygen. *J. Heterocycl. Chem*. **1990**, *27*, 367.

[31](a) Tsang, W. P.; Zheng, N.; Buchwald, S. L. Combined C− H functionalization/C− N bond formation route to carbazoles. *J. Am. Chem. Soc*, **2005**, *127*, 14560-14561. (b) Brasche, G.; Buchwald, S. L. C- H Functionalization/C-N Bond Formation: Copper-Catalyzed Synthesis of Benzimidazoles from Amidines. *Angew. Chem. Int. Ed*. **2008**, *47*, 1932-1934.

[32]Lauer, W. M.; Sprung, M. M.; Langkammerer, C. M. The Piria Reaction. III. 1 Mechanism Studies *J. Am. Chem. Soc.* **1936**, *58*, 225.

[33]Pyrolysis at 240 °C: Suschitzky, H.; Sutton, M. E. Thermal cyclisation of aromatic nitrocompounds. *Tetrahedron Lett,* **1967**, *8*, 3933.

[34] (a) Shen, M.; Leslie, B. E.; Driver, T. G.; Shen, M.; Leslie, B. E.; Driver, T. G. Dirhodium (II)-Catalyzed Intramolecular C-H Amination of Aryl Azides. *Angew. Chem., Int. Ed*. **2008**, *47*, 5056. (b) Stokes, B. J.; Jovanovic, B.; Dong, H.; Richert, K. J.; Riell, R. D.; Driver, T. G. Rh_2 (II)-Catalyzed synthesis of carbazoles from biaryl azides. *J. Org. Chem.* **2009**, *74,* 3225. (c) Sun, K.; Liu, S.; Bec, P. M.; Driver, T. G. *Angew. Chem., Int. Ed.* **2011**, *50*, 1702. (d) Pumphrey, A. L.; Dong, H.; Driver, T. G. RhII2-Catalyzed Synthesis of α-, β-, or δ-Carbolines from Aryl Azides. *Angew. Chem., Int. Ed.* **2012**, *51*, 5920.

[35](a) Archibald, T. *In Managing Hazardous Reactions and Compounds in Process Chemistry*; American Chemical Society: Washington, DC, 2014; pp 87−109. (b) Gonzalez-Bobes, F.; Kopp, N.; Li, L.; Deerberg, J.; Sharma, P.; Leung, S.; Davies, M.; Bush, J.; Hamm, J.; Hrytsak, M. Scale-up of azide chemistry: a case study. *Org. Process Res. Dev.* **2012**, *16*, 2051.

[36]Lebel, H.; Huard, K.; Lectard, S. N-Tosyloxycarbamates as a source of metal nitrenes: rhodium-catalyzed C–H insertion and aziridination reactions. *J. Am. Chem. Soc.* **2005**, *127*, 14198–14199. (b) Lebel, H.; Huard, K. De novo synthesis of troc-protected amines: intermolecular rhodium-catalyzed C–H amination with N-tosyloxycarbamates. *Org. Lett.* **2007**, *9*, 639–642. (c) Reddy, R. P.; Davies, H. M. L. Dirhodium tetracarboxylates derived from adamantylglycine as chiral catalysts for enantioselective C–H aminations. *Org. Lett.* **2006**, *8*, 5013–5016.

[37]Xing, Q.; Chan, C. M.; Yeung, Y. W.; Yu, W. Y. Ruthenium (II)-catalyzed enantioselective γ-lactams formation by intramolecular C–H amidation of 1, 4, 2-dioxazol-5-ones. *J. Am. Chem. Soc.* **2019**, *141*, 3849

[38]Thu, H. Y.; Yu, W. Y.; Che, C. M. Intermolecular amidation of unactivated sp^2 and sp^3 C− H bonds via palladium-catalyzed cascade C− H activation/nitrene insertion. *J. Am. Chem. Soc.* **2006**, *128*, 9048.

[39]Nykaza, T. V.; Cooper, J. C.; Li, G.; Mahieu, N.; Ramirez, A.; Luzung, M. R.; Radosevich, A. T. Intermolecular Reductive C−N Cross Coupling of Nitroarenes and Boronic Acids by P^{III}/P^{V}=O Catalysis. *J. Am. Chem. Soc*. **2018**, *140*, 15200−15205.

[40]Grantham, R. K.; Meth-Cohn, O. Dihydrobenzimidazole chemistry. Part V. The reaction of quaternised dihydrobenzimidazoles with nucleophiles. *J. Chem. Soc.* **1969**, *1444,* 1354-1356.

[41]Xie, M. S.; Huang, B.; Li, N.; Tian, Y.; Wu, X. X.; Deng, Y.; Guo, H. M. Rational Design of 2-Substituted DMAP-N-oxides as Acyl Transfer Catalysts: Dynamic Kinetic Resolution of Azlactones. *J. Am. Chem. Soc*. **2020**, *142*, 19226-19238.

[42]Huisgen, R.; Vossius, D.; Appl, M. Die Thermolyse des Phenylazids in primären Aminen; die Konstitution des Dibenzamils. *Chem. Ber.* **1958**, *91*, 1−12

Chapter 3.

Mechanistic Investigations into C(sp^3)–H Amination

This chapter will detail the mechanistic studies performed to better understand the described organophosphorus catalyzed C(sp^3)–H amination reaction. More specifically, studies probing the catalyst resting state and the C–N cyclization event are investigated experimentally and computationally by Density Functional Theory (DFT).

3.1 – Probing Catalyst Resting State

To gain insight into the catalytic resting state and possible relevant catalytic intermediates, in situ ^{31}P and ^{1}H NMR experiments were conducted. Monitoring the catalytic reaction – 1 equiv of **3.2**, 20 mol% **P1**·[O], 2.5 equiv of phenylsilane, 1 equiv of DBU, 50 μL toluene-d_8, 0.5 M in benzonitrile, 100 °C – in the ^{31}P NMR channel (163 Hz) showed rapid depletion of **P1**·[O], ($t_{1/2}$ ~5 min) at δ 55.5 ppm, with appearance of resonances at δ 31.7 and δ 28.5 ppm, corresponding to the *anti* and *syn* diastereomers of **P1** respectively, which remain constant throughout the rest of the experiment. This result is in line with previous reactions, where the critical observation is phosphine oxide reduction occurs rapidly at high temperatures with the *anti*-**P1** acting as the predominant catalyst resting state.

In terms of product formation, monitoring in the ^{1}H NMR channel (500 MHz) of the same catalytic reaction showed little consumption of *o*-N, N-dibenzyl nitroaniline over ca. 80 min along with concomitant appearance of dihydrobenzimidazole. These results implicate the catalyst resting state and the turnover limiting step occur during the first deoxygenation step with no observable intermediates, including the nitroarene. This presumably occurs via a [3+1] cycloaddition, similarly to our previous reports. This also implicates the C–N bond forming step occurs post-rate-limiting and detection of intermediates spectroscopically will be futile.

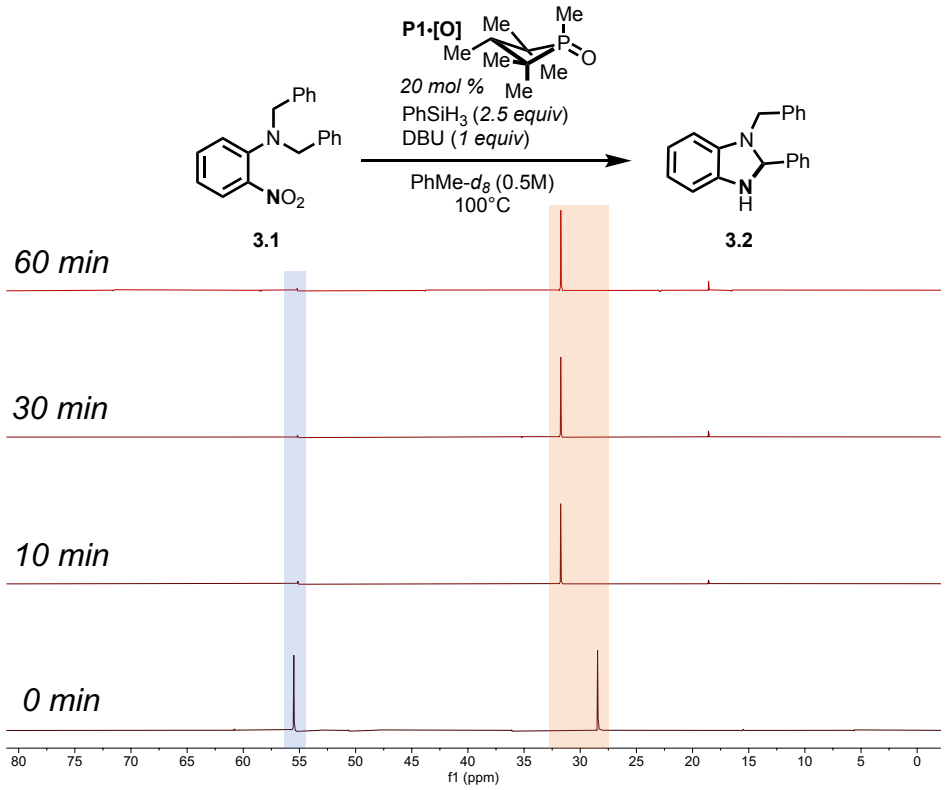

Figure 3.1. Monitored cyclization of nitroaniline **3.1** to dihydrobenzimidazole. A) Time-stacked in situ ^{31}P NMR spectra (T = 100 °C, toluene-d$_8$) at t = 0 min, 10 min, 30 min, and 60 min. Chemical shifts: P1•[O], δ 55.5 ppm (blue); *anti*-**P1**, δ 31.7 (orange) and *syn*-**P1** δ 28.5 ppm.

3.2 – Mechanistic Discussion Supported by Computational Studies

In order to probe possible intermediates, a catalytic cycle supported by density functional theory calculations conducted at the M06-2X/6-311++G(d,p) level was proposed (Figure 3.2). Analogous to previously reported nitroarene reductions by P^{III},[1, 2, 3] the first deoxygenation step occurs via a [3+1] cycloaddition of the *o*-nitroaniline **(3.3)** with phosphetane **P1** for the formation of the pentacoordinate azadioxaphosphetane **Int-3.4**. The energy barrier of the transition state towards this intermediate was calculated as the highest energetic barrier ($\Delta G^{\ddagger}_{rel}$ = +28.1 kcal/mol) for this system, in line with previous calculated barriers. This rate-determining step is also supported by the P^{III} catalyst resting state as confirmed by NMR in experimental studies. **Int-3.4** decomposes by a [2+2] retro fragmentation step[1] giving the *o*-nitrosoaniline **Int-3.5** and one equivalent of the phosphetane oxide **P1•[O]**, a thermodynamically favorable process (ΔG_{rel} = -34.5 kcal/mol with only a $\Delta\Delta G^{\ddagger}_{rel}$ = +7.5 kcal/mol kinetic barrier).

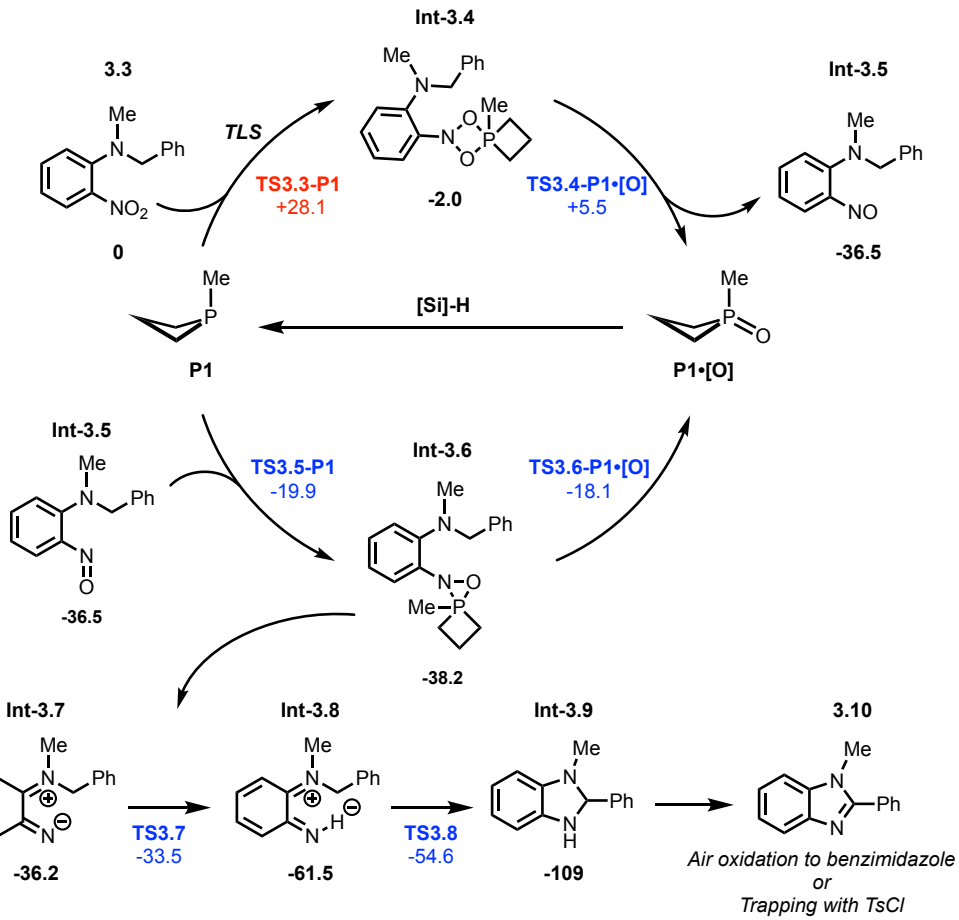

Figure 3.2. Proposed mechanism for benzimidazole formation through a nitrenoid intermediate supported by DFT calculations.

In terms of the C–N bond-forming step, one possible pathway may proceed through a second deoxygenation event by forming the favorable anti-diastereomer of the oxazaphosphirane intermediate **Int-3.6** (ΔG_{rel} = -38.2 kcal/mol). **Int-3.6** could then decompose into the nitrenoid species **Int-3.7**, which is depicted here as the favorable *o*-quinodiimide resonance form (ΔG_{rel} = -36.2 kcal/mol). An intramolecular proton transfer to the nitrenoid position from the benzylic position would, with <3 kcal/mol barrier, produces an energetically downhill deprotonated intermediate **Int-3.8** ($\Delta\Delta G_{rel}$ = 2.7 kcal/mol, $\Delta G^{\ddagger}_{rel}$ = -61.5 kcal/mol). This intermediate would then proceed through a 6π electrocyclization process that is both kinetically ($\Delta G^{\ddagger}_{rel}$ = -54.6 kcal/mol) and thermodynamically (ΔG_{rel} = -109 kcal/mol) favorable. The dihydrobenzimidazole species **Int-3.9** would then be oxidized during work up to provide the aromatic product **3.10**. The next sections will provide experimental insight into this C–N bond-forming step.

3.3 – Hammett Study Probing C–N Bond Forming Event

In order to probe the electronic demand for the C–N bond forming event, a series of N, N-dibenzylated substrates with differing *p*-substitution patterns were prepared. By evaluating the product ratios in an intramolecular competition study, the kinetic selectivity of the presumed post-turnover limiting C(sp^3)–H functionalization step, which must necessarily be selectivity-determining, can be directly measured. For ease of characterization, some substrates were designed as competition against a trifluoromethyl-substituted benzyl group as opposed to the parent benzyl group. These reactions were carried out for 12 h, and their products were analyzed relative to an internal standard for yield (1,3,5-trimethoxybenzene) by ^{1}H NMR and to extract the product ratios by both ^{1}H and ^{19}F NMR spectroscopy when appropriate. A plot of log([X]/[Y]) versus substituent constant σ_{p-} is shown in Figure 3.3, from which a Hammett sensitivity constant $\rho = +0.21$ was derived. A general trend was observed with a preference for C–H functionalization of the benzylic positions of electron-deficient arenes. The σ_{p-} parameter was used to consider the strong inductive effect by resonance and the sigma induction displayed by the ester group substrate. This positive ρ value informs us of a negative charge buildup on the arene ring during the selectivity-determining transition state that could be stabilized by electron-withdrawing substituents. This can be explained by a stabilization effect of the charged intermediate **Int-3.8** (Figure 3.2) that would be enhanced by electron-withdrawing substituents in the transition state leading to the dihydrobenzimidazole, **Int-3.9** (Figure 3.2).

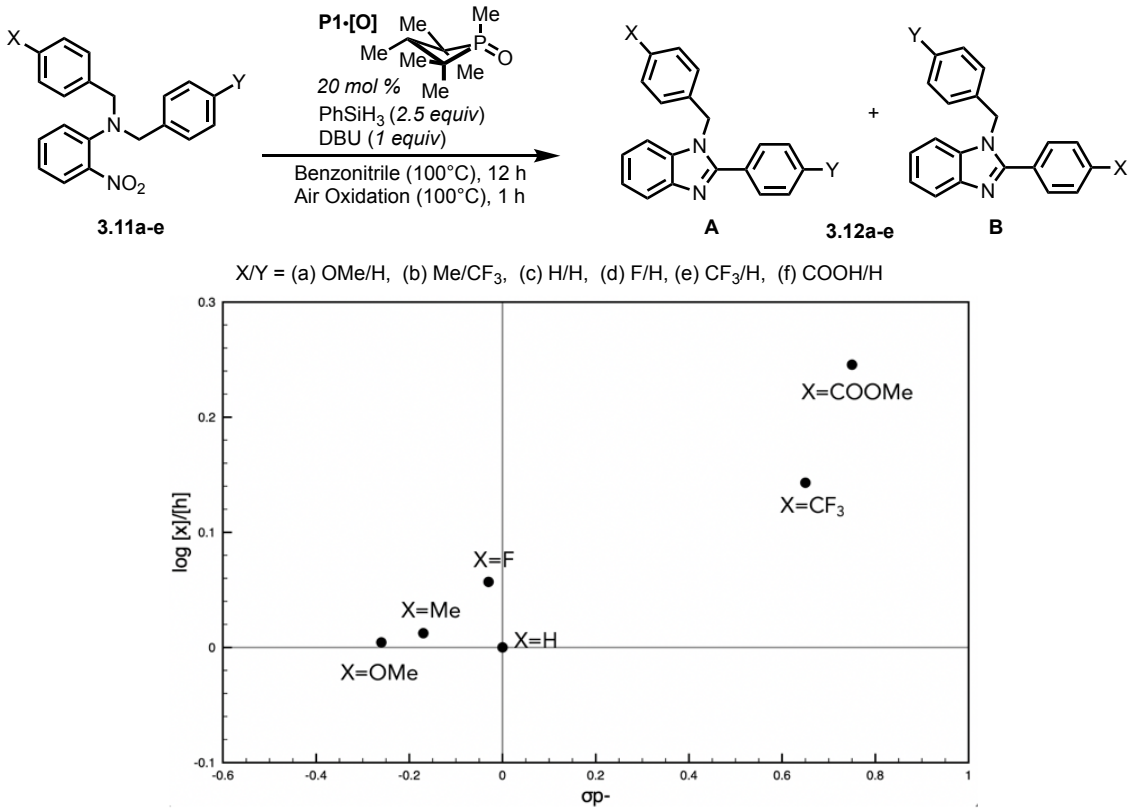

Figure 3.3. Hammett plot of log(X/Y) for benzimidazole formation according to the reaction depicted against the σ_{p-} parameter. Equation: y = 0.2136x + 0.0575; R^2= 0.88.

3.4 – Intramolecular Competition KIE Study

Based on the proposed reaction mechanism, an intramolecular competition kinetic isotope effect (KIE) study would provide insight into the product determining step, where a primary isotope effect would be expected. With 1 equiv of the corresponding deuterated substrate, *N*-benzyl-2-nitro-*N*-(phenylmethyl-d_2) aniline **3.13-*d*$_2$**, ran under catalytic conditions, a kinetic isotope effect ratio of 2.24 k_H/k_D was determined. This value indicates a primary KIE, informing the C–N bond-forming step does indeed occur post rate-limiting step. Additionally, the absence of isotopic scrambling **3.16** indicates that this process is not in equilibrium. This result agrees with the DFT studies where the transition state of the proton transfer leading to deprotonated intermediate **Int-3.9** (Figure 3.2) is an energetically downhill process ($\Delta\Delta G_{rel}$ = 2.7 kcal/mol, $\Delta G^{\ddagger}$ = -61.5 kcal/mol).

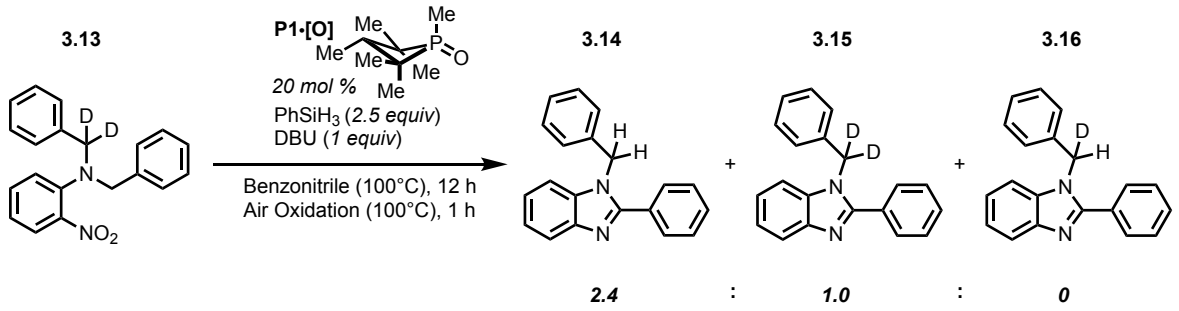

Figure 3.4. KIE of 2.24 k_H/k_D from intramolecular competition.

3.5 – Possible Alternative Mechanism

While the mechanistic results are in support of the proposed reaction mechanism, a possible alternative can be envisioned based on previously reported *o*-nitroso aniline reactivity (Figure 3.5).[20, 21] Instead of the nitroso intermediate undergoing a second deoxygenation event catalyzed by the phosphetane, a non-phosphorus-involved pathway could also be conceived leading to the desired product. First, challenging proton transfer from the benzylic position to the nitroso-group would yield zwitterion **Int-3.17** (ΔG_{rel} = -10.8 kcal/mol. This intermediate proceeds to form the cyclic hydroxylamine **Int-3.18** with a strong thermodynamic driving force (ΔG_{rel} = -54 kcal/mol). Dehydration would drive the formation of the aromatic product. While evidence of an uncatalyzed nitroso cyclization for synthesis of benzimidazoles,[4] is reported, the barriers are almost 20 kcal/mol higher than the catalyzed pathway, and the presence of a hydroxylamine intermediate was never observed by ^{1}H-NMR or mass spectroscopy in the crude reaction mixture. Furthermore, the observation and isolation of dihydrobenzimidazole product would be precluded if this mechanism were operative. Accordingly, this alternative pathway seems unlikely to be operative. Synthesis of an *o*-nitroso aniline is ongoing to evaluate this pathway experimentally.

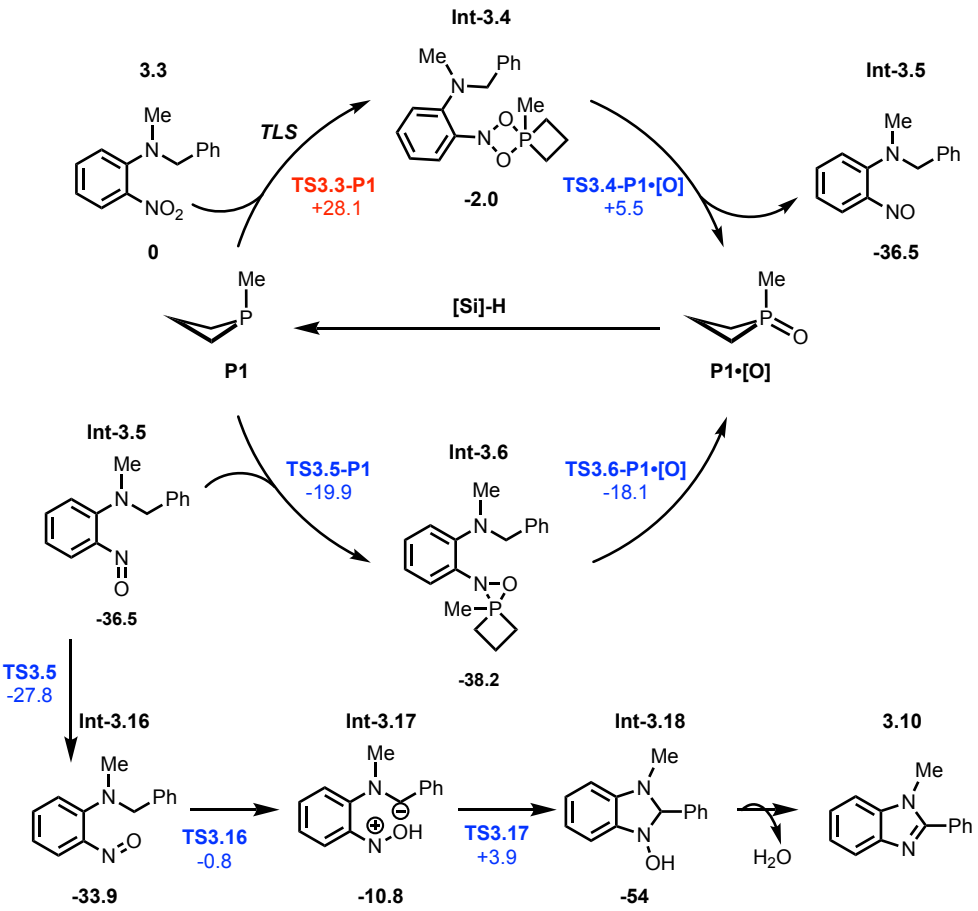

Figure 3.5. Alternative mechanism for benzimidazole formation through *o*-nitrosoaniline pathway.

3.6 – Summary

The mechanism of the organophosphorus catalyzed C(sp^3)–H amination reaction was studied. The catalyst resting state was determined to be the P^{III} phosphetane by analysis by ^{31}P NMR spectroscopy. The C–N cyclization event supported by DFT is believed to proceed through a second deoxygenation event arriving at the oxazaphosphirane intermediate **Int-3.6**. This intermediate proceeds through an intramolecular proton transfer followed by a 6π electrocyclization process to arrive at the dihydrobenzimidazole. A ρ value of +0.21 derived from the Hammett plot indicates a buildup of negative charge in the transition state supporting the proposed mechanism. Additionally, the KIE study displayed a ratio k_H/k_D of 2.24, indicating a primary isotope effect and support for the C–N cyclization occurring post rate-limiting step. Ongoing work is focused on the synthesis of an *o*-nitroso aniline that will allow us to probe reactivity and understand reaction mechanism stoichiometrically at lowered temperature. The

results of this work and future directions will contribute to broadening the repertoire of nitro-modifying reactions and provide a mechanistic rationale for iterative reaction design based on organophosphorus catalysis.

3.7 – References

[1]Nykaza, T. V.; Harrison, T. S.; Ghosh, A.; Putnik, R. A.; Radosevich, A. T. A Biphilic Phosphetane Catalyzes N-N Bond Forming Cadogan Heterocyclization via P^{III}/P^{V}=O Redox Cycling. *J. Am. Chem. Soc.* **2017**, *139*, 6839−6842

[2]Nykaza, T. V.; Ramirez, A.; Harrison, T. S.; Luzung, M. R.; Radosevich, A. T. Biphilic Organophosphorus-Catalyzed Intramolecular Csp^2−H Amination: Evidence for a Nitrenoid in Catalytic Cadogan Cyclizations. *J. Am. Chem. Soc.* **2018**, *140*, 3103−3113.

[3]Nykaza, T. V.; Cooper, J. C.; Li, G.; Mahieu, N.; Ramirez, A.; Luzung, M. R.; Radosevich, A. T. Intermolecular Reductive C−N Cross Coupling of Nitroarenes and Boronic Acids by P^{III}/P^{V}=O Catalysis. *J. Am. Chem. Soc*. **2018**, *140*, 15200−15205.

[4]Purkait, A.; Roy, S. K.; Srivastava, H. K.; Jana, C. K. Metal-Free Sequential C (sp^2)–H/OH and C (sp^3)–H Aminations of Nitrosoarenes and N-Heterocycles to Ring-Fused Imidazoles. *Org. Lett.* **2017**, *10*, 2540-2543.

Chapter 4

Experimental Section

I. General Notes

All reagents were purchased from commercial vendors (Sigma-Aldrich, Alfa Aesar, Acros, TCI, Oakwood Chemical, or Combi-Blocks) and used without further purification unless otherwise indicated. Indicated substrates were synthesized according to literature procedure. Acetonitrile, dichloromethane, diethyl ether, dimethylformamide, toluene, and tetrahydrofuran were purified and collected under argon using a Glass Contour Solvent Purification System. Anhydrous benzonitrile was obtained from a Sigma-Aldrich (sure-seal® bottle) and used as received. All other solvents were ACS grade or better and were used without further purification unless otherwise noted. Manipulations were conducted under an atmosphere of dry N2 gas unless otherwise noted. The reductive C(sp^3)–N coupling reactions were carried out in glass culture tubes with a threaded end (13 x 100 mm; Fisher Scientific part # 14-959-35C), outfitted with a phenolic screw-thread open top cap with red PTFE/white silicone (VWR part #82028-444). Column chromatography was carried out on silica gel (SiliFlash® Irregular Silica Gel, P60 40-63μm) or aluminum oxide (activated, neutral, Brockmann I) as noted. ^{1}H, ^{13}C, ^{15}N, ^{19}F, and ^{31}P NMR were collected with either Bruker AVANCE III HD 400 (BBO Prodigy nitrogen cryoprobe) or Bruker Neo 500 (BBO Prodigy nitrogen cryoprobe or BBFO SmartProbe) spectrometers and processed using MestReNova software. ^{1}H NMR chemical shifts are given in ppm with respect to solvent residual peak (chloroform-*d*, δ 7.26 ppm; DMSO-d_6, δ 2.50 ppm; C_6D_6 7.16 ppm). $^{13}C\{^{1}H\}$ NMR shifts are given in ppm with respect to (chloroform-*d,* δ 77.16 ppm). ^{31}P NMR shifts are given in ppm with respect to 85% H_3PO_4 (δ 0.0 ppm) as an external standard. Multiplicities are described as s = singlet, br s = broad singlet, d = doublet, t = triplet, q = quartet, dd = doublet of doublets, td = triplet of doublets, m = multiplet. Coupling constants are reported in Hertz (Hz). High-resolution ESI mass spectra were obtained from the Mass Spectrometry Laboratory at the MIT department of chemistry instrumentation using Agilent QTOF 6545 with ESI ionization source. All yields reported are isolated yields unless stated otherwise.

II. Optimization of Reaction Conditions

A. Optimization with *N,N*-dibenzyl *o*-nitroaniline (2.1)

Optimization-scale reactions were conducted at 0.25 mmol of limiting substrate. To a 4 mL vial with magnetic stir bar was added *N,N*-dibenzyl *o*-nitroaniline (**2.1**), phosphine oxide catalyst

(P•[O], 20 mol%), and 1,3,5-trimethoxybenzene (14.0 mg, 98%, 0.33 mmol) as the internal standard. The thread was lined with teflon tape, capped with a black septum cap, and the septum was punctured with a needle under N_2. The atmosphere was exchanged by three evacuation/N_2 backfill cycles. Solvent (Toluene, Dioxane, $PhCF_3$, DMF, or Benzonitrile, 0-0.5 M) was added under N_2, followed by additive (water, MeOH, NEt_3, DIPEA, Pyridine, or DBU, 0-2.5 equiv) and silane (Ph_2SiH_2, PMHS, $PhSiH_3$, 0–3.0 equiv.) were added. The black septum cap was wrapped in parafilm, and reaction vial placed in a thermostatted (60-100 °C) aluminum heating block and stirred at 300 rpm. After 12-24 h, the product was oxidized with rigorous bubbling of air through the solution for 1 h at 100°C. After cooling down an aliquot was transferred to an NMR tube, diluted to total volume ~0.6 mL, and analyzed by ^{1}H NMR spectroscopy. The yield was determined by relative integration between 1,3,5- trimethoxybenzene (δ = 6.04 ppm, s, 3 H, 0.33 equiv.), and product **2.3** (δ = 5.45 ppm, s, 2H). Number of scans = 8 and relaxation delay = 4 seconds.

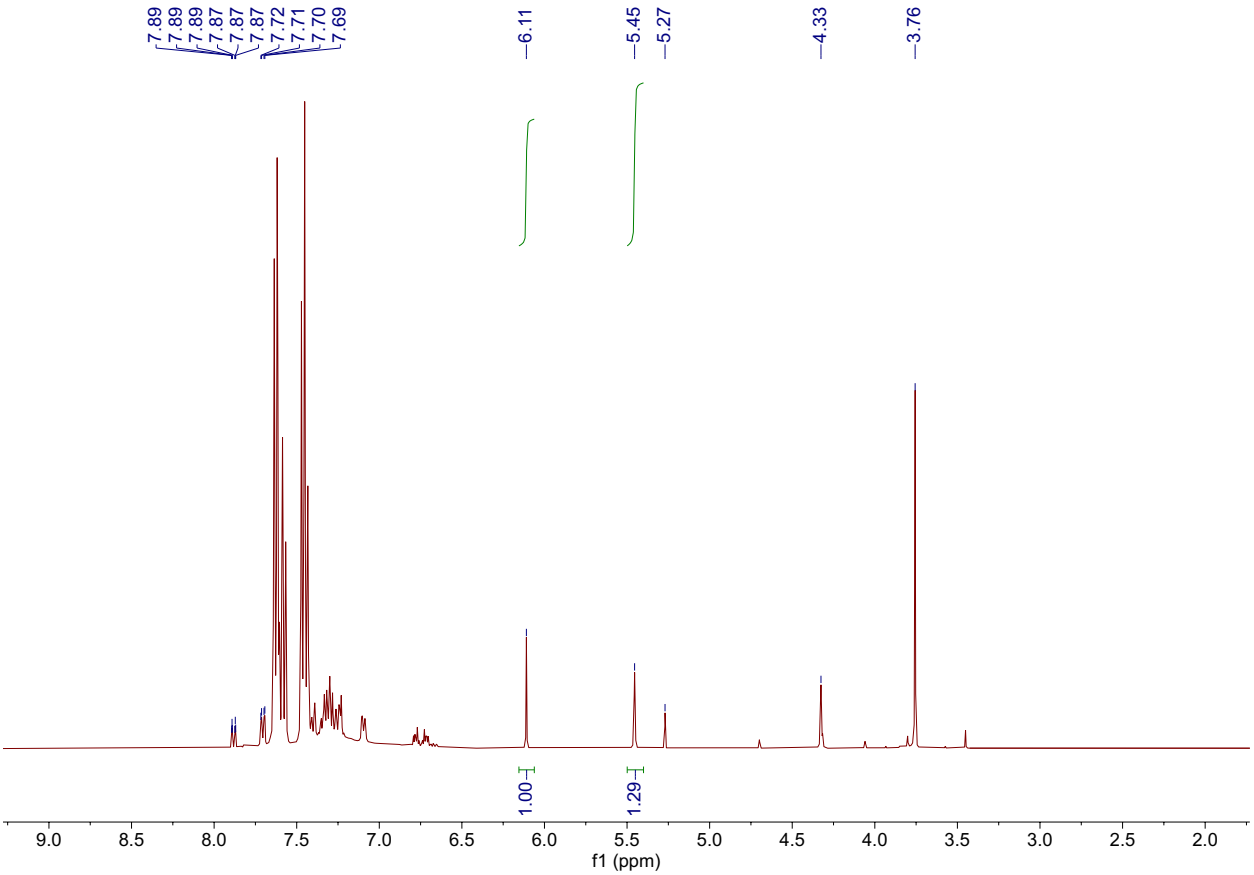

Figure 4.10. Representative ^{1}H NMR spectrum for yield determination for optimization of reductive C–N cyclization of *N,N*-dibenzyl *o*-nitroaniline (**2.1**) by **P1**•[O] (optimal conditions, 88% **2.3**)

Table 4.1. Complete Optimization Table

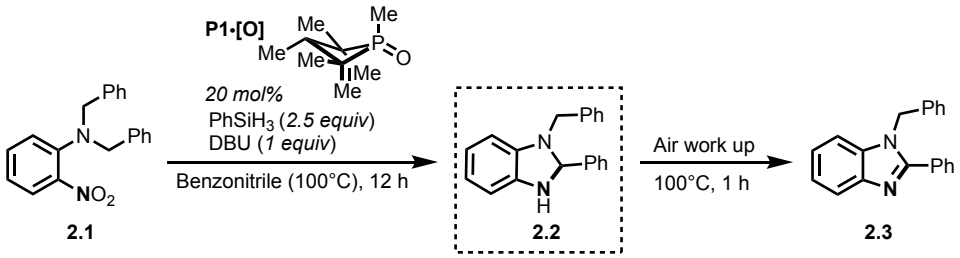

Entry	Deviation from standard	Yield (%)
1	Toluene	40%
2	Dioxane	27%
3	$PhCF_3$	24%
4	DMF	51%
5	Benzonitrile	64%
6	Water	72%
7	MeOH	61%
8	NEt_3	60%
9	DIPEA	49%
10	Pyridine	65%
12	DBU	88%
12	Ph-phosphetane	33%
13	Py-phosphetane	42%
14	O'Brien catalyst	47%
15	Rutjes catalyst	5%
16	Triphenylphosphine	4%
17	0.1 M	62%
18	0.5 M	97% (87%[b])
19	No catalyst	0%
20	No silane	0%
21	Ph_2SiH_2	77%
22	PMHS	29%
23	0.67 eq $PhSiH_3$	34%
24	2% cat. 12h	35%
25	5% cat. 12h	50%
26	10% cat. 24h	82%
27	60 °C	19%
28	80 °C 48h	64%
29	DBU 0.5 eq	86%
30	DBU 2.5 eq	82%

[a]Standard conditions: 0.25 mmol substrate 2.1, 20 mol% **P1**•[O], 0.5 M in benzonitrile 1.5 eq. $PhSiH_3$, 1.0 eq DBU at 100°C, 12h. Yield determined by ^1H NMR analysis of crude reaction mixture with 1,3,5-trimethoxybenzene added as internal standard. [b]Isolated Yield

III. Procedures for the Preparation of Starting Materials

A. Preparation of phosphorus compounds

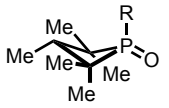

R = Me: **P1•[O]**
R = Ph
R = pyrrolidino

1,2,2,3,4,4-Hexamethylphosphetane 1-oxide (**P1•**[O]), *2,2,3,4,4-Pentamethyl-1-phenylphosphetane 1-oxide*, *2,2,3,4,4-Pentamethyl-1-(purrolidin-1-yl)phosphetane 1-oxide* were prepared according to literature methods.[1]

3-Methyl-1-phenylphospholane 1-oxide:

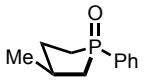

Prepared according to the literature procedure[2] via hydrogenation (Pd/C) of commercially available 3-methyl-1-phenyl-2-phospholene 1-oxide. Clear pale-yellow oil obtained, 973 mg, 96%. Spectral data are in agreement with the literature reported values.

5-Phenylbenzo[b]phosphindole 5-oxide:

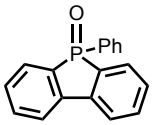

According to the literature procedure,[2,3] triphenylphosphine oxide was treated with phenyllithium, and the corresponding phosphine (5-phenyl-5*H*- benzo[b]phosphindole) was oxidized using H_2O_2. The phosphine can be columned prior to oxidation (silica, ethyl acetate/n-heptane 1:1 ratio) and recrystallized in ethyl acetate if necessary. White solid obtained, 672 g, 81%. Spectral data are in agreement with the literature reported values.

B. Preparation of Benzimidazole Precursors

General method A: Dibenzylamine (1.0 equiv) was added dropwise to 1-fluoro-2-nitrobenzene (3.0 equiv) at rt. The resulting mixture was stirred at 120°C for 24h. The reaction mixture was cooled to room temperature, diluted with a minimum amount of dichloromethane, and purified by column chromatography (hexane/DCM).

General method B: Benzylbromide (2.0 equiv), 2-nitroaniline (1.0 equiv) and potassium carbonate (1.0 equiv) were stirred in acetonitrile (1M) at reflux overnight. After cooling down the mixture was extracted with ethyl acetate and water. The combined organic layers were washed

with brine, dried over MgSO4 and concentrated in vacuo. Product was isolated by column chromatography (hexane/DCM).

General method C: 1-Fluoro-2-nitrobenzene (1.0 eqiuv), N-benzylmethylamine (1.1 equiv) and potassium carbonate (1.45 eq) were reacted in DMSO (0.2M) at 120°C. After 3 days, the reaction was allowed to cool to room temperature and added to water. The solid is filtered and washed with additional water. The filtrate was extracted with ethyl acetate. The combined organic layers were washed with brine, dried over $MgSO_4$ and concentrated in vacuo. Product was isolated by column chromatography (hexane/DCM).

N,N-dibenzyl-2-nitroaniline (2.4-SM)

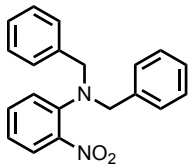

Synthesized according to general method A and isolated as orange oil (85%). ^{1}H NMR (400 MHz, Chloroform-*d*) δ 7.76 (dd, *J* = 8.1, 1.6 Hz, 1H), 7.38 (ddd, *J* = 8.6, 7.3, 1.7 Hz, 1H), 7.35 – 7.21 (m, 10H), 7.11 (dd, *J* = 8.3, 1.2 Hz, 1H), 7.02 (ddd, *J* = 8.3, 7.3, 1.3 Hz, 1H), 4.24 (s, 4H). Spectral data is consistent with literature characterization.[4]

N,N-di-p-xylyl-2-nitroaniline (2.5-SM)

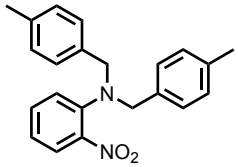

Synthesized according to general method B and isolated as orange oil (31%). ^{1}H NMR (500 MHz, Chloroform-*d*) δ 7.76 (dd, *J* = 8.1, 1.7 Hz, 1H), 7.36 (ddd, *J* = 8.7, 7.2, 1.7 Hz, 1H), 7.17 – 7.05 (m, 9H), 7.00 (ddd, *J* = 8.3, 7.3, 1.3 Hz, 1H), 4.19 (s, 4H), 2.34 (s, 6H). ^{13}C NMR (101 MHz, $CDCl_3$) δ 144.99, 144.08, 137.07, 134.15, 132.76, 129.22, 128.45, 125.81, 123.46, 121.38, 56.40, 21.26. HRMS(ESI$^+$) calcd. for $C_{22}H_{23}N_2O_2$ $[M+H]^+$ 347.1760, found 347.1658. IR (neat) ν 3022, 2921, 2857, 1567, 1486, 1346, 808 cm^{-1}

N,N-di-(p-methoxybenzyl)-2-nitroaniline (2.6-SM)

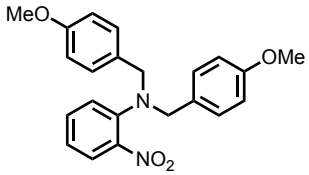

Synthesized according to general method A and isolated as yellow solid (90%). ^{1}H NMR (400 MHz, Chloroform-*d*) δ 7.75 (dd, *J* = 8.1, 1.7 Hz, 1H), 7.37 (ddd, *J* = 8.7, 7.3, 1.7 Hz, 1H), 7.14 (d, *J* = 8.7 Hz, 3H), 7.08 (dd, *J* = 8.3, 1.2 Hz, 1H), 7.01 (ddd, *J* = 8.3, 7.3, 1.2 Hz, 1H), 6.84 (d, *J* = 8.6 Hz, 3H), 4.15 (s, 4H), 3.80 (s, 6H). ^{13}C NMR (101 MHz, $CDCl_3$) δ 158.84, 144.83, 144.16, 132.59, 129.60, 129.12, 125.59, 123.55, 121.40, 113.75, 55.85, 55.22. IR (neat) ν 3068, 2835, 1603, 1510, 1246, 1173, 1033, 823 cm^{-1}.

N,N-di-(p-fluorobenzyl)-2-nitroaniline (2.7-SM)

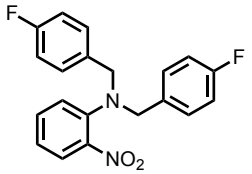

Synthesized according to general method B and isolated as orange oil (23%). ^{1}H NMR (400 MHz, Chloroform-*d*) δ 7.74 (dd, *J* = 8.0, 1.6 Hz, 1H), 7.40 (ddd, *J* = 8.6, 7.3, 1.7 Hz, 1H), 7.25 – 7.16 (m, 4H), 7.13 – 7.06 (m, 2H), 7.06 – 6.94 (m, 4H), 4.16 (s, 4H). ^{13}C NMR (101 MHz, Chloroform-*d*) δ 162.14 (d, *J* = 245.6 Hz), 144.84, 144.26, 132.66, 132.60 (d, *J* = 3.5 Hz), 129.99 (d, *J* = 8.0 Hz), 125.49, 123.78, 122.42, 115.34 (d, *J* = 21.5 Hz), 56.08. ^{19}F NMR (376 MHz, $CDCl_3$) δ -114.94. HRMS(ESI^{+}) calcd. for $C_{20}H_{16}F_2N_2O_2$ $[M+H]^+$ 355.1253, found 355.1256. IR (neat) ν 3071, 2847, 1601, 1507, 1220, 827 cm^{-1}.

N,N-di-(p-trifluoromethylbenzyl)-2-nitroaniline (2.8-SM)

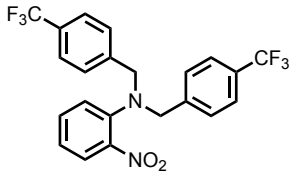

Synthesized according to general method A and isolated as orange oil (23%). ^{1}H NMR (400 MHz, $CDCl_3$) δ 7.80 – 7.62 (m, 1H), 7.58 (d, *J* = 8.0 Hz, 2H), 7.49 – 7.36 (m, 2H), 7.16 – 7.08 (m, 1H), 4.27 (s, 2H). ^{13}C NMR (101 MHz, $CDCl_3$) δ 145.06, 143.77, 144.99, 144.92, 140.89, 132.88, 130.06, 129.74, 128.58, 127.24, 125.61, 125.56, 125.53, 125.49, 125,40, 123.62, 123.14, 122.70, 77.34, 77.02, 76.70, 56.79. ^{19}F NMR (376 MHz, $CDCl_3$) δ -62.54.

***N,N*-dibenzyl-3-nitropyridin-2-amine (2.9-SM)**

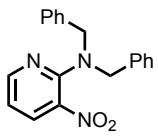

Synthesized according to general method A and isolated as orange oil (1.470 g, 91% Yield). ^{1}H NMR (400 MHz, $CDCl_3$) δ 8.40 (dd, *J* = 4.5, 1.8 Hz, 1H), 8.14 (dd, *J* = 8.0, 1.8 Hz, 1H), 7.29 (pd, *J* = 8.0, 2.0 Hz, 7H), 7.21 – 7.15 (m, 4H), 6.80 (dd, *J* = 8.0, 4.5 Hz, 1H), 4.63 (s, 4H). Spectral data is consistent with literature characterization.[5]

N,N-dipropyl-2-nitroaniline (2.11-SM)

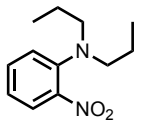

Synthesized according to general method A and isolated as orange oil (64%). ^{1}H NMR (400 MHz, Chloroform-*d*) δ 7.68 (dd, *J* = 8.1, 1.7 Hz, 1H), 7.40 (ddd, *J* = 8.6, 7.2, 1.7 Hz, 1H), 7.15 (dd, *J* = 8.4, 1.2 Hz, 1H), 6.91 (ddd, *J* = 8.3, 7.2, 1.2 Hz, 1H), 3.12 – 3.03 (m, 4H), 1.55 (dq, *J* = 14.7, 7.4 Hz, 4H), 0.87 (t, *J* = 7.4 Hz, 6H). ^{13}C NMR (101 MHz, $CDCl_3$) δ 145.12, 143.13, 132.51, 125.78, 122.18, 119.67, 54.32, 20.66, 11.39. HRMS(ESI$^+$) calcd. for $C_{12}H_{19}N_2O_2$ $[M+H]^+$ 223.1447, found 223.1443. IR (neat) ν 2962, 2874, 1602, 1513, 1343, 850, 742 cm^{-1}.

N,N-dibutyl-2-nitroaniline (2.12-SM)

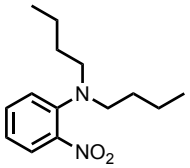

Synthesized according to general method A and isolated as orange oil (84%). ^{1}H NMR (400 MHz, Chloroform-*d*) δ 7.66 (dd, *J* = 8.1, 1.6 Hz, 1H), 7.38 (ddd, *J* = 8.7, 7.2, 1.6 Hz, 1H), 7.12 (dd, *J* = 8.5, 1.2 Hz, 1H), 6.94 – 6.83 (m, 1H), 3.08 (t, *J* = 7.3 Hz, 4H), 1.67 – 1.42 (m, 4H), 1.28 (dt, *J* = 15.0, 7.4 Hz, 4H), 0.87 (t, *J* = 7.3 Hz, 6H). Spectral data is consistent with literature characterization.[6]

3-nitro-2-(piperidin-1-yl)pyridine (2.14-SM)

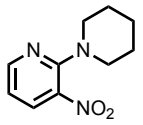

Synthesized according to general method A and isolated as orange solid (96%). ^{1}H NMR (400 MHz, $CDCl_3$) δ 8.33 (dd, *J* = 4.5, 1.8 Hz, 1H), 8.13 (dd, *J* = 8.0, 1.8 Hz, 1H), 6.70 (dd, *J* = 8.0, 4.5 Hz, 1H), 3.46 – 3.39 (m, 5H), 1.71 (q, *J* = 2.5 Hz, 7H). Spectral data is consistent with literature characterization.[7]

1-(2-Nitrophenyl)azepane (2.16-SM)

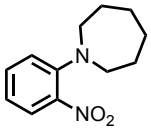

Synthesized according to general method A and isolated as orange oil (94%). ^{1}H NMR (400 MHz, Chloroform-*d*) δ 7.71 (dd, *J* = 8.2, 1.7 Hz, 1H), 7.37 (ddd, *J* = 8.7, 7.0, 1.7 Hz, 1H), 7.09 (dd, *J* = 8.7, 1.1 Hz, 1H), 6.76 (ddd, *J* = 8.2, 7.0, 1.1 Hz, 1H), 3.42 – 3.22 (m, 4H), 1.83 (tp, *J* = 6.1, 1.8 Hz, 4H), 1.62 (dt, *J* = 5.9, 2.7 Hz, 4H). Spectral data is consistent with literature characterization.[6]

N-phenyl-N-methyl-2-nitroaniline (2.17-SM)

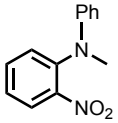

To a solution of 2-nitrodiphenylamine (2.14 g, 10 mmol) in DMF (25 mL) was added KOtBu (1.46 g, 13 mmol) and subsequently iodomethane (0.81 mL, 13 mmol). The mixture was stirred at room temperature for 2 h, poured onto water and extracted with ethyl acetate. The organic phase was evaporated and the remaining oily product purified by column chromatography on silica gel (hexane/ethyl acetate). The product was isolated as dark red oil (0.80 g, 3.5 mmol, 35%). ^{1}H NMR (400 MHz, DMSO-d_6) δ 7.93 (dd, *J* = 8.1, 1.6 Hz, 1H), 7.76 (td, *J* = 7.8, 1.6 Hz, 1H), 7.54 (dd, *J* = 8.1, 1.3 Hz, 1H), 7.44 (ddd, *J* = 8.5, 7.5, 1.4 Hz, 1H), 7.22 – 7.12 (m, 2H), 6.79 (tt, *J* = 7.3, 1.1 Hz, 1H), 6.65 (dq, *J* = 7.1, 1.5, 1.0 Hz, 2H), 3.26 (s, 3H). Spectral data is consistent with literature characterization.[8]

N-benzyl-N-methyl-2-nitroaniline (2.18-SM)

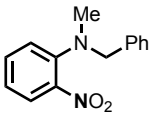

Synthesized according to general method C, the reaction was heated for 5h, and isolated as orange oil (56%). ^{1}H NMR (400 MHz, Chloroform-*d*) δ 7.79 (dd, *J* = 8.2, 1.7 Hz, 1H), 7.50 – 7.20 (m, 6H), 7.10 (dd, *J* = 8.4, 1.1 Hz, 1H), 6.92 (ddd, *J* = 8.1, 7.1, 1.2 Hz, 1H), 4.41 (s, 2H), 2.81 (s, 3H). ^{13}C NMR (101 MHz, $CDCl_3$) δ 145.86, 140.89, 137.04, 133.08, 128.64, 127.62, 127.43, 126.32, 120.20, 119.24, 58.71, 40.35. HRMS(ESI$^+$) calcd. for $C_{14}H_{15}N_2O_2$ $[M+H]^+$ 243.1128, found 243.1134. IR (neat) ν 3063, 2805, 1603, 1511, 1344, 735, 698 cm^{-1}.

4-(2-Nitrophenyl)morpholine (2.21-SM)

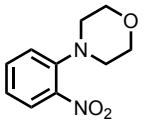

Synthesized according to general method A, except that it was heated for 1h, and isolated as orange oil (82%). ^{1}H NMR (400 MHz, Chloroform-*d*) δ 7.76 (dd, *J* = 8.1, 1.6 Hz, 1H), 7.55 – 7.41 (m, 1H), 7.15 (d, *J* = 8.2 Hz, 1H), 7.07 (t, *J* = 7.7 Hz, 1H), 3.89 – 3.74 (m, 4H), 3.15 – 2.98 (m, 4H). Spectral data is consistent with literature characterization.[6]

1-(2-nitrophenyl)pyrrolidin-2-one (2.22-SM)

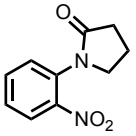

Synthesized according to general method A, and isolated as orange oil (95%).^{1}H NMR (400 MHz, $CDCl_3$) δ 7.98 (dd, *J* = 8.2, 1.5 Hz, 1H), 7.65 (td, *J* = 7.7, 1.5 Hz, 1H), 7.43 (td, *J* = 7.8, 1.4 Hz, 1H), 7.37 (dd, *J* = 8.0, 1.4 Hz, 1H), 3.91 (t, *J* = 7.0 Hz, 2H), 3.72 (s, 7H), 2.56 (t, *J* = 8.0 Hz, 2H), 2.29 (tt, *J* = 7.7, 6.7 Hz, 2H), 2.06 (s, 1H), 1.27 (t, *J* = 7.1 Hz, 1H). Spectral data is consistent with literature characterization.[9]

N-benzyl-N-phenyl-2-nitroaniline (2.23-SM)

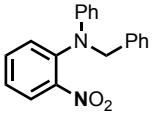

To a solution of 2-nitrodiphenylamine (2.14 g, 10 mmol) in DMF (25 mL) was added KOtBu (1.46 g, 13 mmol) and subsequently benzyl bromide (1.55 mL, 13 mmol). The mixture was stirred at room temperature for 2 h. The solvent was removed under vacuum, 1,4- diazabicyclo[2,2,2]octane (DABCO; 560 mg, 5 mmol) was added to precipitate unreacted benzyl bromide from ethanol, followed by crystallization of the product from ethanol in the fridge overnight. The product was isolated as an orange/red solid (2.50 g, 8.2 mmol, 82%). 1H NMR (400 MHz, DMSO-d6) δ 7.90 (dd, J = 8.1, 1.6 Hz, 1H), 7.71 (ddd, J = 8.2, 7.4, 1.6 Hz, 1H), 7.55 (dd, J = 8.2, 1.3 Hz, 1H), 7.41 – 7.35 (m, 3H), 7.34 – 7.28 (m, 2H), 7.28 – 7.20 (m, 1H), 7.16 – 7.10 (m, 2H), 6.84 – 6.76 (m, 1H), 6.75 – 6.66 (m, 2H), 4.98 (s, 2H). Spectral data is consistent with literature characterization.[10]

C. Substrates used for Mechanistic Studies

General Procedure:

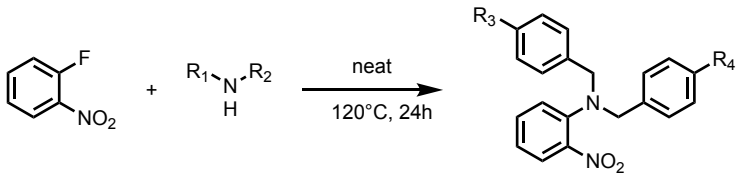

To a round bottom flask with a stir bar was added o-halonitrobenzene (1.5 equiv), followed by the addition of amine (1.0 equiv) dropwise at rt. The mixture was moved to an oil bath at 120°C for 24h. The reaction mixture cooled to rt was diluted with minimum amount CH_2Cl_2, filtered through a short path of silica gel. The orange fractions were collected and evaporated to afford the corresponding o-nitroanilines.

***N*-benzyl-*N*-(4-methoxybenzyl)-2-nitroaniline (3.11a-SM):**

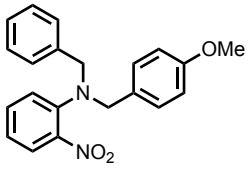

Following a modification of the general procedure using *N*-benzyl-1-(4-methoxyphenyl)methanamine (1.9 g, 8.42 mmol) was added dropwise to 1-fluoro-2-nitrobenzene (0.59 mL, 5.62 mmol) at rt. The crude product was purified by column chromatography on silica gel by hexane/DCM to yield product as an orange oil (812 mg, 41%). ^{1}H NMR (400 MHz, Chloroform-*d*) δ 7.73 (d, *J* = 8.0 Hz, 1H), 7.41-7.20 (m, 7H), 7.17-7.10 (d, *J* = 8.4 Hz, 2H), 7.10-7.06 (d, *J* = 8.1 Hz, 1H), 7.03-6.96 (t, *J* = 7.7 Hz, 1H), 6.87-6.77 (m, 2H), 4.20 (s, 2H), 4.15 (s, 2H), 3.78 (s, 3H). ^{13}C NMR (101 MHz, $CDCl_3$) δ 159.02, 144.92, 144.30, 137.32, 135.73, 135.64, 132.77, 129.77, 129.14, 128.55, 128.50, 127.47, 126.31, 126.28, 125.77, 124.71, 124.66, 123.61, 121.63, 118.69, 118.49, 113.91, 56.49, 56.33, 55.35.

***N*-(4-methylbenzyl)-2-nitro-*N*-(4-(trifluoromethyl)benzyl)aniline (3.11b-SM):**

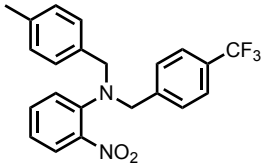

Following a modification of the general procedure using *N*-(4-methylbenzyl)-1-(4-(trifluoromethyl)phenyl)methanamine (2.1 g ,7.52 mmol) was added dropwise to 1-fluoro-2-nitrobenzene (0.52 mL, 5.01 mmol) at rt. The crude product was purified by column chromatography on silica gel by hexane/DCM to yield product as an orange oil (311 mg, 16%). ^{1}H NMR (500 MHz, $CDCl_3$) δ 7.74 (dd, *J* = 8.1, 1.6 Hz, 1H), 7.54 (d, *J* = 8.1 Hz, 2H), 7.38 (d, *J*

= 8.6 Hz, 3H), 7.14 – 6.97 (m, 6H), 4.24 (s, 2H), 4.15 (s, 2H), 2.32 (s, 3H). ^{13}C NMR (126 MHz, $CDCl_3$) δ 144.65, 144.49, 141.59, 137.43, 133.63, 132.89, 129.87, 129.61, 129.36, 128.66, 128.53, 125.79, 125.55, 125.52, 125.36, 123.60, 123.20, 122.33, 57.33, 55.95, 21.26. ^{19}F NMR (471 MHz, $CDCl_3$) δ -62.46.

***N*-benzyl-*N*-(4-fluorobenzyl)-2-nitroaniline (3.11c-SM):**

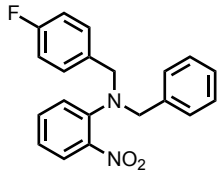

Following a modification of the general procedure using *N*-benzyl-1-(4-fluorophenyl) (1.77 g, 8.22 mmol) was added dropwise to 1-fluoro-2-nitrobenzene (0.58 mL, 5.48 mmol) at rt. The crude product was purified by column chromatography on silica gel by hexane/DCM to yield product as an orange oil (739 mg, 40%). ^{1}H NMR (400 MHz, $CDCl_3$) δ 7.74– 7.71 (dd, *J* = 8.1, 1.6 Hz, 1H), 7.39-7.34 (t, *J* = 8.0, 1H), 7.30– 7.17 (m, 9H), 7.24 – 7.14 (m, 1H), 7.11 – 6.91 (m, 4H), 4.18 (s, 2H), 4.16 (s, 2H). ^{13}C NMR (101 MHz, $CDCl_3$) δ 163.51, 161.07, 144.99, 144.40, 132.81, 132.76, 132.73, 130.18, 130.10, 125.63, 123.92, 122.56, 115.59, 115.38, 56.22. ^{19}F NMR (376 MHz, $CDCl_3$) δ -115.12.

***N*-benzyl-2-nitro-*N*-(4-(trifluoromethyl)benzyl)aniline (3.11d-SM):**

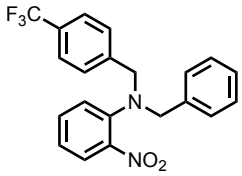

Following a modification of the general procedure using *N*-benzyl-1-(4-(trifluoromethyl)phenyl)methanamine (2.12 g, 8.00 mmol) was added dropwise to 1-fluoro-2-nitrobenzene (0.56 mL, 5.33 mmol) at rt. The crude product was purified by column chromatography on silica gel by hexane/DCM to yield product as an orange oil (313 mg, 15%). ^{1}H NMR (500 MHz, $CDCl_3$) δ 7.74 (dd, *J* = 8.1, 1.6 Hz, 1H), 7.54 (d, *J* = 8.0 Hz, 2H), 7.41 – 7.34 (m, 3H), 7.34 – 7.17 (m, 5H), 7.12 – 7.01 (m, 2H), 4.25 (s, 2H), 4.20 (s, 2H). ^{13}C NMR (126 MHz, $CDCl_3$) δ 144.75, 144.40, 141.47, 136.75, 132.92, 129.68, 128.70, 128.57, 127.77, 125.80, 125.62, 125.59, 125.56, 125.53, 123.65, 122.51, 57.55, 56.19. ^{19}F NMR (471 MHz, $CDCl_3$) δ -62.49.

Methyl 4-((benzyl(2-nitrophenyl)amino)methyl)benzoate (3.11e-SM):

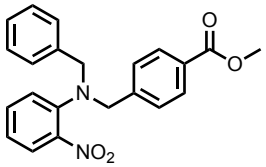

Following a modification of the general procedure using methyl 4-((benzylamino)methyl)benzoate (1.50 g, 5.87 mmol) was added dropwise to 1-fluoro-2-nitrobenzene (0.41 mL, 3.92 mmol) at rt. The crude product was purified by column chromatography on silica gel by hexane/DCM to yield product as an orange oil (324 mg, 21%). ^{1}H NMR (500 MHz, $CDCl_3$) δ 8.07 – 7.87 (m, 2H), 7.73 (dd, *J* = 8.1, 1.6 Hz, 1H), 7.36 (ddd, *J* = 8.6, 7.3, 1.6 Hz, 1H), 7.22 – 7.17 (m, 2H), 7.07 (dd, *J* = 8.4, 1.2 Hz, 1H), 7.03 (td, *J* = 7.7, 1.2 Hz, 1H), 4.22 (d, *J* = 24.4 Hz, 4H), 3.89 (s, 3H). ^{13}C NMR (126 MHz, $CDCl_3$) δ 142.62, 136.84, 132.89, 130.64, 129.93, 129.46, 128.67, 128.59, 128.45, 127.73, 125.81, 123.64, 122.30, 57.52, 56.32, 52.23.

_N_-benzyl-2-nitro-_N_-(phenylmethyl-_d_$_2$)aniline (3.13-SM):

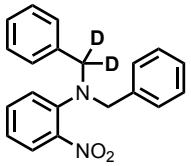

Following a modification of the general procedure using *N*-benzyl-1-phenylmethan-*d*2-amine (3.00 g, 15.1 mmol) was added dropwise to 1-fluoro-2-nitrobenzene (0.79 mL, 7.52 mmol) at rt. The crude product was purified by column chromatography on silica gel by hexane/DCM to yield product as an orange oil (555 mg, 23%). ^{1}H NMR (600 MHz, $CDCl_3$) δ 7.74 (dd, *J* = 8.2, 1.7 Hz, 1H), 7.38 – 7.32 (m, 1H), 7.31 – 7.20 (m, 9H), 7.07 (dd, *J* = 8.3, 1.3 Hz, 1H), 6.99 (ddd, *J* = 8.4, 7.3, 1.2 Hz, 1H), 4.21 (s, 2H). ^{13}C NMR (101 MHz, $CDCl_3$) δ 144.88, 144.23, 137.22, 137.07, 132.82, 128.57, 128.55, 128.52, 127.55, 127.52, 125.83, 123.51, 121.67, 108.03, 56.72.

IV. Synthetic Examples.

A. General Procedure

General method E: The nitrocompound (0.50 mmol, 1.0 equiv) and phosphetane oxide (0.10 mmol, 0.20 equiv) were weighed into an oven-dried 4-mL vial charged with stirring bar. The thread was lined with teflon tape and the vial was then purged with N_2. Next dry benzonitrile (1.0 mL, 0.5 M) was added, followed by phenylsilane (154 µL, 1.25 mmol, 2.5 eq) and DBU (75 µL, 0.50 mmol, 1.0 equiv). The reactions were then heated and stirred overnight at 100°C. The intermediate dihydrobenzimidazole was then oxidized by bubbling air through the solution for 1 h at

100°C. After cooling, ammonium fluoride in methanol was added to degrade the silanes. This mixture was stirred for 1 h after which the reaction was filtered over a silica plug and rinsed with EtOAc, concentrated in vacuo and purified by column.

General method F: The nitrocompound (0.50 mmol, 1.0 eq) and phosphetane oxide (0.10 mmol, 0.20 eq) were weighed into an oven-dried 4-mL vial charged with stirring bar. The thread was lined with teflon tape and the vial was then purged with N_2. Next dry benzonitrile (1.0 mL, 0.5 M) was added, followed by phenylsilane (154 µL, 1.25 mmol, 2.5 equiv) and DBU (75 µL, 0.50 mmol, 1.0 equiv). The reactions were then heated and stirred overnight at 100°C. After cooling, a 1M aqueous solution of NaOH was added to degrade the silanes. This mixture was stirred for 1 h after which the reaction was extracted 3x with EtOAc and 2x with DCM, the combined organic layers were dried over $MgSO_4$, concentrated in vacuo and purified by column.

B. Analytical Data

1-benzyl-2-phenyl-1H-benzo[d]imidazole (2.4):

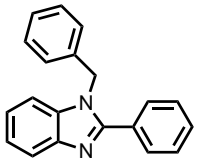

Prepared according to general method **E** using *N*,*N*-dibenzyl-2-nitroaniline (159 mg, 0.50 mmol). The crude product was purified by column chromatography on silica gel (Hex/EtOAc = 4.2:1.8) to yield product as a white solid (123 mg, 87%). ^{1}H NMR (400 MHz, Chloroform-*d*) δ 7.90 (d, *J* = 8.0 Hz, 1H), 7.76 – 7.68 (m, 2H), 7.56 – 7.43 (m, 3H), 7.40 – 7.30 (m, 4H), 7.31 – 7.21 (m, 2H), 7.17 – 7.08 (m, 2H), 5.49 (s, 2H). Spectral data is consistent with literature characterization.[13]

1-(4-methylbenzyl)-2-(p-tolyl)-benzo[d]imidazole (2.5):

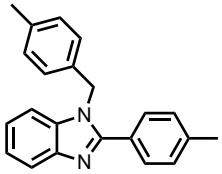

Prepared according to general method **E** using *N*,*N*-bis(4-methylbenzyl)-2-nitroaniline (173 mg, 0.50 mmol). The crude product was purified by column chromatography on silica gel (Hex/EtOAc = 4.2:1.8) to yield product as a white solid (139 mg, 89%). ^{1}H NMR (400 MHz, Chloroform-*d*) δ 7.89 (d, *J* = 8.0 Hz, 1H), 7.62 (d, *J* = 8.0 Hz, 2H), 7.18-7.33 (m, 5H), 7.15 (d, *J* = 8.0 Hz, 2H), 7.01

(d, *J* = 8.0 Hz, 2H), 5.43 (s, 2H), 2.43 (s, 3H), 2.36 (s, 3H). Spectral data is consistent with literature characterization.[13]

1-(4-methoxybenzyl)-2-(4-methoxyphenyl)-benzo[d]imidazole (2.6):

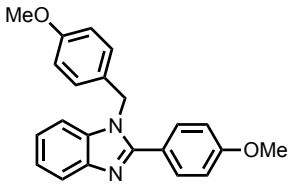

Prepared according to general method **E** using *N*,*N*-bis(4-methoxybenzyl)-2-nitroaniline (189 mg, 0.50 mmol). The crude product was purified by column chromatography on silica gel (Hex/EtOAc = 7:3) to yield product as a white solid (164 mg, 95%). ^{1}H NMR (500 MHz, Chloroform-*d*) δ 7.87 (d, *J* = 8.2 Hz, 1H), 7.71 – 7.58 (m, 2H), 7.31 (ddd, *J* = 8.1, 5.5, 2.9 Hz, 1H), 7.26 – 7.21 (m, 2H), 7.05 (d, *J* = 8.6 Hz, 2H), 6.99 (d, *J* = 8.8 Hz, 2H), 6.93 – 6.82 (m, 2H), 5.40 (s, 2H), 3.86 (s, 3H), 3.80 (s, 3H). Spectral data is consistent with literature characterization.[13]

1-(4-fluorobenzyl)-2-(4-fluorophenyl)-1H-benzo[d]imidazole (2.7):

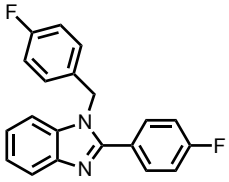

Prepared according to general method **E** using *N*,*N*-bis(4-fluorobenzyl)-2-nitroaniline (177 mg, 0.50 mmol). The crude product was purified by column chromatography on silica gel (Hex/EtOAc = 4.2:1.8) to yield product as a white solid (120 mg, 74%). ^{1}H NMR (400 MHz, Chloroform-*d*) δ 7.86 (d, *J* = 8.0 Hz, 1H), 7.68-7.58 (m, 2H), 7.36-7.08 (m, 5H), 7.07-6.93 (m, 4H), 5.39 (s, 2H). ^{13}C{^{1}H} NMR (101 MHz, $CDCl_3$) δ 165.09, 163.60, 162.60, 161.14, 153.16, 143.15, 135.98, 132.05, 131.34, 127.76, 126.27, 123.38, 123.00, 120.16, 116.31, 116.20, 116.09, 115.99, 110.42, 47.78.^{19}F NMR (565 MHz, $CDCl_3$) δ -110.02, -114.06.

1-(4-(trifluoromethyl)benzyl)-2-(4-(trifluoromethyl)phenyl)-1H-benzo[d]imidazole (2.8):

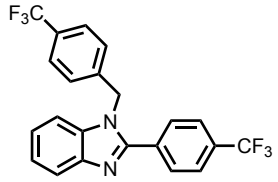

Prepared according to general method **E** using 2-nitro-*N*,*N*-bis(4-(trifluoromethyl)benzyl)aniline (227 mg, 0.50 mmol). The crude product was purified by column chromatography on silica gel

(Hex/EtOAc = 4.2:1.8) to yield product as a white solid (185 mg, 88%). ^{1}H NMR (400 MHz, Chloroform-*d*) δ 7.91 (d, *J* = 8.0 Hz, 1H), 7.78 (d, *J* = 8.0 Hz, 2H), 7.73 (d, *J* = 8.0 Hz, 2H), 7.62 (d, *J* = 8.0 Hz, 2H), 7.37 (t, *J* = 8.0 Hz, 1H), 7.31 (t, *J* = 8.0 Hz, 1H), 7.21 (t, *J* = 8.0 Hz, 3H), 5.52 (s, 2H). ^{13}C{^{1}H} NMR (101 MHz, $CDCl_3$) δ 152.54, 143.29, 140.15, 136.08, 133.48, 132.27, 132.01, 130.78, 130.52, 129.67, 126.44, 126.41, 126.33, 126.05, 126.02, 125.03, 124.08, 123.52, 122.87, 120.65, 110.44, 48.18. ^{19}F NMR (565 MHz, $CDCl_3$) δ -62.67, -62.90.

3-benzyl-2-phenyl-3*H*-imidazo[4,5-*b*]pyridine (2.9):

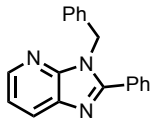

Prepared according to general method **E** using *N*,*N*-dibenzyl-3-nitropyridin-2-amine (160 mg, 0.50 mmol). The crude product was purified by column chromatography on silica gel (Hex/EtOAc = 4:1) to yield product as a white solid (141 mg, 98%). ^{1}H NMR (500 MHz, Chloroform-*d*) δ 8.42 (dd, *J* = 3.4 Hz, 1.4 Hz, 1H), 8.12 (dd, *J* = 6.5 Hz, 1.3 Hz, 1H), 7.73 – 7.60 (m, 2H), 7.55 – 7.40 (m, 3H), 7.34 – 7.21 (m, 4H), 7.16 – 7.04 (m, 2H), 5.62 (s, 2H). Spectral data is consistent with literature characterization.[14]

1-methyl-1H-benzo[d]imidazole (2.10):

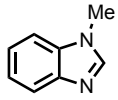

Prepared according to general method **E** using *N*,*N*-dimethyl-2-nitroaniline (83 mg, 0.50 mmol). The crude product was purified by column chromatography on silica gel (EtOAc) to yield product as a brown liquid (52 mg, 79%). ^{1}H NMR (500 MHz, Chloroform-*d*) δ 7.79 (m, 2H), 7.36 (m, 1H), 7.28 (m, 2H), 3.79 (s, 3H). Spectral data is consistent with literature characterization.[6]

1-propyl-2-ethyl-1H-benzo[d]imidazole (2.11):

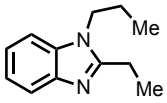

Prepared according to general method **E** using 2-nitro-*N*,*N*-dipropylaniline (111 mg, 0.50 mmol). The crude product was purified by column chromatography on silica gel (EtOAc) to yield product as a brown oil (73 mg, 81%). ^{1}H NMR (500 MHz, Chloroform-*d*) δ 7.72 (dt, *J* = 8 Hz, 3Hz, 1H), 7.29-7.24 (m, 1H), 7.23-7.17 (m, 2H), 4.02 (t, *J* = 7 Hz, 2H), 2.86 (q, *J* = 8 Hz, 2H), 1.80 (h, *J* = 7

Hz, 2H), 1.45 (t, *J* = 8 Hz, 2H), 0.94 (h, *J* = 8 Hz, 3H). Spectral data is consistent with literature characterization.[6]

1-butyl-2-propyl-1H-benzo[d]imidazole (2.12):

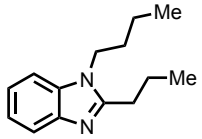

Prepared according to general method **E** using *N*,*N*-dibutyl-2-nitroaniline (125 mg, 0.50 mmol). The crude product was purified by column chromatography on silica gel (EtOAc) to yield product as a brown oil (67 mg, 62%). ^{1}H NMR (500 MHz, Chloroform-*d*) δ 7.72 (m, 1H), 7.31-7.26 (m, 1H), 7.23-7.18 (m, 2H), 4.08 (t, *J* = 8 Hz, 2H), 2.83 (t, *J* = 8 Hz, 2H), 1.93 (h, *J* = 1 Hz, 2H), 1.77 (m, 2H), 1.39 (h, *J* = 1 Hz, 2H), 1.07 (t, *J* = 2 Hz, 3H), 0.96 (t, *J* = 2 Hz, 3H). Spectral data is consistent with literature characterization.[6]

1,2,3,4-tetrahydrobenzo[4,5]imidazo[1,2-a]pyridine (2.13):

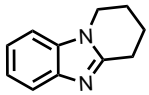

Prepared according to general method **E** using 1-(2-nitrophenyl)piperidine (103 mg, 0.50 mmol). The crude product was purified by column chromatography on silica gel (EtOAc) to yield product as a brown solid (68 mg, 77%). ^{1}H NMR (400 MHz, Chloroform-*d*) δ 7.72 – 7.61 (m, 1H), 7.35 – 7.12 (m, 3H), 4.04 (t, *J* = 6.0 Hz, 2H), 3.08 (t, *J* = 6.4 Hz, 2H), 2.23 – 2.08 (m, 2H), 2.01 (ddp, *J* = 9.3, 6.2, 3.4, 3.0 Hz, 2H). Spectral data is consistent with literature characterization.[6]

6,7,8,9-tetrahydroimidazo[1,2-*a*:5,4-*b'*]dipyridine (2.14):

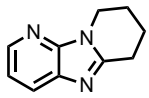

Prepared according to general method **E** using 3-nitro-2-(piperidin-1-yl)pyridine (103 mg, 0.50 mmol). The crude product was purified by column chromatography on silica gel (Hex/EtOAc = 4:1) to yield product as a white solid (32 mg, 41%). ^{1}H NMR (500 MHz, Chloroform-*d*) δ 7.78 (dd, *J* = 3.2 Hz, 1.6 Hz, 1H), 6.91 (dd, *J* = 7.9 Hz, 1.6 Hz, 1H), 6.84-6.75 (m, 1H), 3.80 (s, 2H), 1.77-1.65 (m, 4H), 1.64-1.54 (m, 2H). Spectral data is consistent with literature characterization.[15]

2,3-dihydro-1H-benzo[d]pyrrolo[1,2-a]imidazole (2.15):

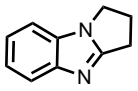

Prepared according to general method **E** using 1-(2-nitrophenyl)pyrrolidine (96 mg, 0.50 mmol). The crude product was purified by column chromatography on silica gel (EtOAc) to yield product as a brown solid (68 mg, 86%). ^{1}H NMR (400 MHz, Chloroform-*d*) δ 7.72-7.66 (m, 1H), 7.32-7.24 (m, 2H), 7.23-7.13 (m, 2H), 4.09 (t, *J* = 6.4 Hz, 2H), 3.05 (t, *J* = 6.4 Hz, 2H), 2.70 (q, *J* = 6.4 Hz, 2H). Spectral data is consistent with literature characterization.[6]

7,8,9,10-tetrahydro-6H-benzo[4,5]imidazo[1,2-a]azepine (2.16):

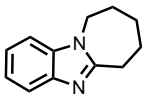

Prepared according to general method **E** using 1-(2-nitrophenyl)azepane (110 mg, 0.50 mmol). The crude product was purified by column chromatography on silica gel (EtOAc) to yield product as a brown solid (83 mg, 89%). ^{1}H NMR (400 MHz, Chloroform-*d*) δ 7.71-7.63 (m, 1H), 7.31-7.15 (m, 3H), 4.02-4.06 (m, 2H), 3.19-3.00 (m, 2H), 2.01-1.88 (m, 2H), 2.01-1.88 (m, 2H), 1.87-1.67 (m, 4H). Spectral data is consistent with literature characterization.[6]

1-phenyl-1*H*-benzo[*d*]imidazole (2.17):

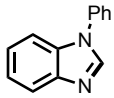

Prepared according to general method **E** using *N*-methyl-2-nitro-*N*-phenylaniline (114 mg, 0.50 mmol). The crude product was purified by column chromatography on silica gel (Hex/EtOAc = 4:1) to yield product as a white solid (68 mg, 70%). ^{1}H NMR (400 MHz, Chloroform-*d*) δ 8.10 (s, 1H), 7.93-7.82 (m, 1H), 7.60-7.41 (m, 6H), 7.38-7.27 (m, 2H). Spectral data is consistent with literature characterization.[16]

1-methyl-2-phenyl-1*H*-benzo[*d*]imidazole (2.19):

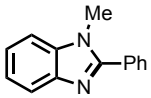

Prepared according to general method **E** using *N*-benzyl-*N*-methyl-2-nitroaniline (121 mg, 0.50 mmol). The crude product was purified by column chromatography on silica gel (Hex/EtOAc = 4:1) to yield product as a white solid (74.9 mg, 72%). ^{1}H NMR (400 MHz, Chloroform-*d*) δ 7.87-7.80 (m, 1H), 7.79-7.72 (m, 2H), 7.57-7.46 (m, 3H), 7.43-7.36 (m, 1H), 7.36-7.27 (m, 2H), 3.83 (s, 3H). Spectral data is consistent with literature characterization.[17]

1-benzyl-1*H*-benzo[*d*]imidazole (2.20):

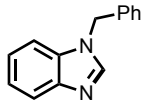

Prepared according to general method **E** using *N*-benzyl-*N*-methyl-2-nitroaniline (121 mg, 0.50 mmol). The crude product was purified by column chromatography on silica gel (EtOAc) to yield product as a white solid (9.37 mg, 9%). ^{1}H NMR (400 MHz, Chloroform-*d*) δ 7.98 (s, 1H), 7.88-7.79 (m, 1H), 7.38-7.32 (m, 6H), 7.22-7.15 (m, 2H), 5.37 (s, 2H). Spectral data is consistent with literature characterization.[18]

3,4-dihydro-1H-benzo[4,5]imidazo[2,1-c][1,4]oxazine (2.21):

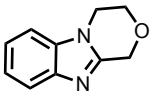

Prepared according to general method **E** using 4-(2-nitrophenyl)morpholine (104 mg, 0.50 mmol). The crude product was purified by column chromatography on silica gel (EtOAc) to yield product as a brown oil (64 mg, 73%). ^{1}H NMR (400 MHz, Chloroform-*d*) δ 7.77-7.69 (m, 1H), 7.38-7.26 (m, 3H), 4.02-4.06 (m, 2H), 5.10-5.00 (s, 2H), 4.26-4.11 (m, 4H). Spectral data is consistent with literature characterization.[6]

1,2-diphenyl-1H-benzo[d]imidazole (2.24):

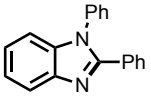

Prepared according to general method **E** using *N*-benzyl-2-nitro-*N*-phenylaniline (152 mg, 0.50 mmol). The crude product was purified by column chromatography on silica gel (EtOAc) to yield product as a brown oil (70 mg, 50%). ^{1}H NMR (400 MHz, Chloroform-*d*) δ 7.90 (d, *J* = 7.9 Hz, 1H) 7.61-7.54 (m, 2H), 7.54-7.43 (m, 3H), 7.40-7.21 (m, 8H). Spectral data is consistent with literature characterization.[19]

5-tosyl-1,2,3,4,4a,5-hexahydrobenzo[4,5]imidazo[1,2-a]pyridine (2.28):

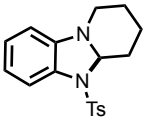

Prepared according to general method **F** using using 1-(2-nitrophenyl)piperidine (103 mg, 0.50 mmol). The crude product was purified by column chromatography on silica gel (Hex/EtOAc = 99:1) to yield product as a white solid (20.8 mg, 25%). ^{1}H NMR (400 MHz, Chloroform-*d*) δ 7.58 (d, *J* = 8.1 Hz, 2H), 7.47 (d, *J* = 7.7 Hz, 1H), 7.17 (d, *J* = 8.0 Hz, 2H), 6.94 (t, *J* = 7.7 Hz, 1H),

6.65 (t, *J* = 7.7 Hz, 1H), 6.26 (d, *J* = 7.7 Hz, 1H), 5.16 (dd, *J* = 10.4, 3.7 Hz, 1H), 3.50 (ddt, *J* = 14.2, 4.2, 1.9 Hz, 1H), 2.83 (ddd, *J* = 14.6, 12.3, 3.5 Hz, 1H), 2.36 (s, 3H), 1.91 (dddd, *J* = 25.4, 12.4, 6.6, 3.3 Hz, 2H), 1.75 (tdd, *J* = 13.1, 10.2, 3.5 Hz, 1H), 1.63 – 1.35 (m, 3H). ^{13}C NMR (101 MHz, $CDCl_3$) δ 143.86, 142.44, 134.65, 130.46, 129.44, 127.22, 125.91, 117.34, 117.31, 105.75, 79.63, 43.55, 31.01, 22.89, 22.60, 21.58. HRMS(ESI$^+$) calcd. for $C_{18}H_{21}N_2O_2S$ $[M+H]^+$ 329.1318, found 329.1324. IR (neat) ν 3055, 2939, 2857, 1597, 1482, 1352, 1165, 1092, 739, 665, 572 cm^{-1}.

C. X-ray Data for N-Tosyl-benzimidazolines

5-tosyl-1,2,3,4,4a,5-hexahydrobenzo[4,5]imidazo[1,2-a]pyridine

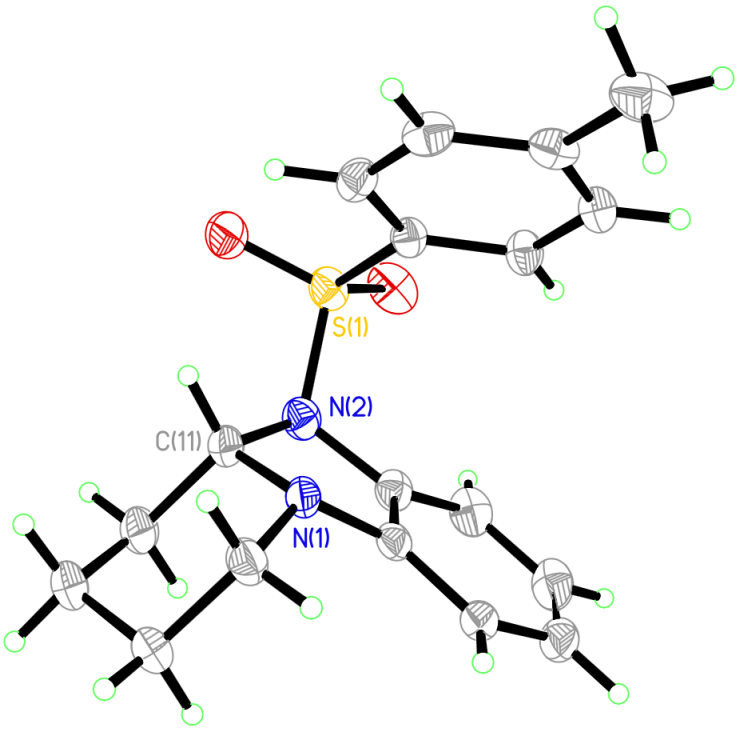

Crystal Data and Structure Refinement Information

Identification code	5-tosyl-1,2,3,4,4a,5-hexahydrobenzo[4,5]imidazo[1,2-a]pyridine
Empirical formula	C18H20N2O2S
Formula weight	328.42
Temperature	100.0 K
Wavelength	0.71073 nm
Crystal system	monoclinic
Unit cell dimensions	a = 11.4707(3) Å = 90 °. b = 11.7864(3) Å = 104.8630(9)°. c = 12.4304(3) Å = 90 °.
Volume	1624.34(7) Å3
Z	4
Density (calculated)	1.343 Mg/m3
Absorption coefficient	0.211mm^{-1}
F(000)	696
Theta range for data collection	2.156 to 31.558 °.
Index ranges	$-16 \leq h \leq 16$, $-17 \leq k \leq 17$, $-18 \leq l \leq 18$
Reflections collected	70051
Independent reflections	5441 [Rint = 0.0296]
Completeness to theta = 25.242°	100.0 %
Absorption correction	None
Refinement method	Full-matrix least-squares on F2
Data / restraints / parameters	5441/0/210
Goodness-of-fit on F2	1.046
Final R indices [I>2sigma(I)]	R1 = 0.0339, wR2 = 0.0932
R indices (all data)	R1 = 0.0392, wR2 = 0.0972
Extinction coefficient	n/a
Largest diff. peak and hole	0.383/-0.391 eÅ-3

V. Mechanistic Experiments.

A. In situ NMR experiments

In situ NMR Studies of Catalytic Reaction: To an oven-dried purged septum-sealed NMR tube was added 3.1 (80 mg, 0.25 mmol, 1 equiv), **P1•**[O] (8.7 mg, 0.05 mmol, 20 mol%), dry benzonitrile (0.5 mL), DBU (38 µL, 0.25 mmol, 1.0 equiv), and toluene-d_8 (50 µL). The tube was inserted into the NMR probe thermostatted at 100°C and a t = 0 spectrum was obtained. The tube was ejected from the probe, phenylsilane (77 µL, 0.625 mmol, 2.5 equiv) was added via syringe, and the NMR tube was reinjected into the probe. The appearance of a methine proton (N–CH–N) at δ 5.33 ppm for 3.2 (δ 7.49 ppm) was monitored by ^{1}H NMR spectroscopy at 100°C. ^{31}P NMR spectra was also obtained contemporaneously. Phosphetane **P1•**[O] (δ 55.5 ppm) is consumed within 5 min and replaced by two signals (δ 31.7 and 28.5 ppm).

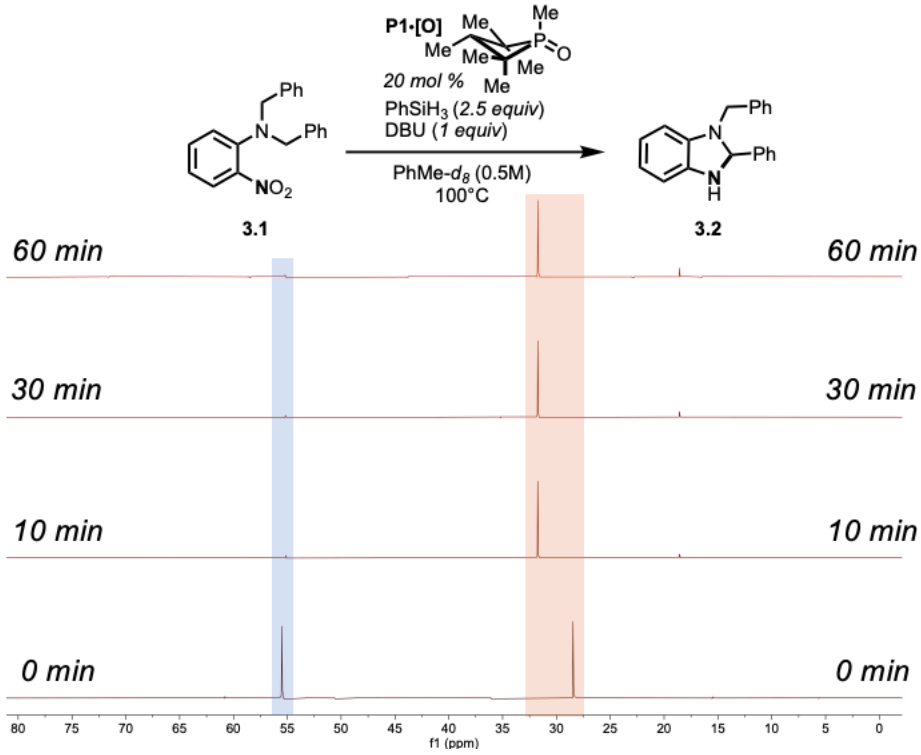

Figure 3.1 (from text)

B. Computational Studies

i. General Computational Information: All calculations were performed using density functional theory (DFT) implemented in Gaussian 09 suite of programs.[11] Geometry optimizations were carried out in the gas phase with DFT Gaussian[12] M06-2X/6-311+G* basis set. Frequency

calculations were conducted at the same level as the geometry optimizations, and thermal free correction terms were found.

ii. DFT Energy Landscape of P III/PV=O redox catalyzed C–N bond forming step

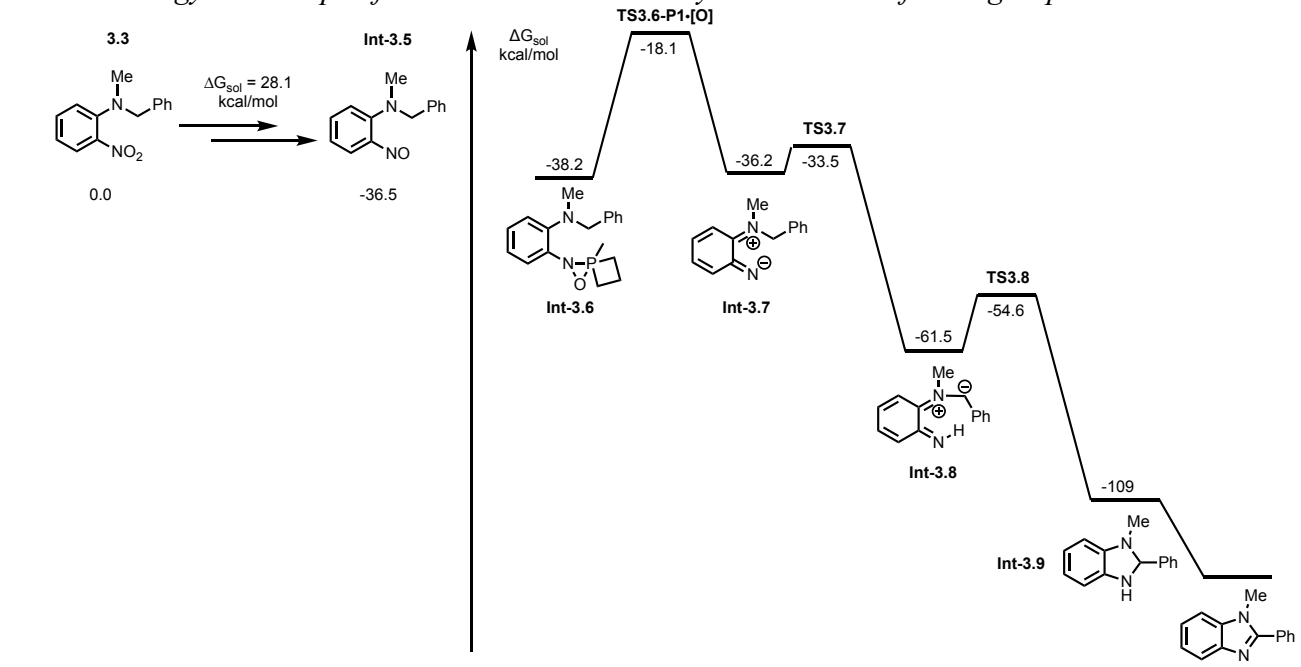

Figure 4.11. Computed reaction profiles from nitroso intermediate **Int-3.5**.

iii. Cartesian Coordinates for Stationary Points

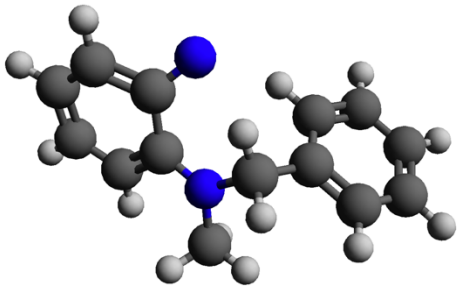

Int. 3.7

Sum of electronic and thermal Free Energies = -650.905340

C	-4.1903660000	-0.5736430000 0.4078910000
C	-3.3656610000	-1.2591370000 -0.4228210000
C	-1.9370880000	-0.9380570000 -0.5857650000
C	-1.5287580000	0.4195580000 -0.0627850000
C	-2.4241970000	1.0818950000 0.8343750000
C	-3.6825020000	0.5913800000 1.0513960000
H	-5.2051990000	-0.8977960000 0.6062170000
H	-3.6664290000	-2.1791910000 -0.9109320000
H	-2.1115340000	1.9678630000 1.3704820000
H	-4.3232830000	1.1250030000 1.7472860000
N	-0.3997010000	1.0081100000 -0.4295190000
N	-1.1363770000	-1.8474880000 -0.9672780000
C	0.6204520000	0.4071690000 -1.3075740000
H	0.8798320000	1.1670830000 -2.0500050000
H	0.1833030000	-0.4652410000 -1.7894160000
C	-0.0451390000	2.3278080000 0.0900840000
H	0.8599780000	2.6639400000 -0.4099830000
H	-0.8461680000	3.0430500000 -0.1010140000
H	0.1586540000	2.2836700000 1.1622910000
C	1.8500660000	0.0085700000 -0.5244490000
C	1.7802130000	-1.0419460000 0.3932070000
C	3.0534950000	0.6893280000 -0.6956780000
C	2.9043040000	-1.3976580000 1.1285490000
H	0.8457880000	-1.5850240000 0.4906090000
C	4.1803000000	0.3304110000 0.0402400000
H	3.1171300000	1.5004720000 -1.4162700000
C	4.1049400000	-0.7119430000 0.9563730000
H	2.8463650000	-2.2199060000 1.8331750000
H	5.1136250000	0.8630700000 -0.1046010000
H	4.9801480000	-0.9937560000 1.5314800000

C. Hammett Correlation Experiments

Catalytic Hammett Studies: The nitrocompound (0.25 mmol, 1.0 equiv), phosphetane oxide **P1•**[O] (8.7 mg, 0.05 mmol, 0.20 equiv), and 1,3,5-trimethoxybenzene (14.0 mg, 0.0832 mmol, 0.33 equiv) were weighed into an oven-dried 4-mL vial charged with stirring bar. The thread was lined with teflon tape, and the vial was then purged with N_2. Dry benzonitrile (0.5 mL, 0.5 M) was added, followed by phenylsilane (77 µL, 0.625 mmol, 2.5 equiv) and DBU (38 µL, 0.25 mmol, 1.0 equiv). The reactions were then heated and stirred overnight at 100°C. The dihydrobenzimidazole was then oxidized by bubbling air through the solution for 1 h at 100°C. After cooling down 0.15 mL of crude reaction mixture was transferred into a NMR tube in addition to 5 mL of chloroform-*d*. In each case complete consumption of starting material was

observed. Spectra were collected and the ratio of the visible benzyl peaks from products was obtained by integration.

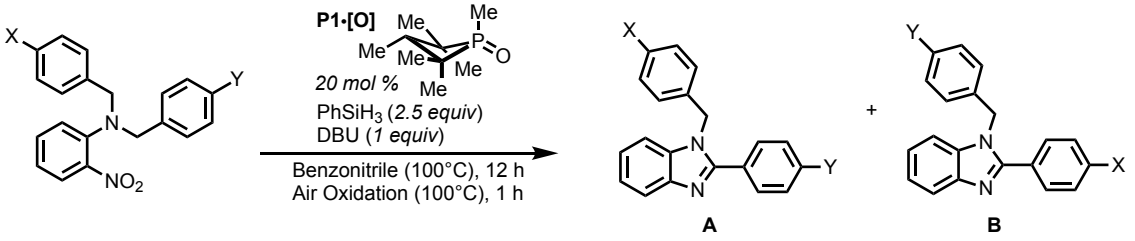

X/Y = (a) OMe/H, (b) Me/CF_3, (c) H/H, (d) F/H, (e) CF_3/H, (f) COOMe/H

Table 4.2: Experimental Hammett Values

-X	σ_p^-	Log(X/Y)
-OMe	-0.26	0.00432137
-Me	-0.17	0.01232124
-F	-0.03	0.05690485
-H	0	0
-CF_3	0.65	0.1430148
-COOMe	0.75	0.24551267

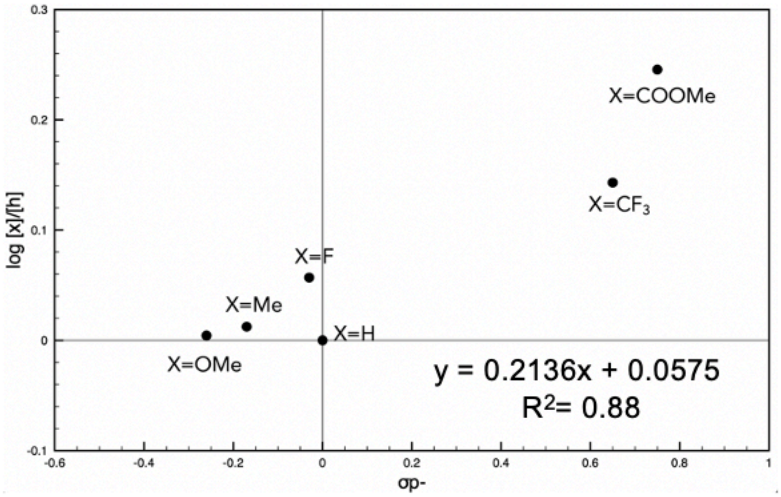

Figure 3.3 (from text).

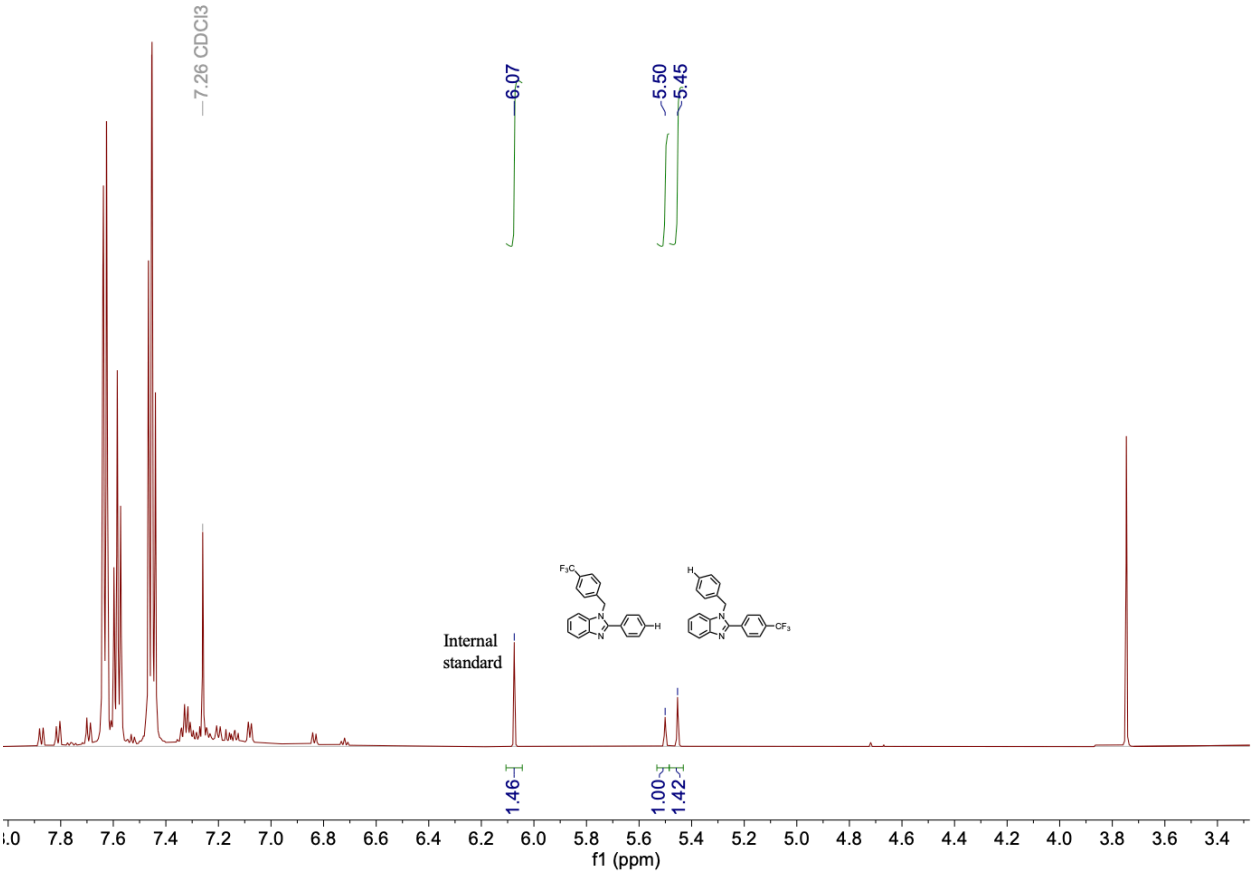

Figure 12.4. Representative ^{1}H NMR spectrum for ratio determination for Hammett correlation experiments of N-benzyl-N-(4-methoxybenzyl)-2-nitroaniline by P**1**•[O].

D. Intramolecular Competition KIE Study

Catalytic KIE Studies: The nitrocompound (0.25 mmol, 1.0 equiv), phosphetane oxide (8.7 mg, 0.05 mmol, 0.20 equiv), and 1,3,5-trimethoxybenzene (14 mg, 0.083 mmol, 0.33 equiv) were weighed into an oven-dried 4-mL vial charged with stirring bar. The thread was lined with teflon tape, and the vial was then purged with N_2. Next dry benzonitrile (0.5 mL, 0.5 M) was added, followed by phenylsilane (77 µL, 0.625 mmol, 2.5 equiv) and DBU (38 µL, 0.25 mmol, 1.0 equiv). The reactions were then heated and stirred overnight at 100°C. The dihydrobenzimidazole was then oxidized by bubbling air through the solution for 1 h at 100°C. After cooling down 0.15 mL of crude reaction mixture was transferred into a NMR tube in addition to 5 mL of chloroform-*d*. In each case complete consumption of starting material was observed. Spectra were collected and the ratio of the visible benzyl peak was integrated against the 4-H aromatic peak from product.

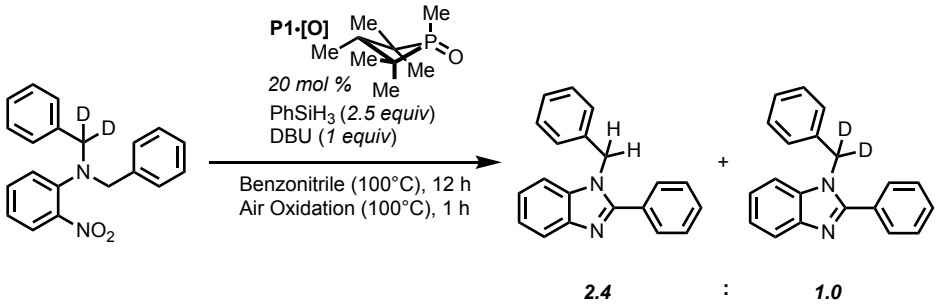

Figure 3.4 (from text).

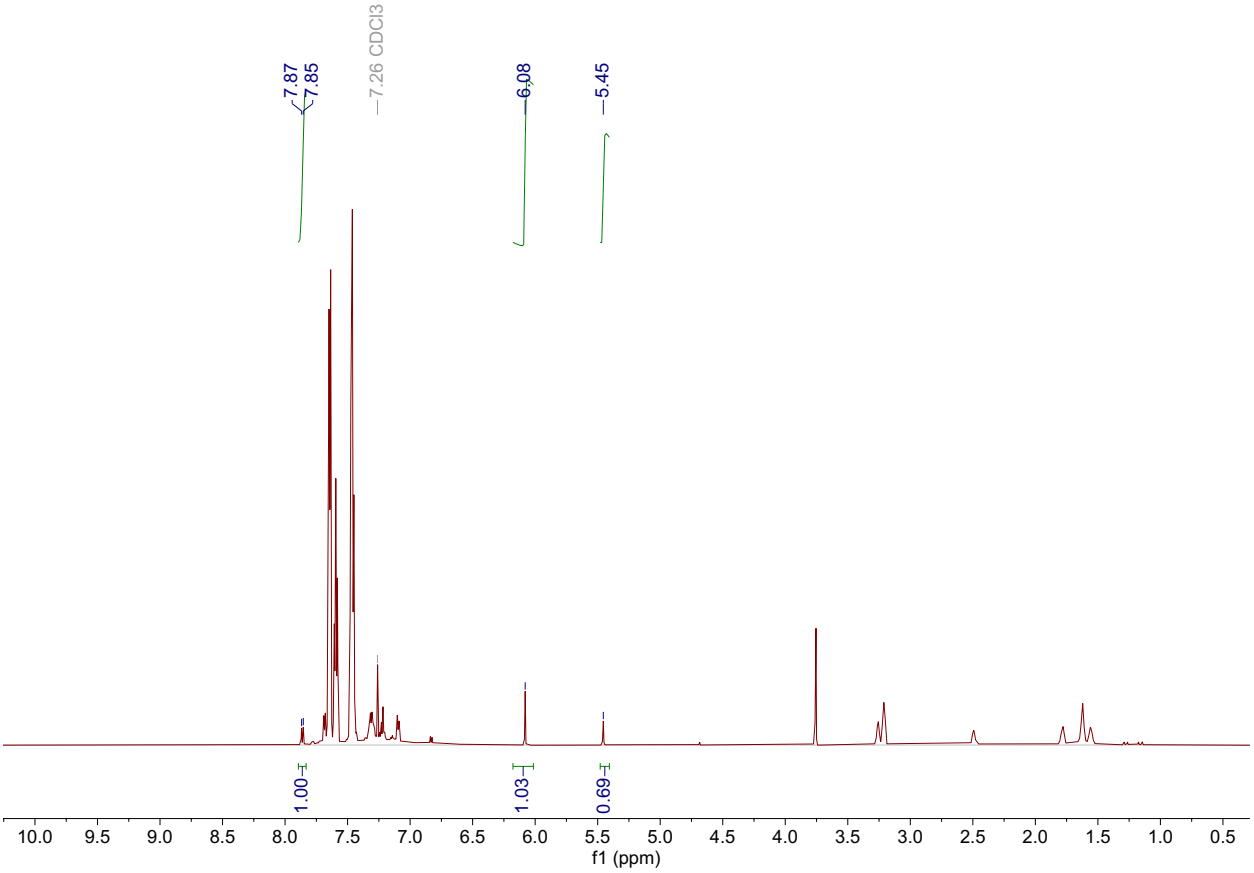

Figure 4.13. Representative ^{1}H NMR spectrum for k_H/k_X ratio determination for Intramolecular Competition KIE experiments of Hammett correlation experiments of *N*-benzyl-2-nitro-*N*-(phenylmethyl-d_2)aniline by **P1•**[O].

VI. Spectral Data

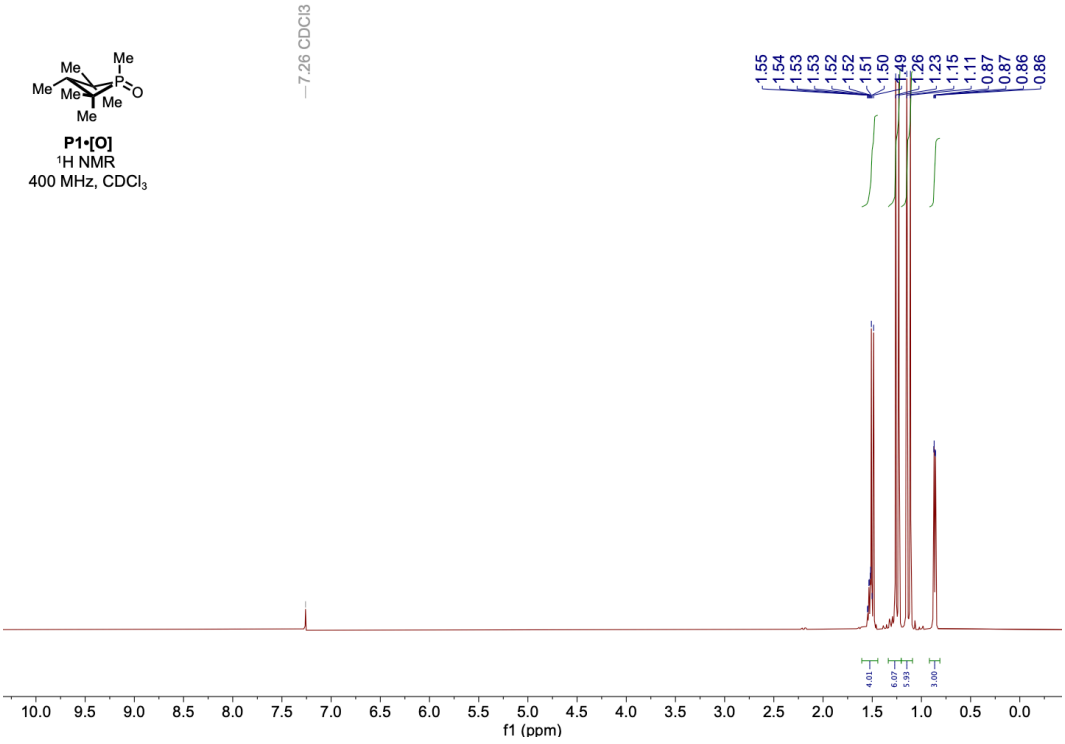

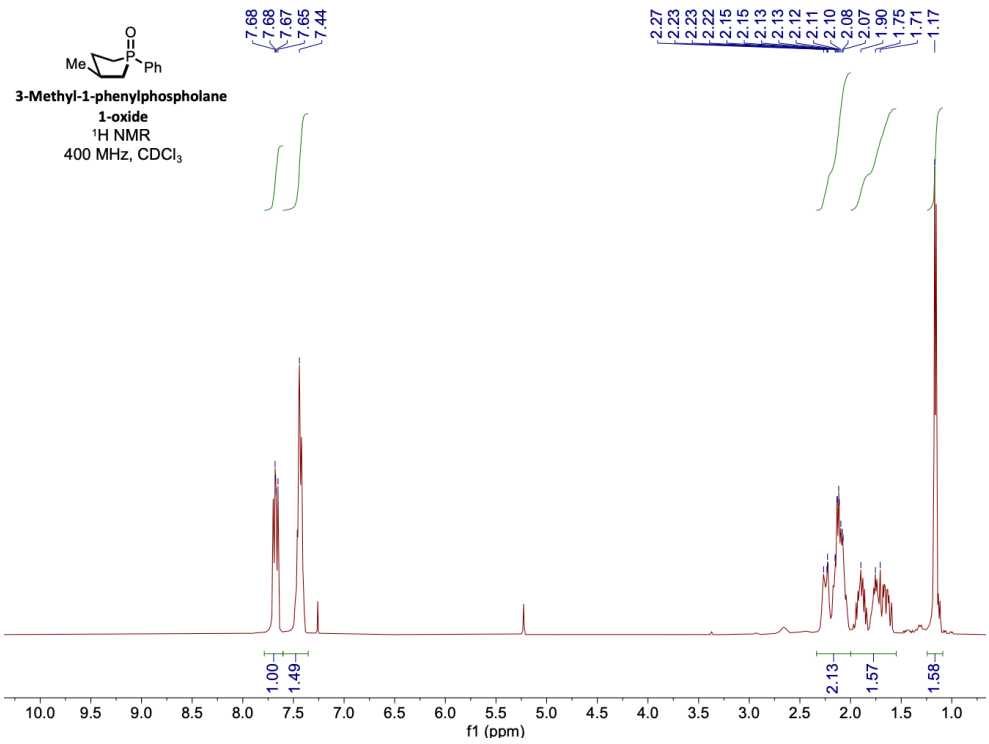

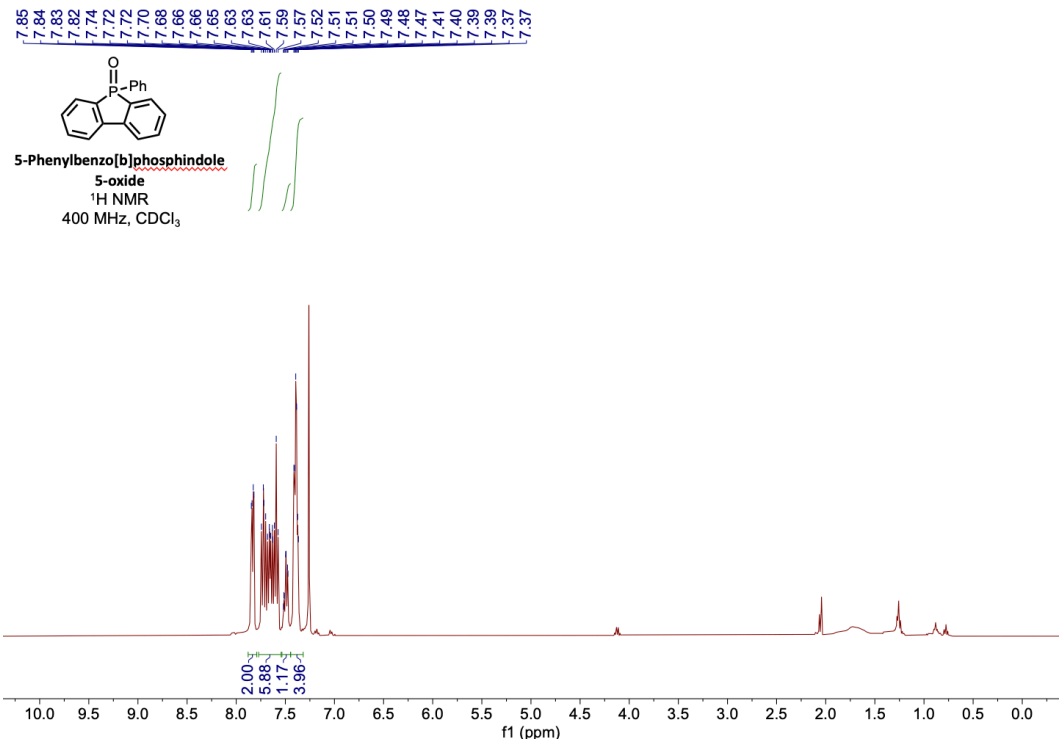
7.85
7.84
7.83
7.82
7.74
7.72
7.72
7.70
7.68
7.66
7.66
7.65
7.63
7.63
7.61
7.59
7.57
7.52
7.51
7.51
7.50
7.49
7.48
7.47
7.41
7.40
7.39
7.39
7.37
7.37
O
P
Ph
5-Phenylbenzo[b]phosphindole
5-oxide
1H NMR
400 MHz, CDCl3
2.00
5.88
1.17
3.96
10.0 9.5 9.0 8.5 8.0 7.5 7.0 6.5 6.0 5.5 5.0 4.5 4.0 3.5 3.0 2.5 2.0 1.5 1.0 0.5 0.0
f1 (ppm)

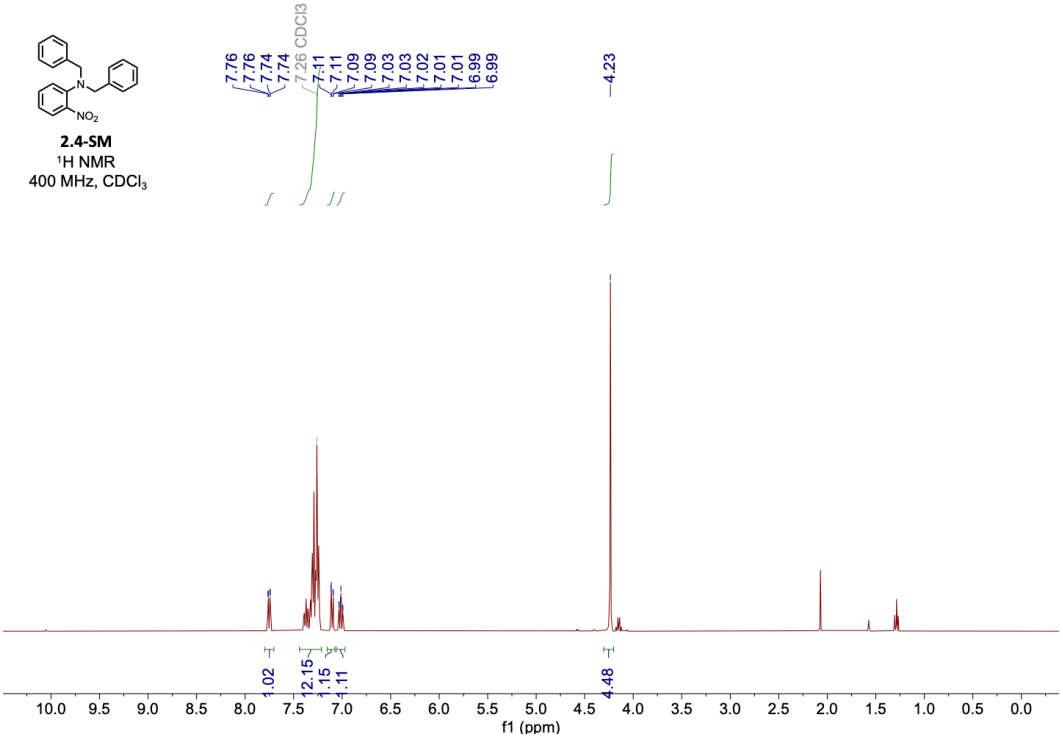
N
NO2
2.4-SM
1H NMR
400 MHz, CDCl3
7.76
7.76
7.74
7.74
7.26 CDCl3
7.11
7.09
7.09
7.03
7.03
7.02
7.01
7.01
6.99
6.99
4.23
1.02
2.15
1.15
1.11
4.48
10.0 9.5 9.0 8.5 8.0 7.5 7.0 6.5 6.0 5.5 5.0 4.5 4.0 3.5 3.0 2.5 2.0 1.5 1.0 0.5 0.0
f1 (ppm)

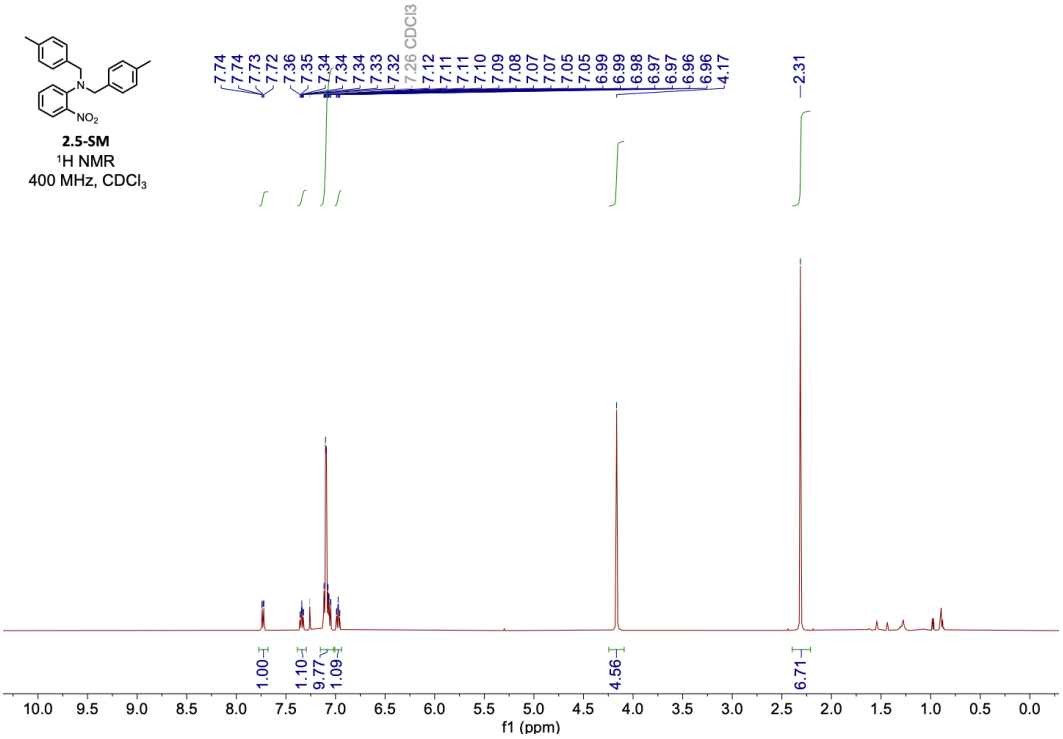
2.5-SM
1H NMR
400 MHz, CDCl3
7.74
7.74
7.73
7.72
7.36
7.35
7.34
7.34
7.34
7.33
7.32
7.26 CDCl3
7.12
7.11
7.11
7.10
7.09
7.08
7.07
7.07
7.05
7.05
6.99
6.99
6.98
6.97
6.96
6.96
4.17
2.31
1.00
1.10
9.77
1.09
4.56
6.71
f1 (ppm)

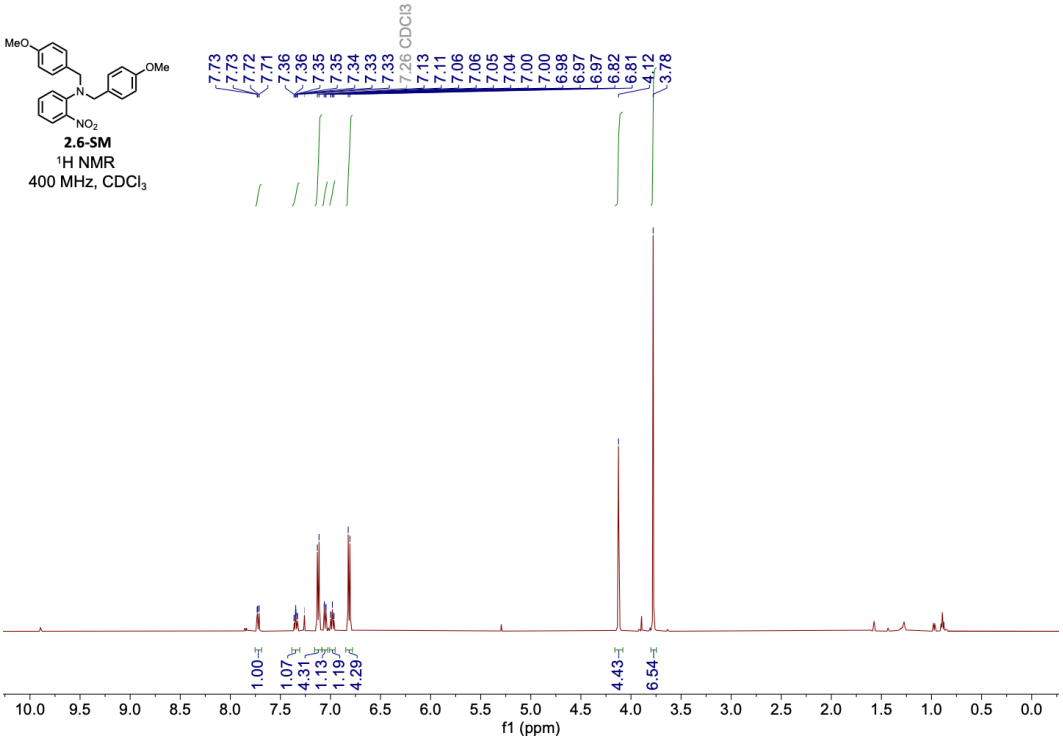
2.6-SM
1H NMR
400 MHz, CDCl3
7.73
7.73
7.72
7.71
7.36
7.36
7.35
7.35
7.34
7.33
7.33
7.26 CDCl3
7.13
7.11
7.06
7.06
7.05
7.04
7.00
7.00
6.98
6.97
6.97
6.82
6.81
4.12
3.78
1.00
1.07
4.31
1.13
1.19
4.29
4.43
6.54
f1 (ppm)

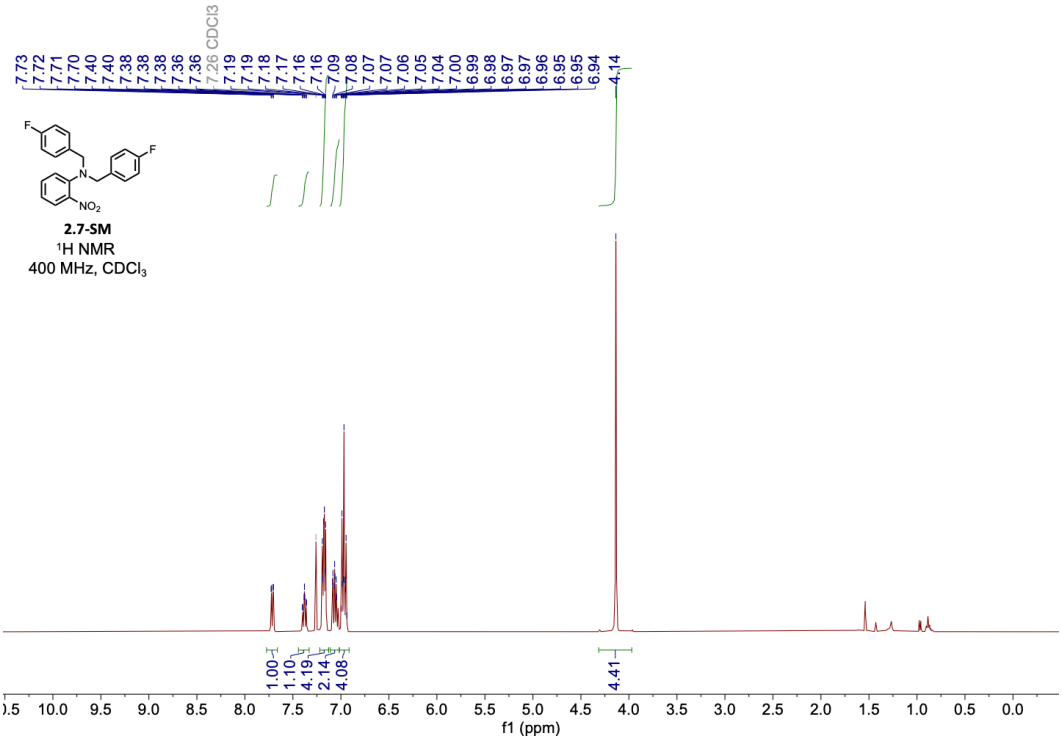
7.73
7.72
7.71
7.70
7.40
7.40
7.38
7.38
7.38
7.36
7.36
7.26 CDCl3
7.19
7.19
7.18
7.17
7.16
7.16
7.09
7.08
7.07
7.07
7.06
7.05
7.04
7.00
6.99
6.98
6.97
6.97
6.96
6.95
6.95
6.94
4.14
F
F
N
NO2
2.7-SM
1H NMR
400 MHz, CDCl3
1.00
1.10
4.19
2.14
4.08
4.41
f1 (ppm)

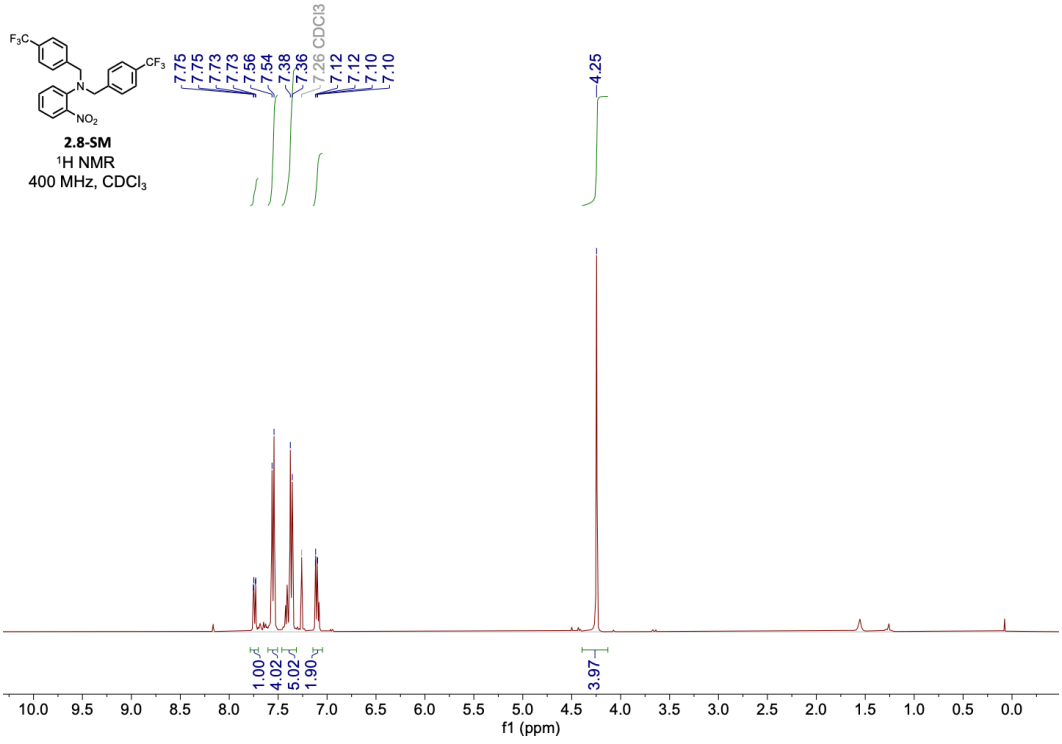
F3C
CF3
N
NO2
2.8-SM
1H NMR
400 MHz, CDCl3
7.75
7.75
7.73
7.73
7.56
7.54
7.38
7.36
7.26 CDCl3
7.12
7.12
7.10
7.10
4.25
1.00
4.02
5.02
1.90
3.97
f1 (ppm)

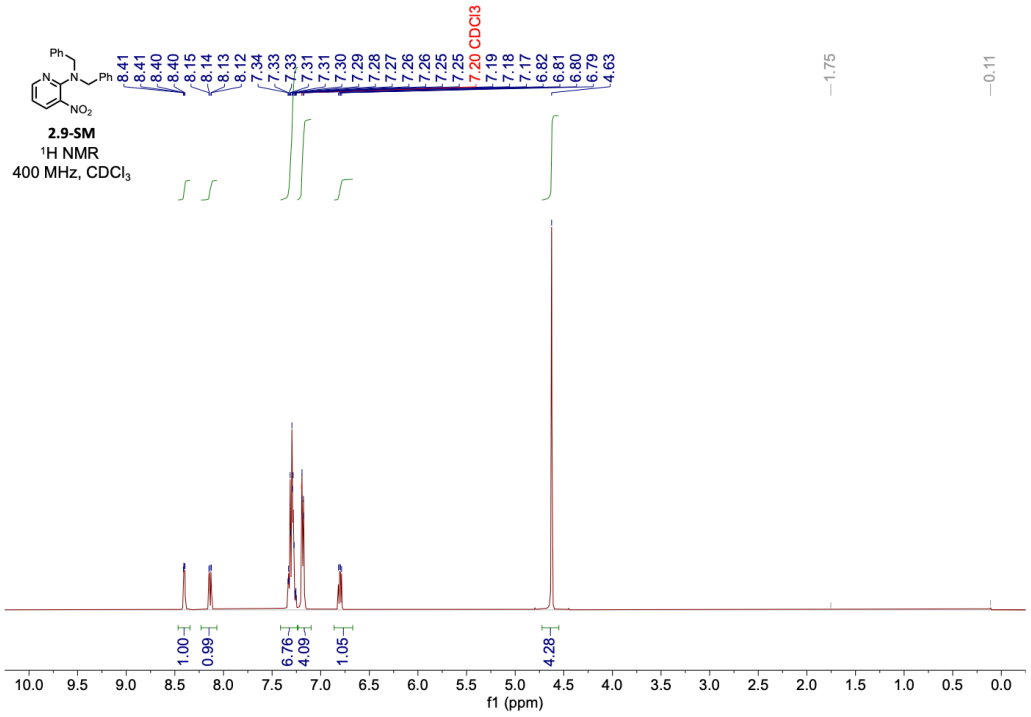
2.9-SM
1H NMR
400 MHz, CDCl3
7.20 CDCl3
f1 (ppm)

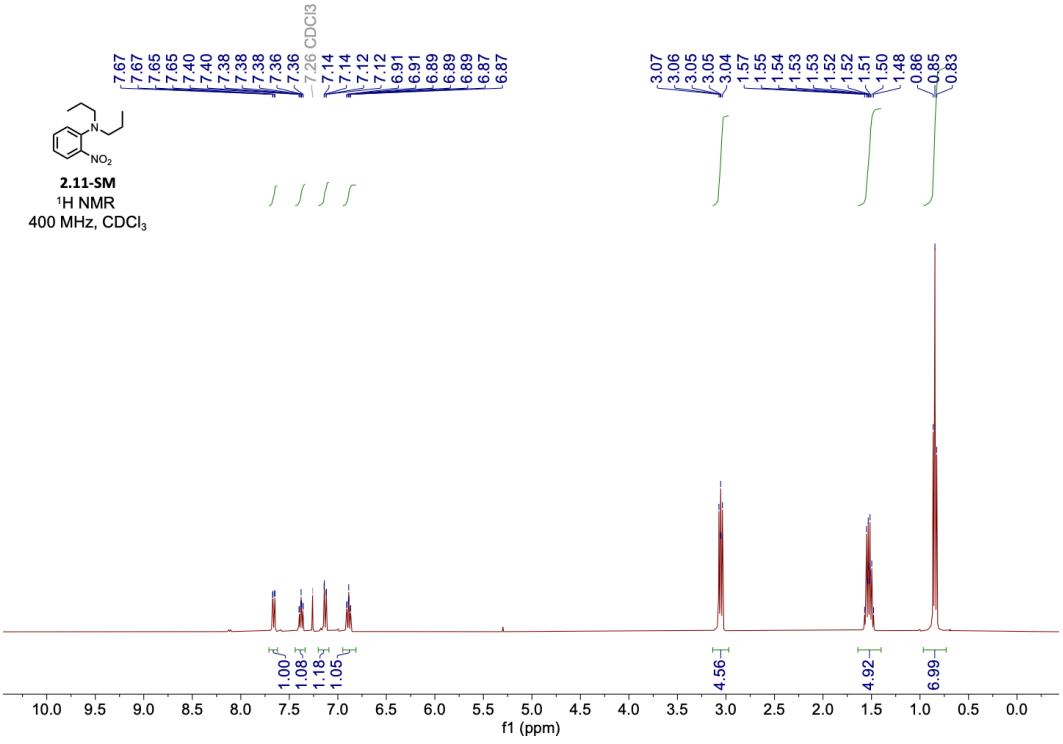
2.11-SM
1H NMR
400 MHz, CDCl3
7.26 CDCl3
f1 (ppm)

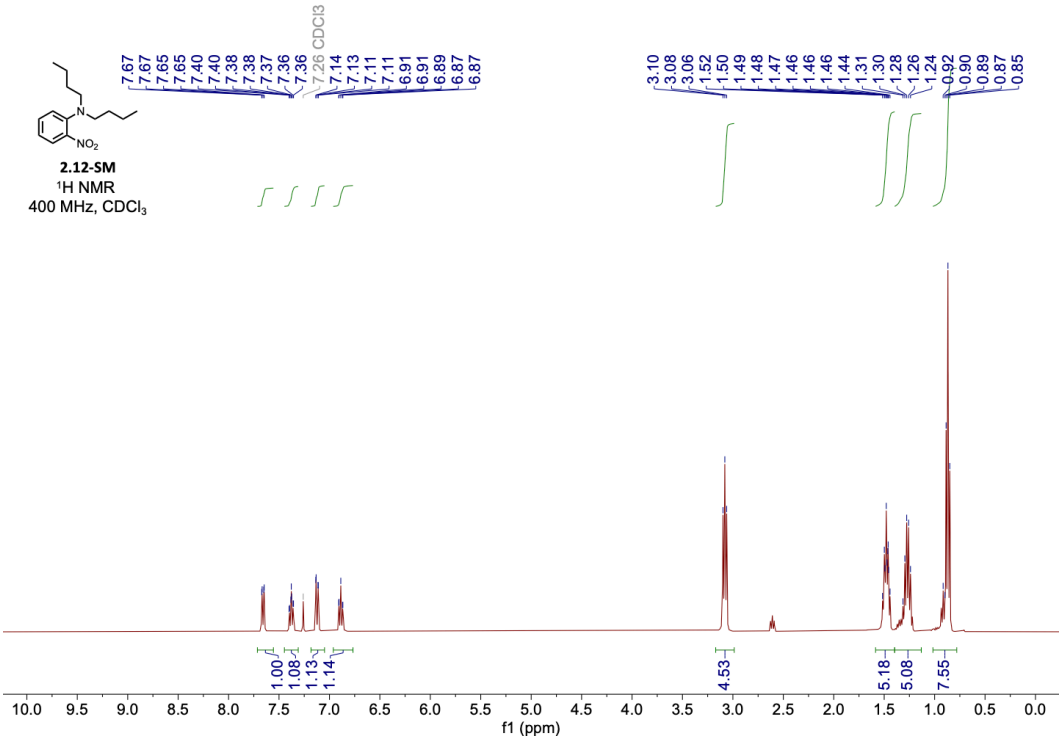
2.12-SM
1H NMR
400 MHz, CDCl3
7.67
7.67
7.65
7.65
7.40
7.40
7.38
7.38
7.37
7.36
7.36
7.26 CDCl3
7.14
7.13
7.11
7.11
6.91
6.89
6.87
6.87
3.10
3.08
3.06
1.52
1.50
1.49
1.48
1.47
1.46
1.46
1.46
1.44
1.31
1.30
1.28
1.26
1.24
0.92
0.90
0.89
0.87
0.85
1.00
1.08
1.13
1.14
4.53
5.18
5.08
7.55
f1 (ppm)

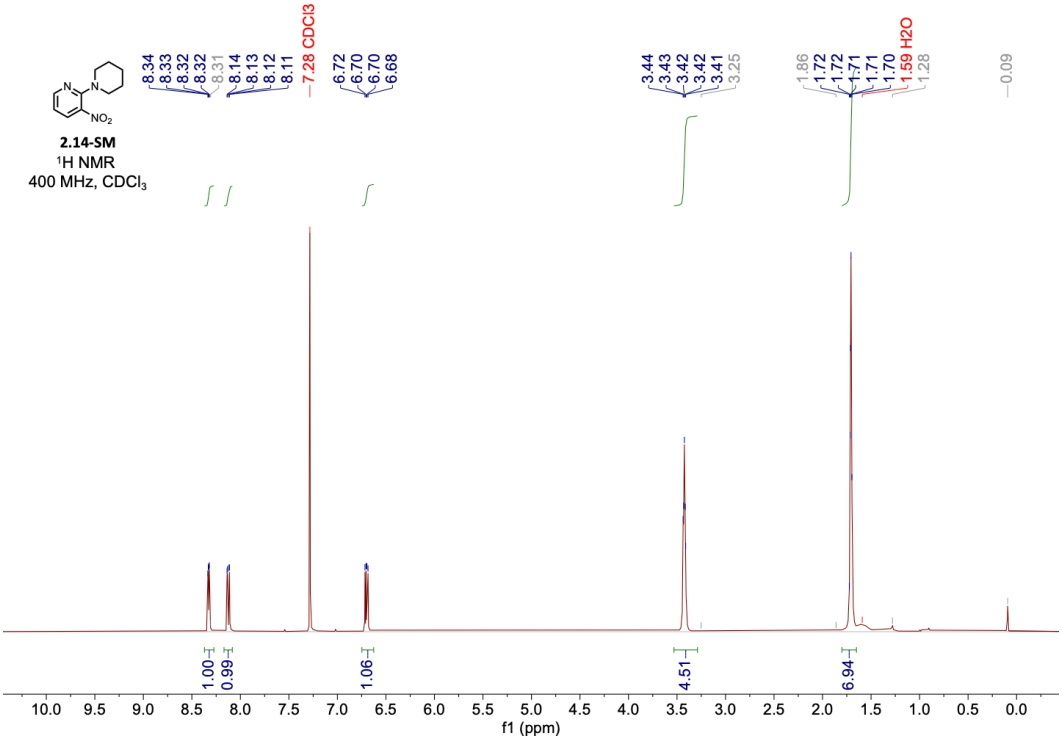
2.14-SM
1H NMR
400 MHz, CDCl3
8.34
8.33
8.32
8.32
8.31
8.14
8.13
8.12
8.11
7.28 CDCl3
6.72
6.70
6.70
6.68
3.44
3.43
3.42
3.42
3.41
3.25
1.86
1.72
1.72
1.71
1.71
1.70
1.59 H2O
1.28
0.09
1.00
0.99
1.06
4.51
6.94
f1 (ppm)

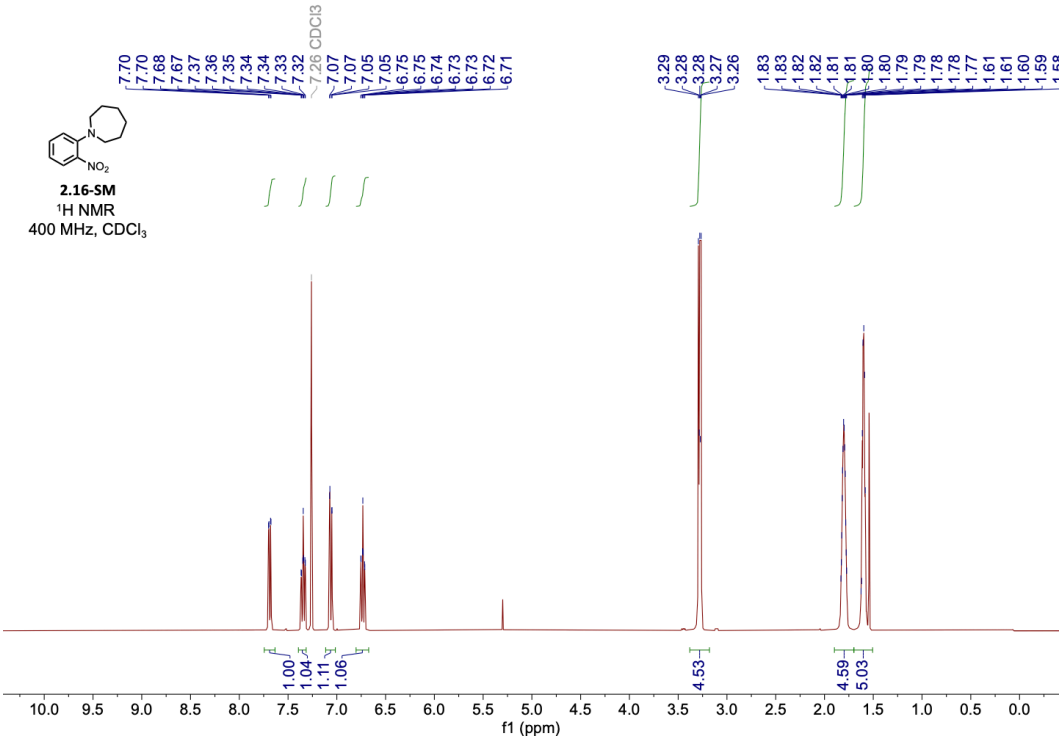
7.70
7.70
7.68
7.67
7.37
7.36
7.35
7.34
7.34
7.33
7.32
7.26 CDCl3
7.07
7.07
7.05
7.05
6.75
6.74
6.73
6.72
6.71
3.29
3.28
3.28
3.27
3.26
1.83
1.83
1.82
1.82
1.81
1.81
1.80
1.80
1.79
1.79
1.78
1.78
1.77
1.61
1.61
1.60
1.59
2.16-SM
1H NMR
400 MHz, CDCl3
1.00
1.04
1.11
1.06
4.53
4.59
5.03
10.0 9.5 9.0 8.5 8.0 7.5 7.0 6.5 6.0 5.5 5.0 4.5 4.0 3.5 3.0 2.5 2.0 1.5 1.0 0.5 0.0
f1 (ppm)

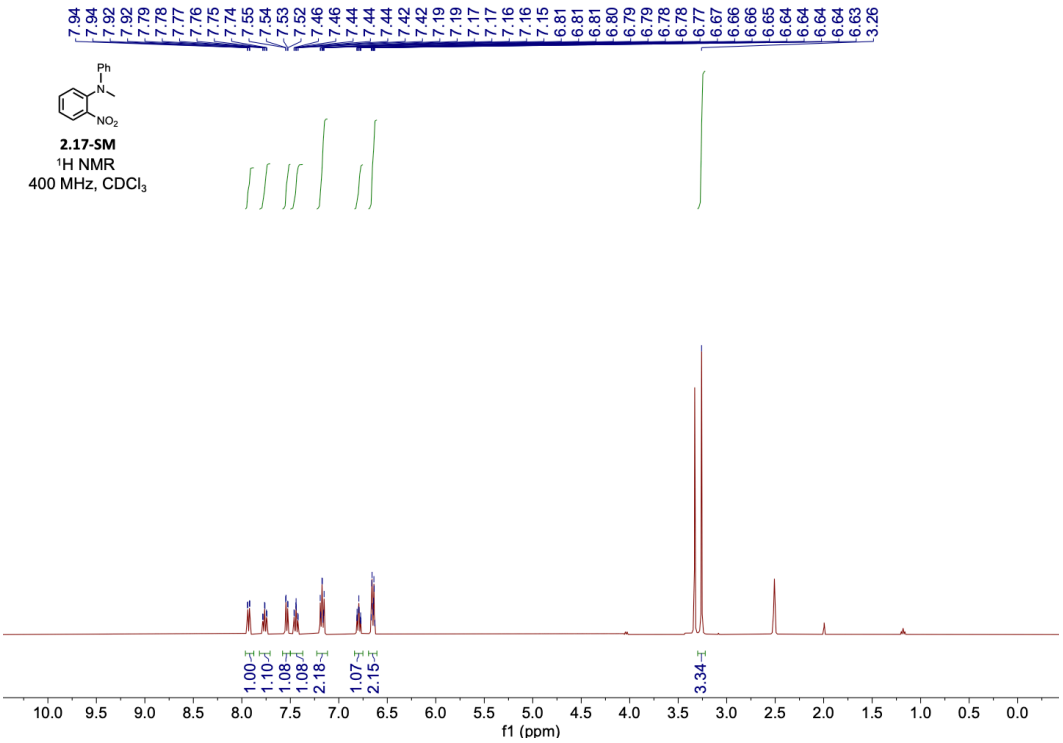
7.94
7.94
7.92
7.92
7.79
7.78
7.77
7.76
7.75
7.74
7.55
7.54
7.53
7.52
7.46
7.44
7.44
7.44
7.42
7.42
7.19
7.19
7.17
7.17
7.16
7.16
7.15
6.81
6.81
6.81
6.80
6.79
6.79
6.78
6.78
6.77
6.67
6.66
6.66
6.65
6.64
6.64
6.64
6.64
6.64
6.63
3.26
2.17-SM
1H NMR
400 MHz, CDCl3
1.00
1.10
1.08
1.08
2.18
1.07
2.15
3.34
10.0 9.5 9.0 8.5 8.0 7.5 7.0 6.5 6.0 5.5 5.0 4.5 4.0 3.5 3.0 2.5 2.0 1.5 1.0 0.5 0.0
f1 (ppm)

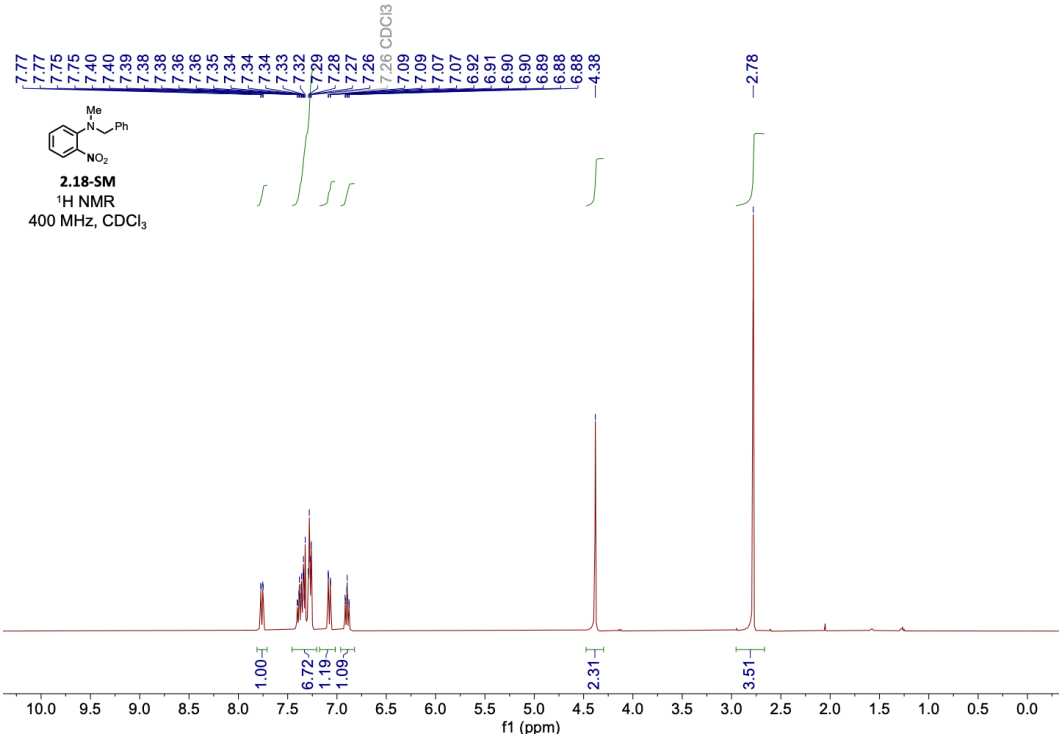
7.77
7.77
7.75
7.75
7.40
7.40
7.39
7.38
7.38
7.36
7.36
7.35
7.34
7.34
7.34
7.33
7.32
7.29
7.28
7.27
7.26
7.26 CDCl3
7.09
7.07
7.07
6.92
6.91
6.90
6.90
6.89
6.88
6.88
4.38
2.78
Me
N
Ph
NO2
2.18-SM
1H NMR
400 MHz, CDCl3
1.00
6.72
1.19
1.09
2.31
3.51
10.0 9.5 9.0 8.5 8.0 7.5 7.0 6.5 6.0 5.5 5.0 4.5 4.0 3.5 3.0 2.5 2.0 1.5 1.0 0.5 0.0
f1 (ppm)

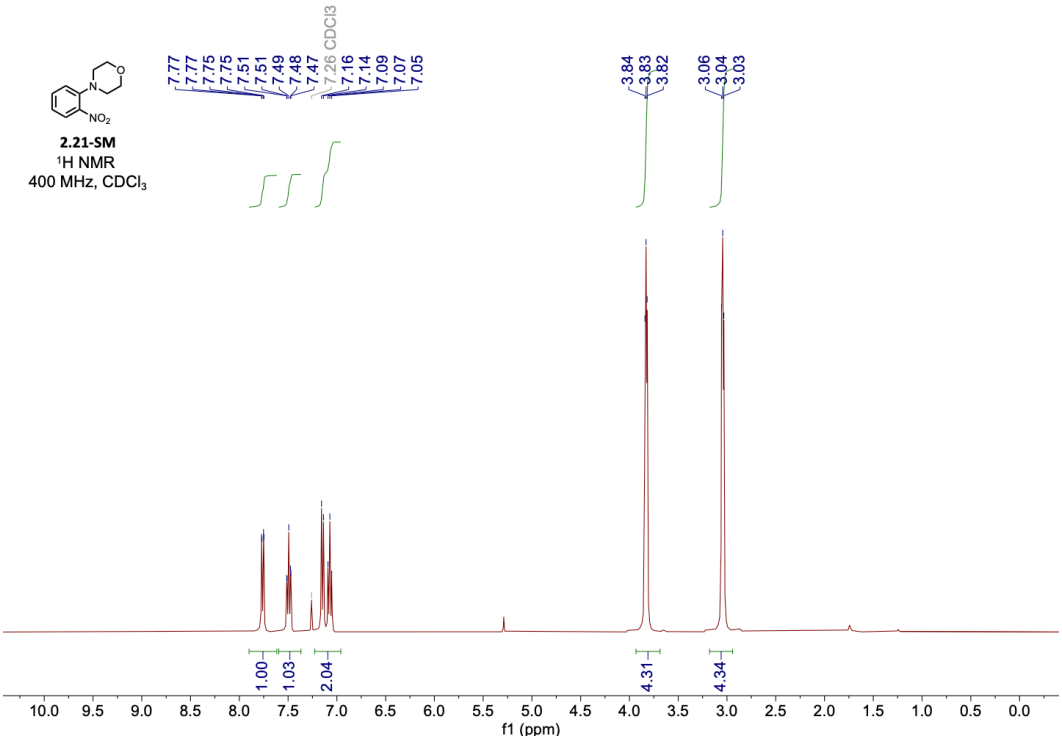
7.77
7.77
7.75
7.75
7.51
7.51
7.49
7.48
7.47
7.26 CDCl3
7.16
7.14
7.09
7.07
7.05
3.84
3.83
3.82
3.06
3.04
3.03
N
O
NO2
2.21-SM
1H NMR
400 MHz, CDCl3
1.00
1.03
2.04
4.31
4.34
10.0 9.5 9.0 8.5 8.0 7.5 7.0 6.5 6.0 5.5 5.0 4.5 4.0 3.5 3.0 2.5 2.0 1.5 1.0 0.5 0.0
f1 (ppm)

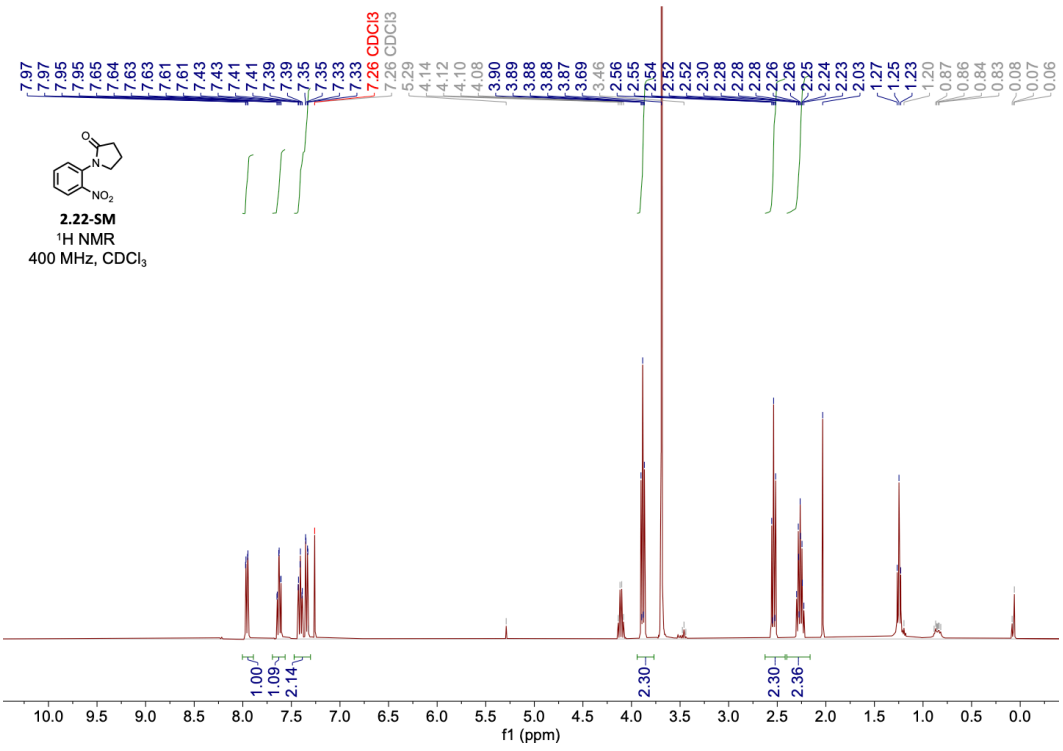
2.22-SM
1H NMR
400 MHz, CDCl3
f1 (ppm)

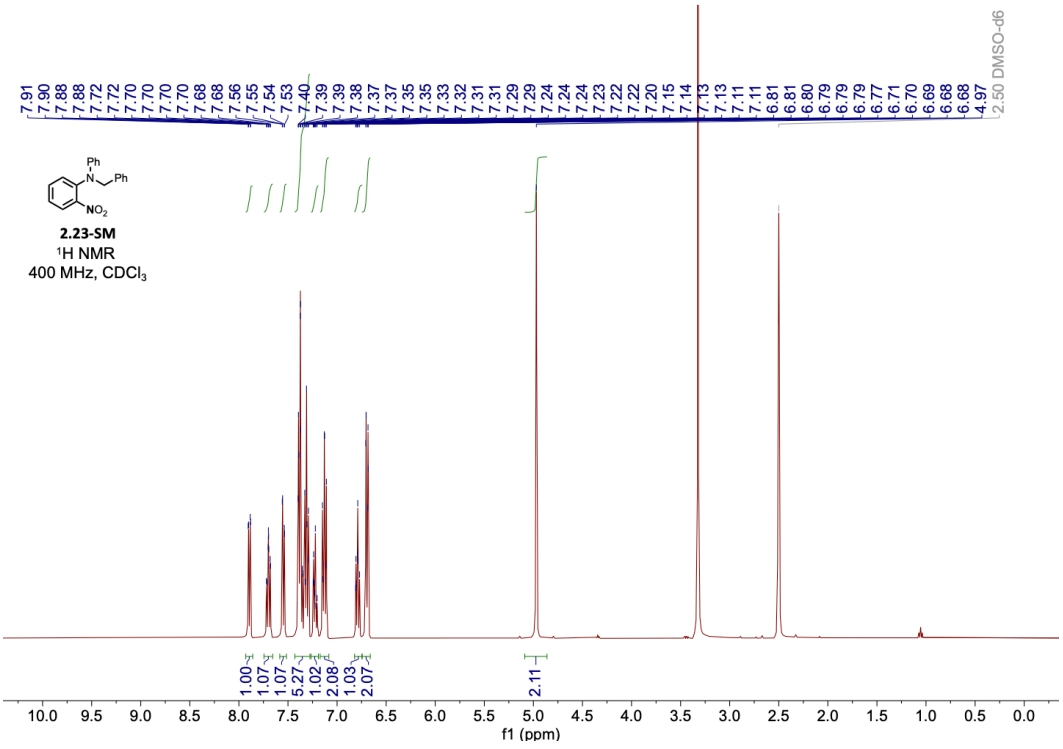
2.23-SM
1H NMR
400 MHz, CDCl3
f1 (ppm)

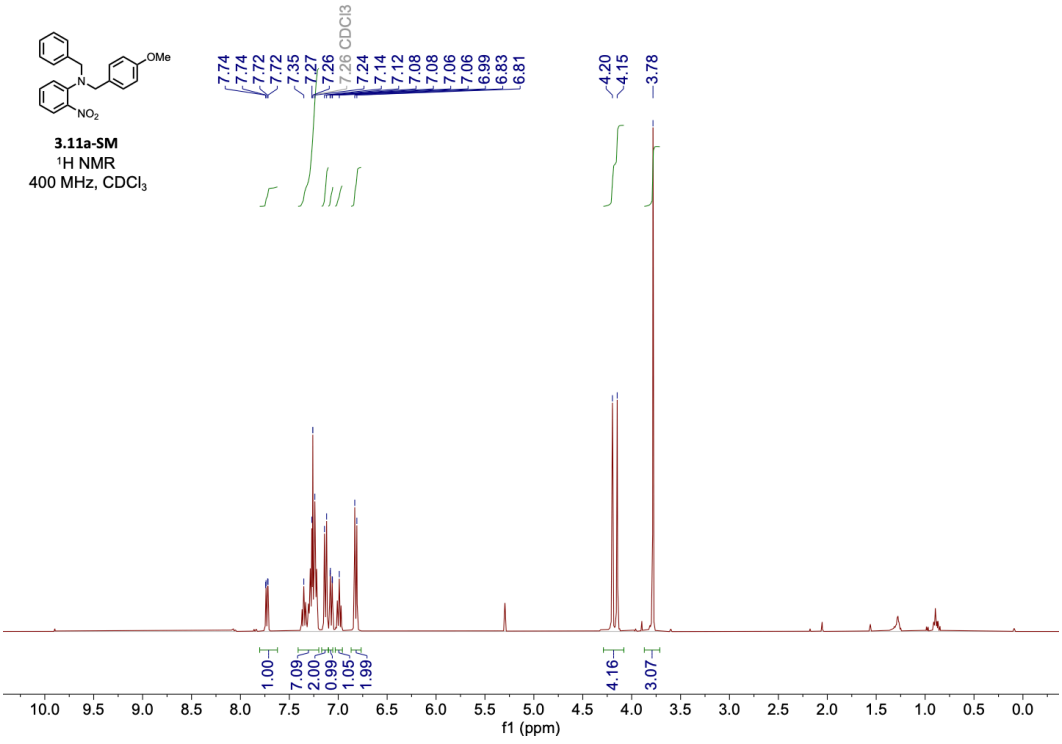
3.11a-SM
1H NMR
400 MHz, CDCl3
7.74
7.74
7.72
7.72
7.35
7.27
7.26
7.26 CDCl3
7.24
7.14
7.12
7.08
7.08
7.06
7.06
6.99
6.83
6.81
4.20
4.15
3.78
1.00
7.09
2.00
0.99
1.05
1.99
4.16
3.07
f1 (ppm)

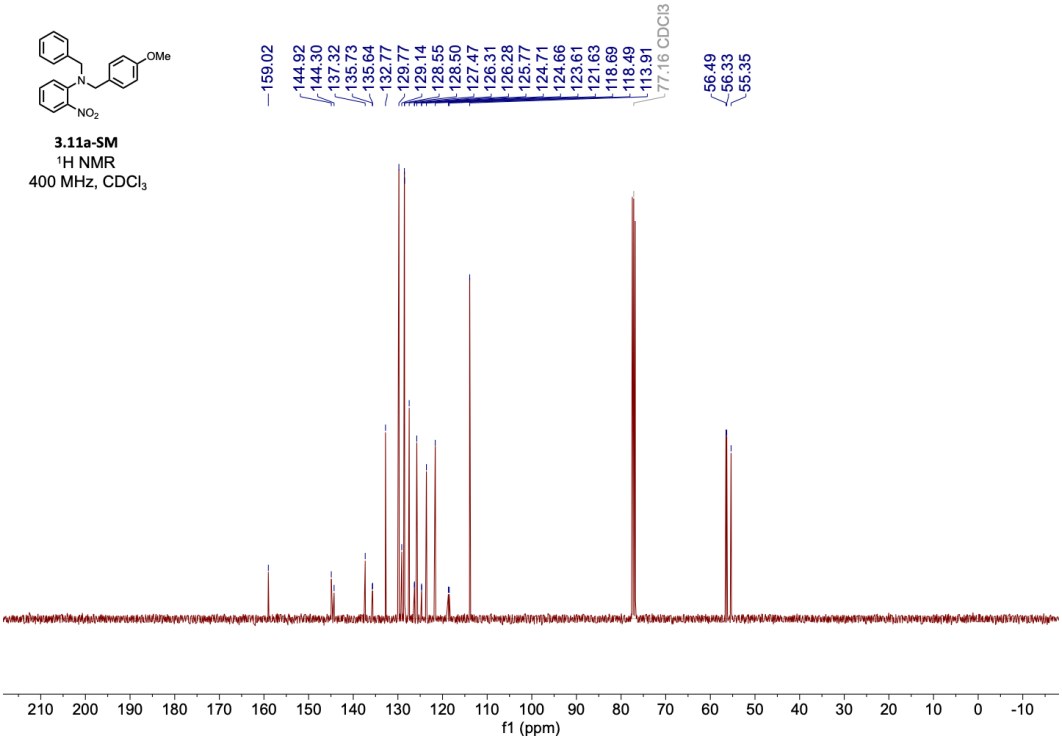
3.11a-SM
1H NMR
400 MHz, CDCl3
159.02
144.92
144.30
137.32
135.73
135.64
132.77
129.77
129.14
128.55
128.50
127.47
126.31
126.28
125.77
124.71
124.66
123.61
121.63
118.69
118.49
113.91
77.16 CDCl3
56.49
56.33
55.35
f1 (ppm)

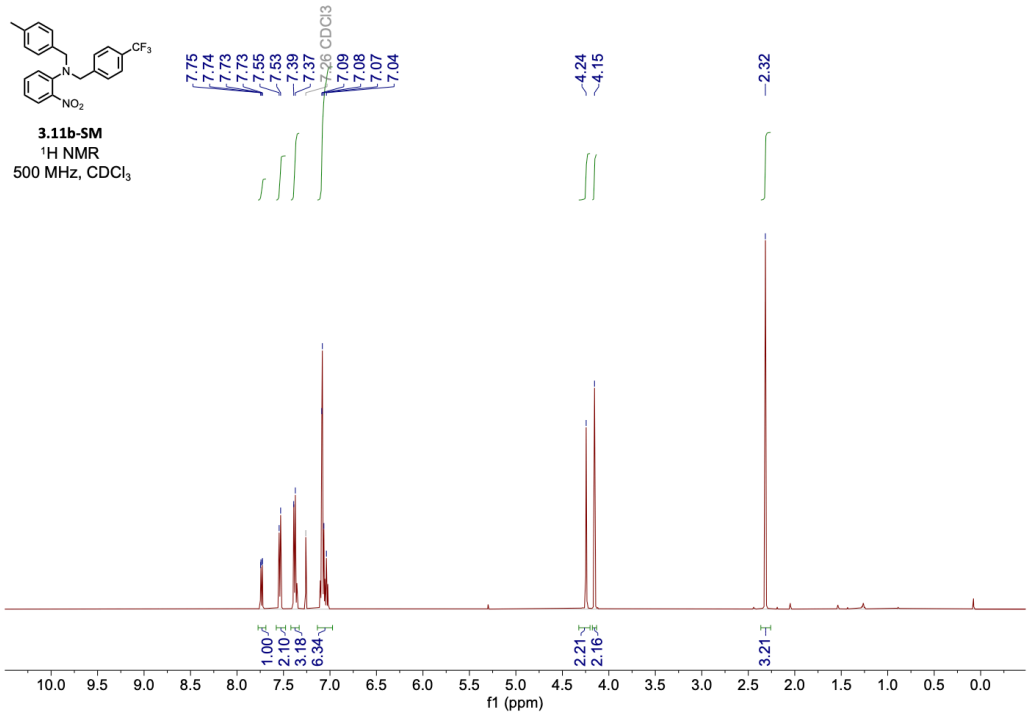
3.11b-SM
1H NMR
500 MHz, CDCl3
7.75
7.74
7.73
7.73
7.55
7.53
7.39
7.37
7.26 CDCl3
7.09
7.08
7.07
7.04
4.24
4.15
2.32
1.00
2.10
3.18
6.34
2.21
2.16
3.21
f1 (ppm)

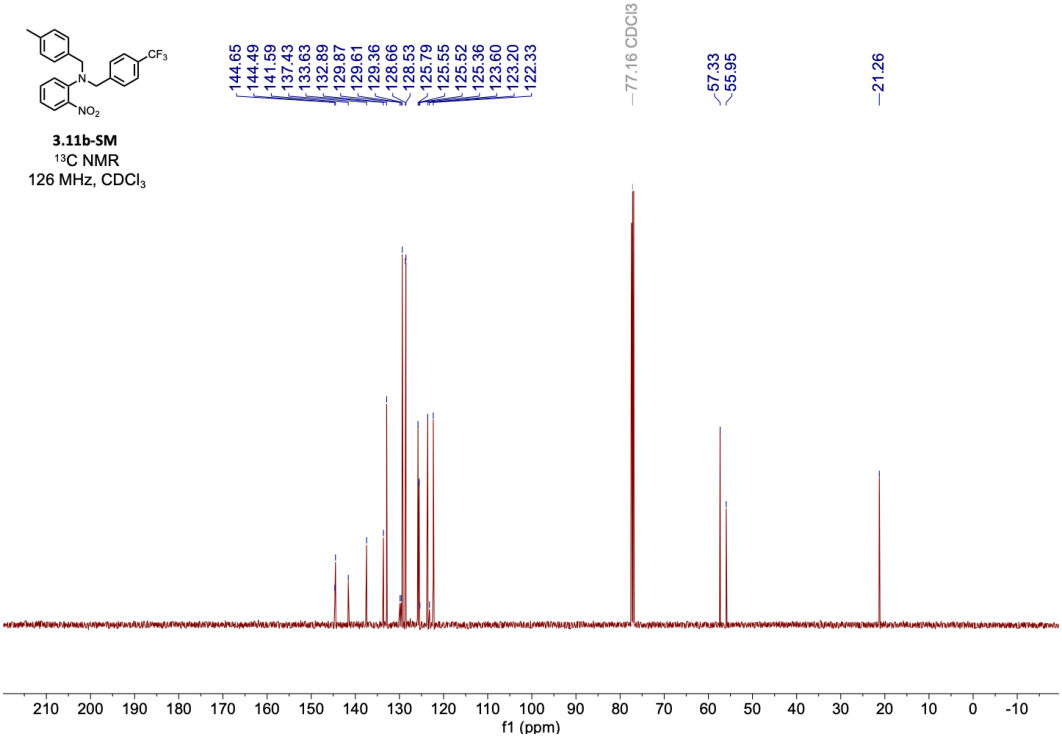
3.11b-SM
13C NMR
126 MHz, CDCl3
144.65
144.49
141.59
137.43
133.63
132.89
129.87
129.61
129.36
128.66
128.53
125.79
125.55
125.52
125.36
123.60
123.20
122.33
77.16 CDCl3
57.33
55.95
21.26
f1 (ppm)

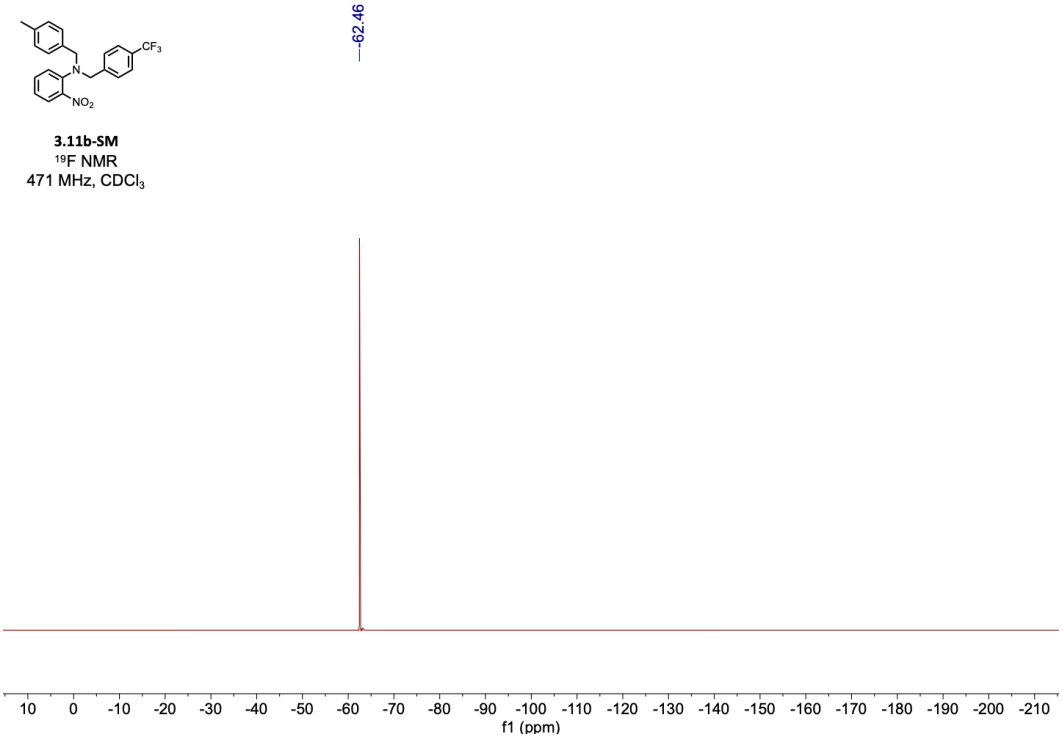

3.11b-SM
^{19}F NMR
471 MHz, $CDCl_3$

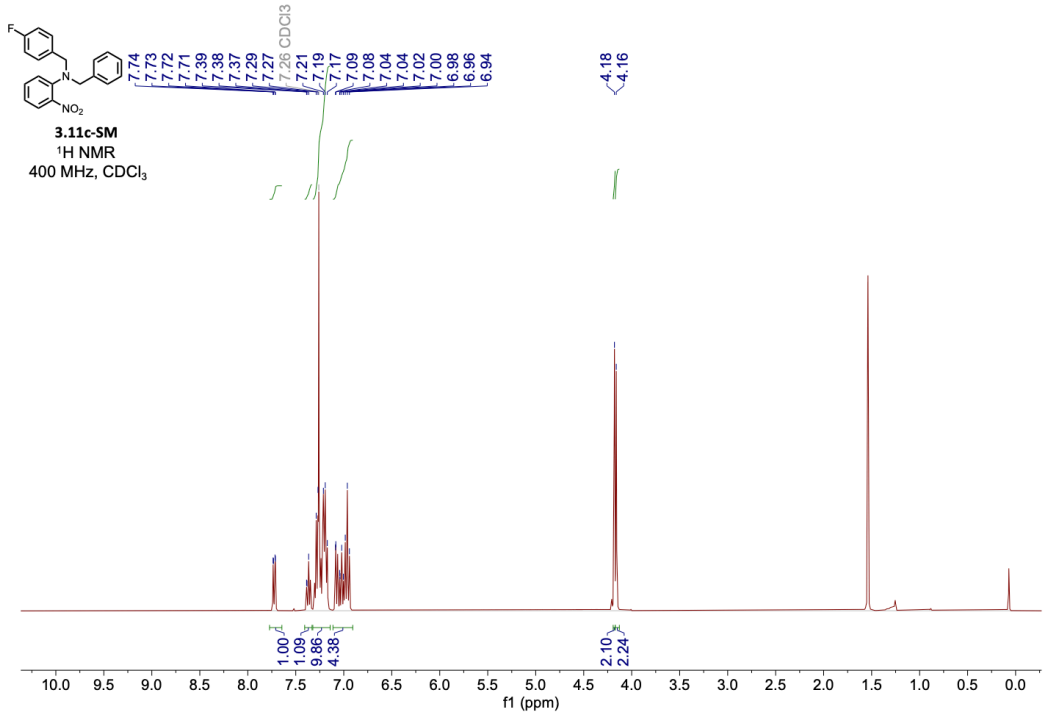

3.11c-SM
^{1}H NMR
400 MHz, $CDCl_3$

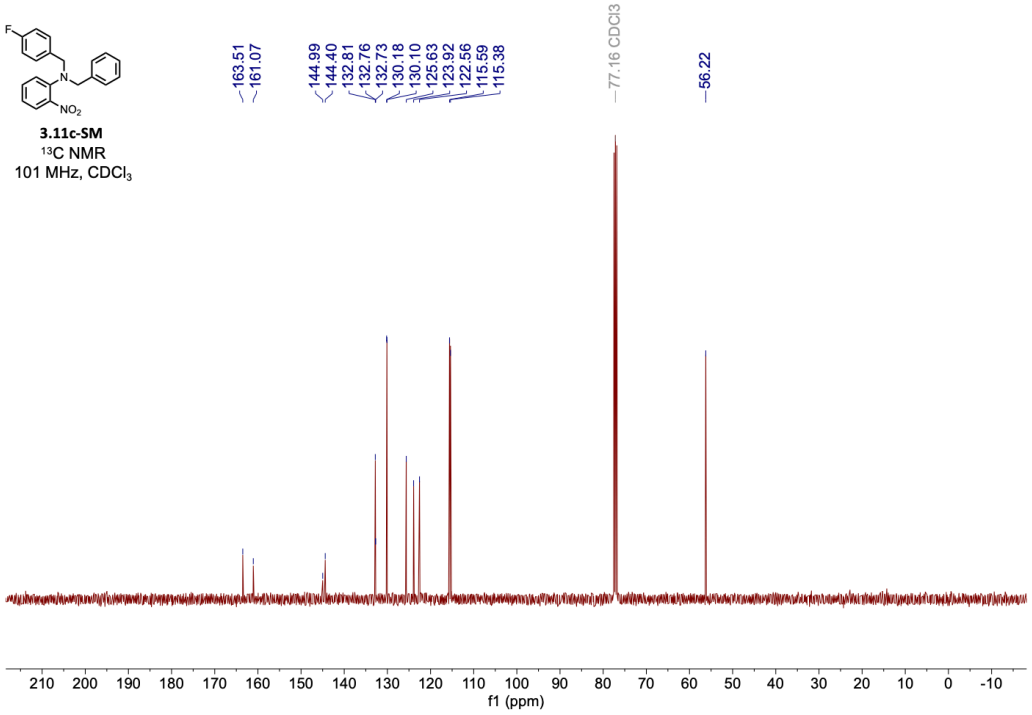
3.11c-SM
13C NMR
101 MHz, CDCl3
163.51
161.07
144.99
144.40
132.81
132.76
132.73
130.18
130.10
125.63
123.92
122.56
115.59
115.38
77.16 CDCl3
56.22
f1 (ppm)

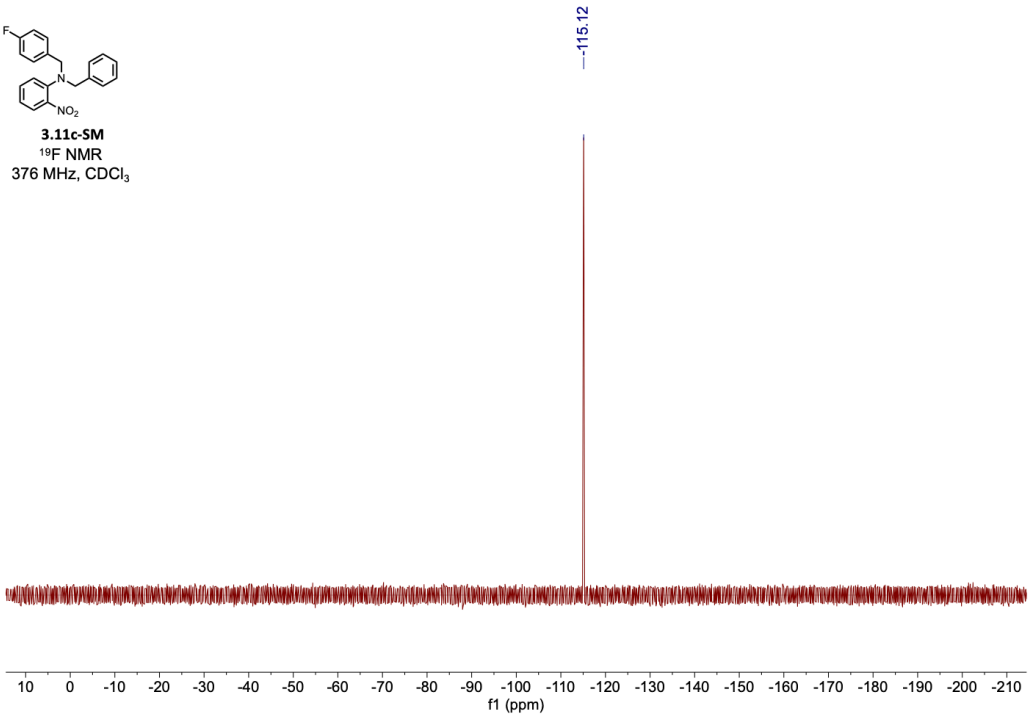
3.11c-SM
19F NMR
376 MHz, CDCl3
-115.12
f1 (ppm)

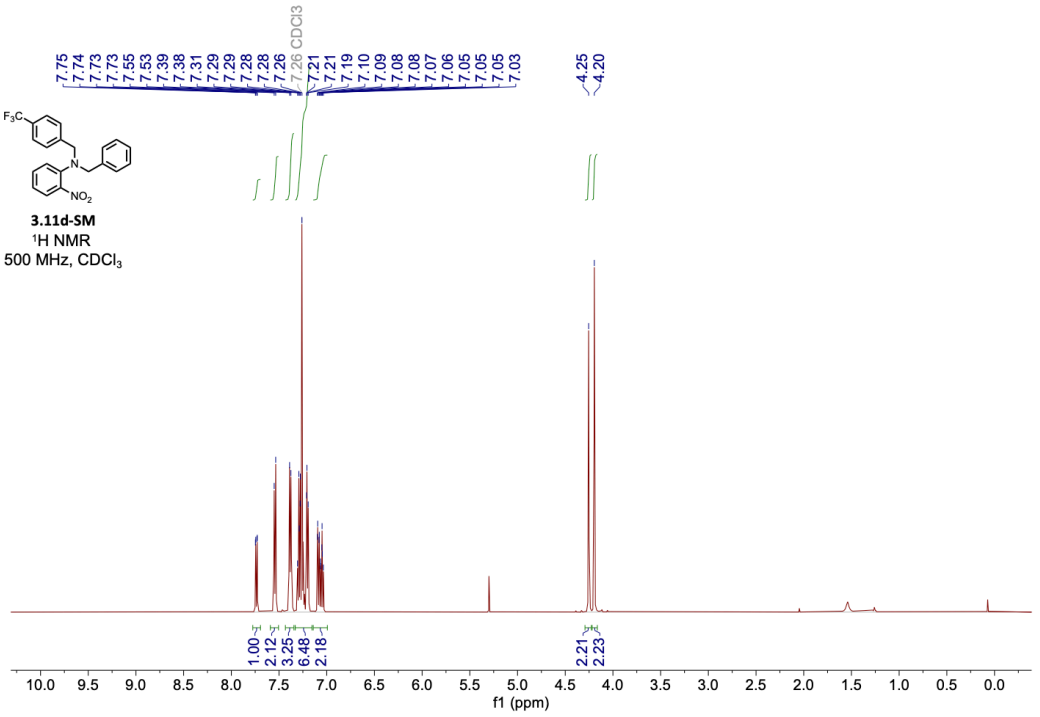
7.75
7.74
7.73
7.73
7.55
7.53
7.39
7.38
7.31
7.29
7.29
7.28
7.28
7.26
7.26 CDCl3
7.21
7.21
7.19
7.10
7.09
7.08
7.08
7.07
7.06
7.05
7.05
7.05
7.03
4.25
4.20
F3C
N
NO2
3.11d-SM
1H NMR
500 MHz, CDCl3
1.00
2.12
3.25
6.48
2.18
2.21
2.23
10.0 9.5 9.0 8.5 8.0 7.5 7.0 6.5 6.0 5.5 5.0 4.5 4.0 3.5 3.0 2.5 2.0 1.5 1.0 0.5 0.0
f1 (ppm)

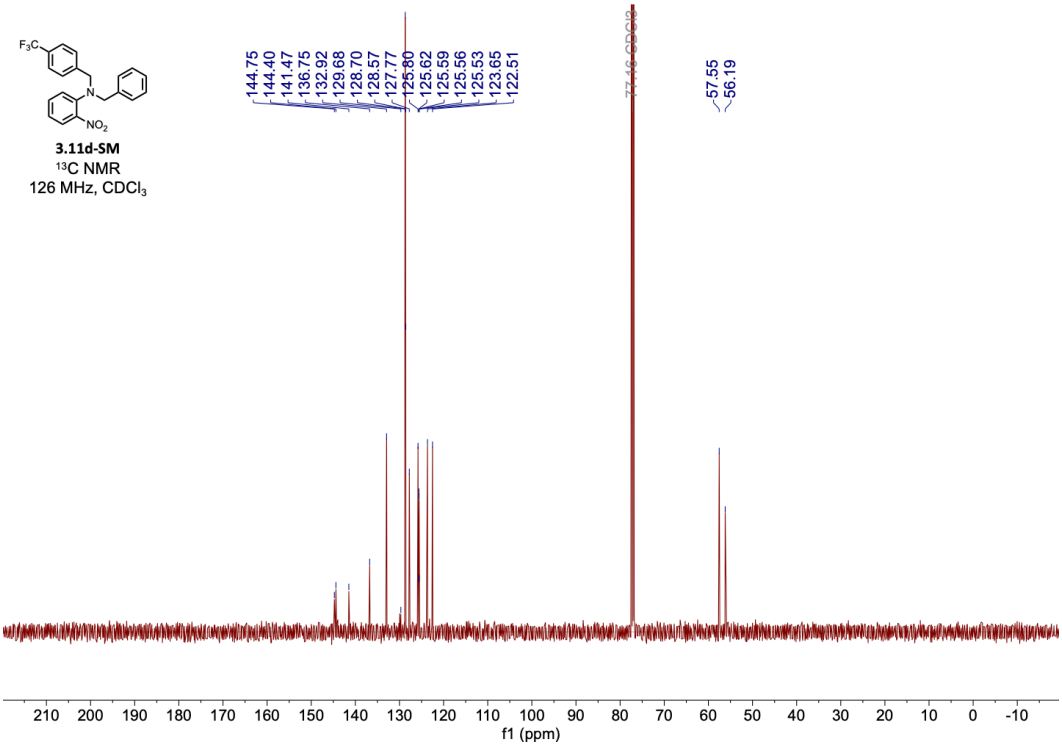
144.75
144.40
141.47
136.75
132.92
129.68
128.70
128.57
127.77
125.80
125.62
125.59
125.56
125.53
123.65
122.51
77.46 CDCl3
57.55
56.19
F3C
N
NO2
3.11d-SM
13C NMR
126 MHz, CDCl3
210 200 190 180 170 160 150 140 130 120 110 100 90 80 70 60 50 40 30 20 10 0 -10
f1 (ppm)

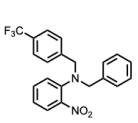

3.11d-SM
^{19}F NMR
471 MHz, $CDCl_3$

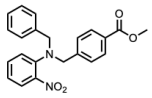

3.11e-SM
^{1}H NMR
500 MHz, $CDCl_3$

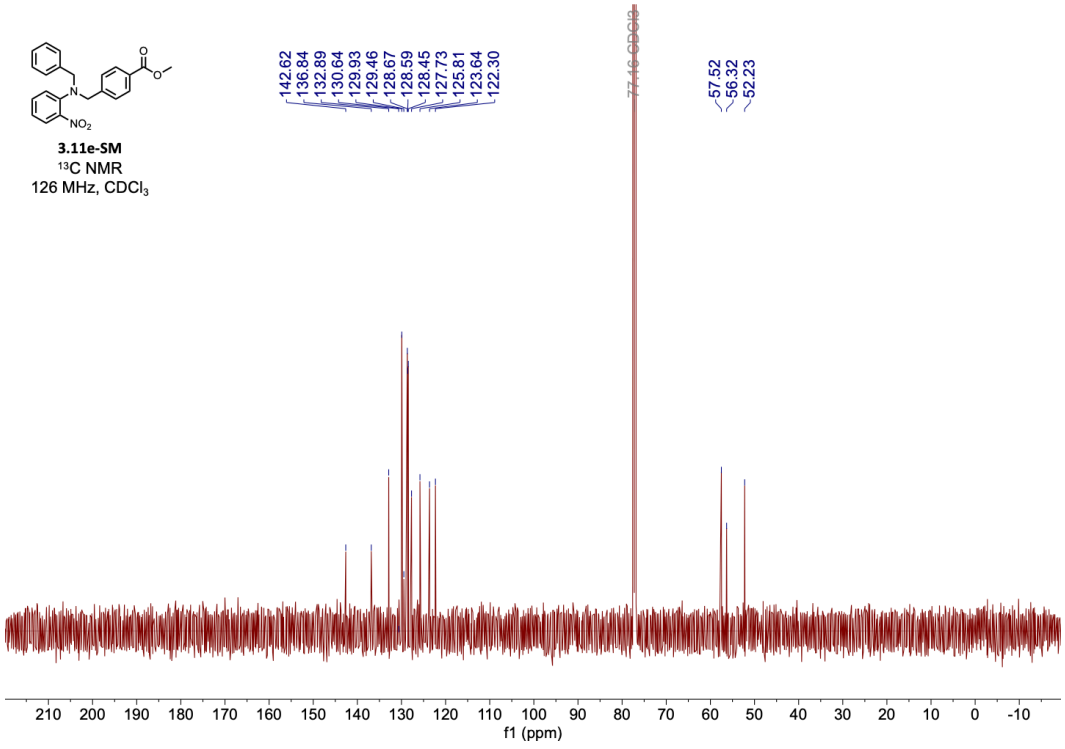

3.11e-SM
^{13}C NMR
126 MHz, $CDCl_3$

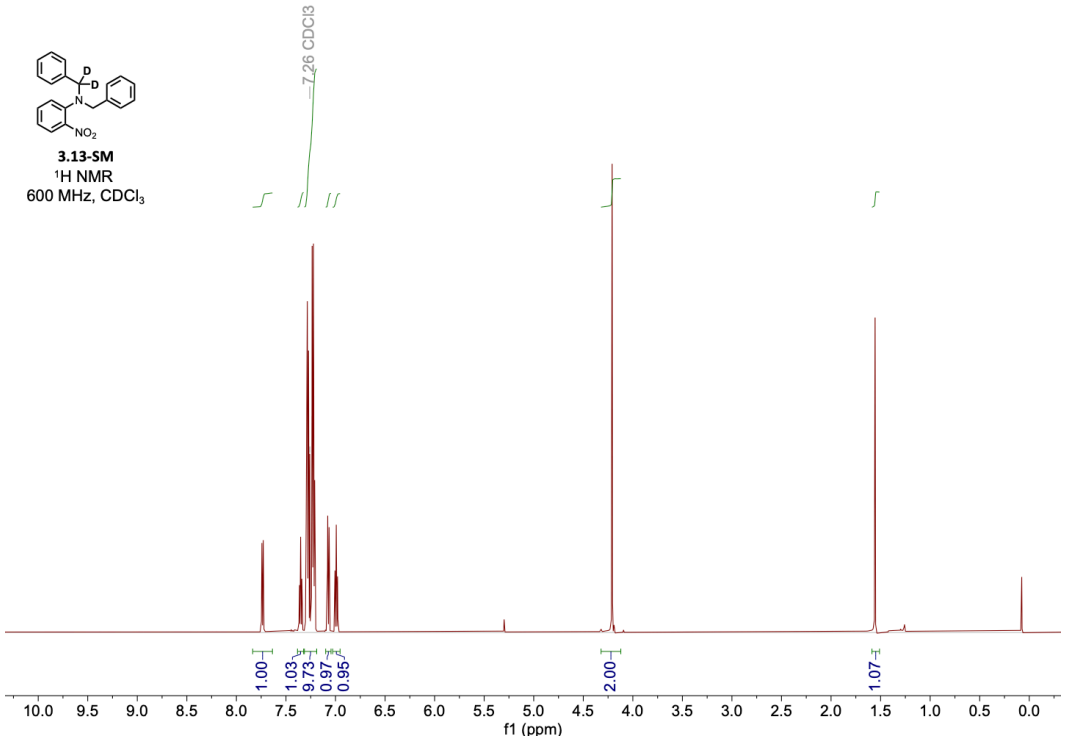

3.13-SM
^{1}H NMR
600 MHz, $CDCl_3$

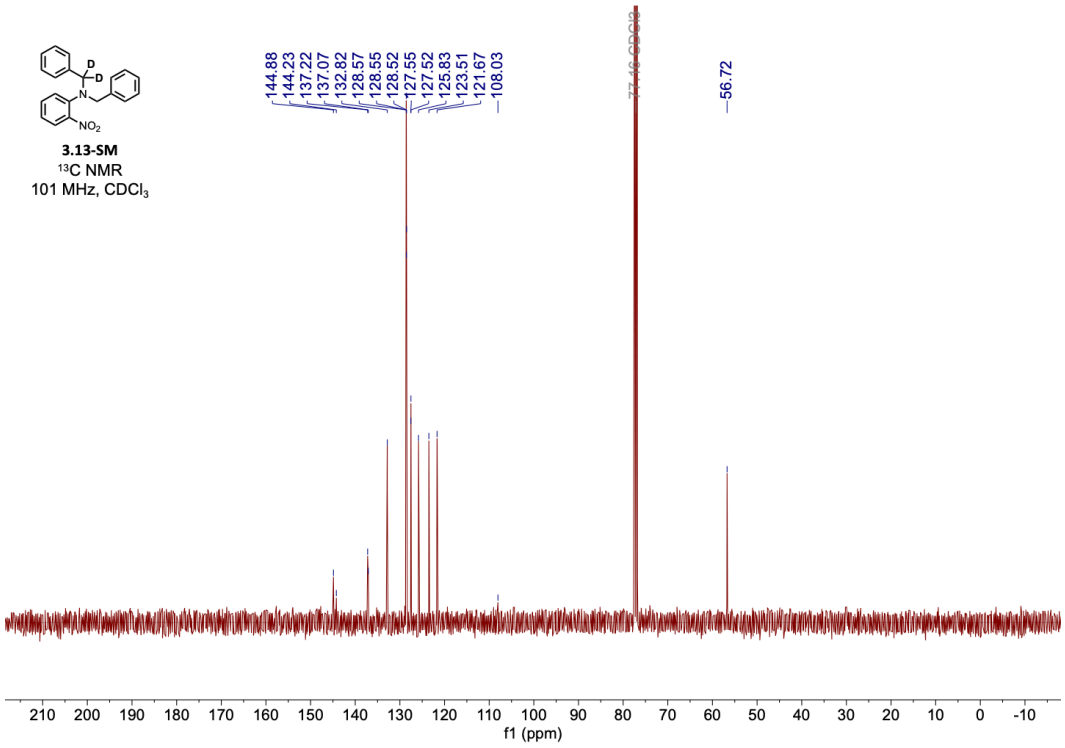
3.13-SM
13C NMR
101 MHz, CDCl3
144.88
144.23
137.22
137.07
132.82
128.57
128.55
128.52
127.55
127.52
125.83
123.51
121.67
108.03
77.46 CDCl3
56.72
f1 (ppm)

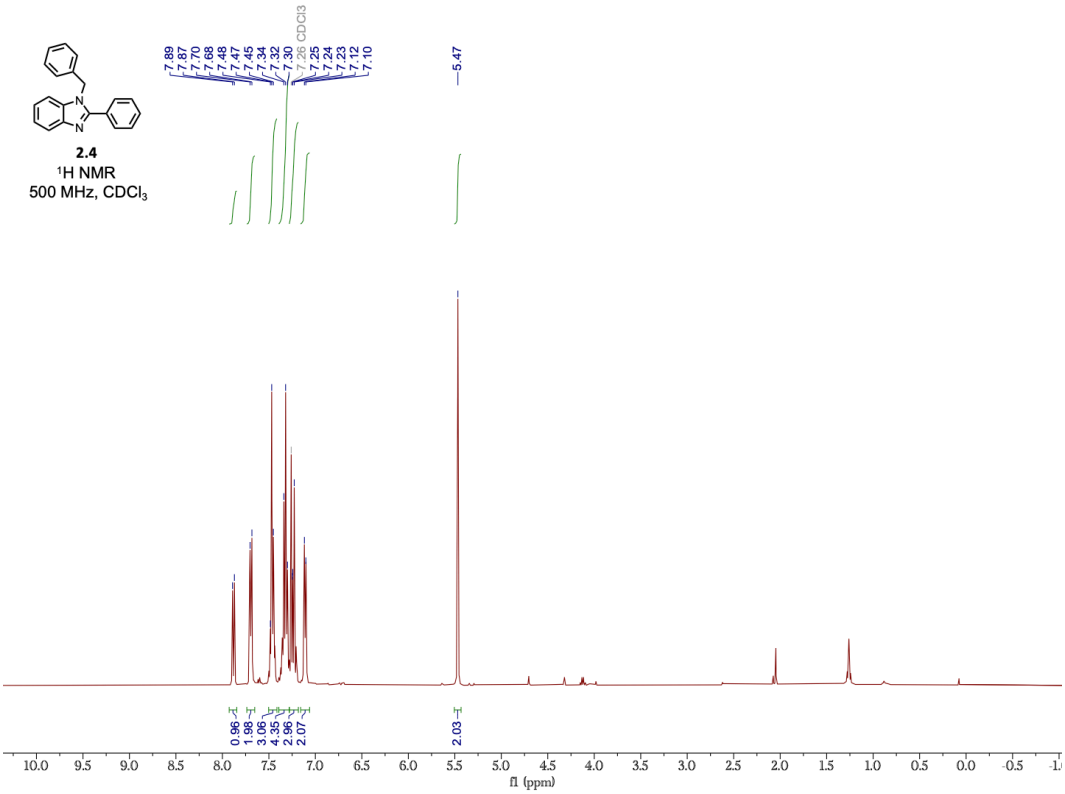
2.4
1H NMR
500 MHz, CDCl3
7.89
7.87
7.70
7.68
7.48
7.47
7.45
7.34
7.32
7.30
7.26 CDCl3
7.25
7.24
7.23
7.12
7.10
5.47
0.96
1.98
3.06
4.35
2.96
2.07
2.03
f1 (ppm)

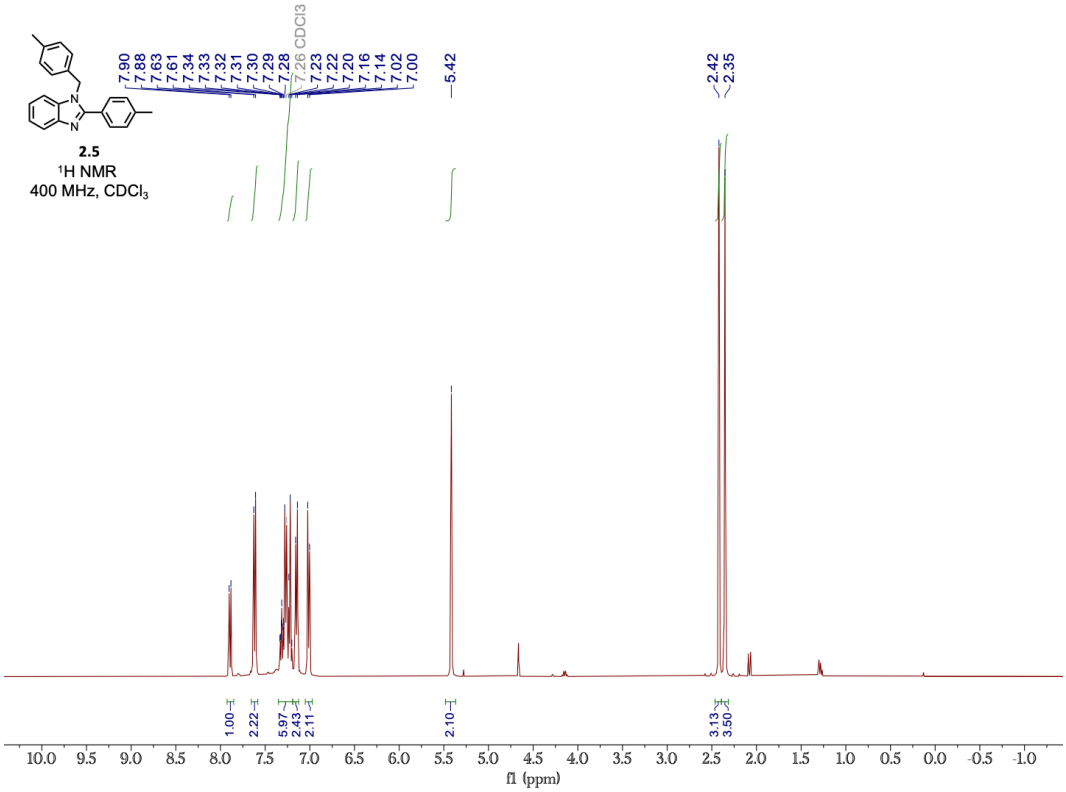
7.90
7.88
7.63
7.61
7.34
7.33
7.32
7.31
7.30
7.29
7.28
7.26 CDCl3
7.23
7.22
7.20
7.16
7.14
7.02
7.00
5.42
2.42
2.35
2.5
1H NMR
400 MHz, CDCl3
1.00
2.22
5.97
2.43
2.11
2.10
3.13
3.50
f1 (ppm)

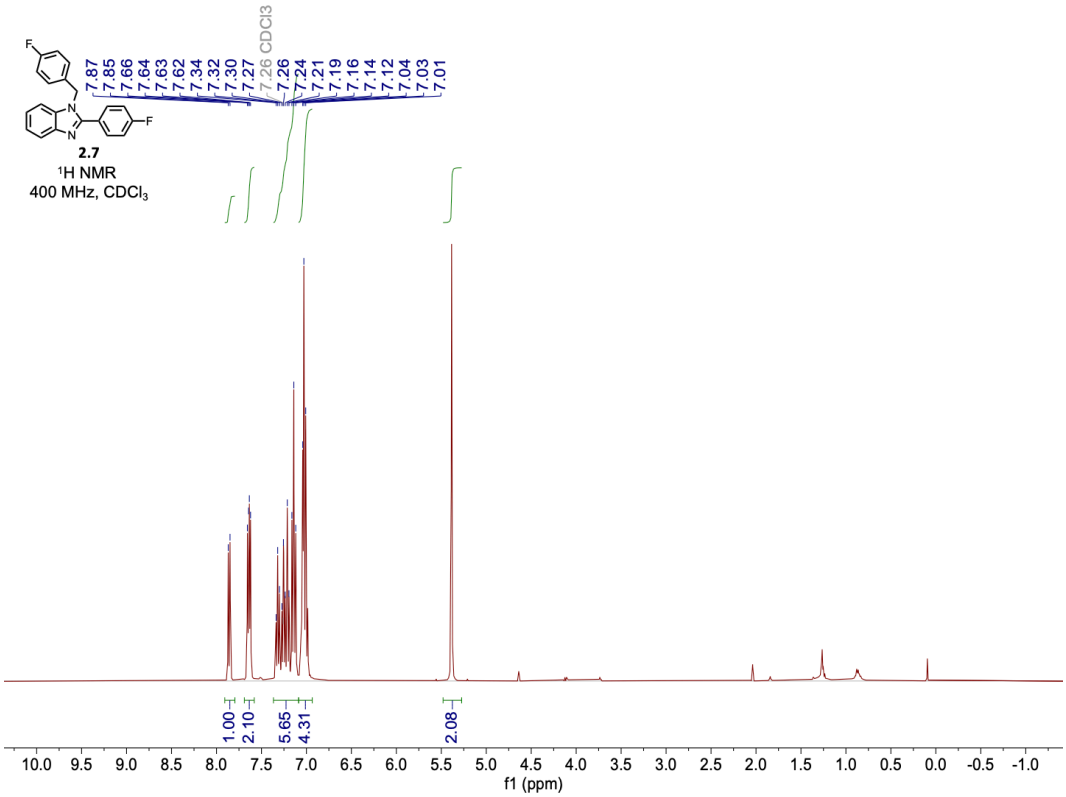
7.87
7.85
7.66
7.64
7.63
7.62
7.34
7.32
7.30
7.27
7.26 CDCl3
7.24
7.21
7.19
7.16
7.14
7.12
7.04
7.03
7.01
F
2.7
1H NMR
400 MHz, CDCl3
1.00
2.10
5.65
4.31
2.08
f1 (ppm)

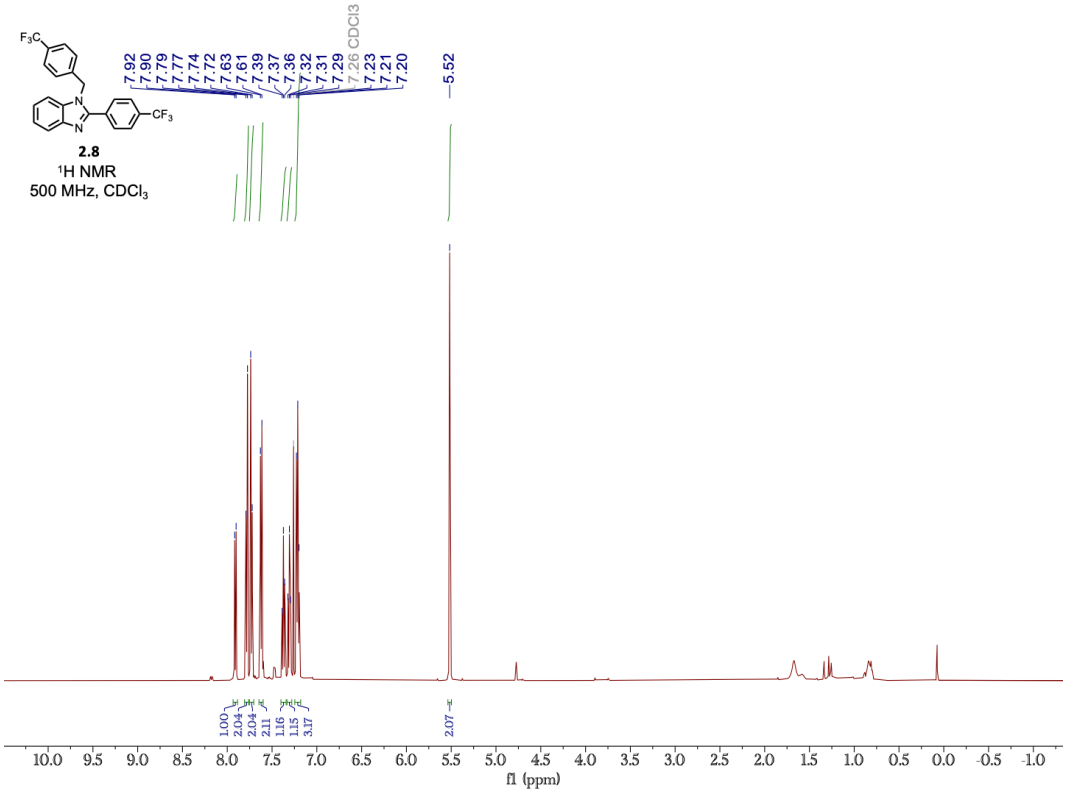
F3C
CF3
N
N
2.8
1H NMR
500 MHz, CDCl3
7.92
7.90
7.79
7.77
7.74
7.72
7.63
7.61
7.39
7.37
7.36
7.32
7.31
7.29
7.26 CDCl3
7.23
7.21
7.20
5.52
1.00
2.04
2.04
2.11
1.16
1.15
3.17
2.07
10.0 9.5 9.0 8.5 8.0 7.5 7.0 6.5 6.0 5.5 5.0 4.5 4.0 3.5 3.0 2.5 2.0 1.5 1.0 0.5 0.0 -0.5 -1.0
f1 (ppm)

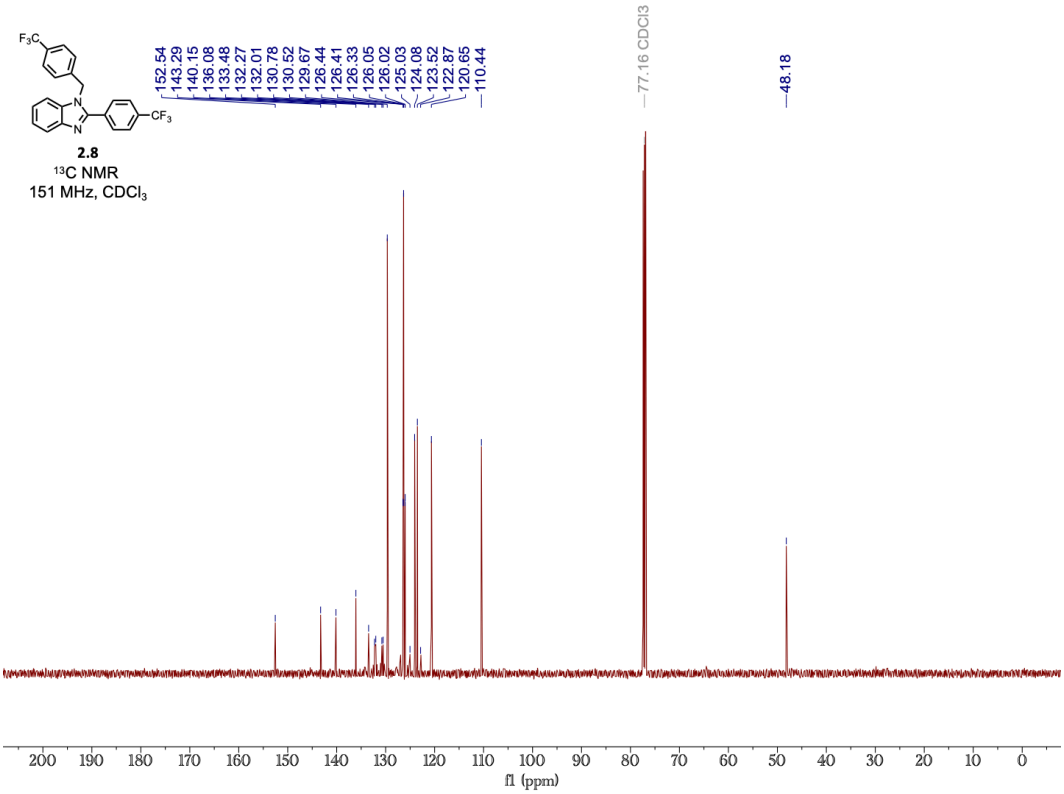
F3C
CF3
N
N
2.8
13C NMR
151 MHz, CDCl3
152.54
143.29
140.15
136.08
133.48
132.27
132.01
130.78
130.52
129.67
126.44
126.41
126.33
126.05
126.02
125.03
124.08
123.52
122.87
120.65
110.44
77.16 CDCl3
48.18
200 190 180 170 160 150 140 130 120 110 100 90 80 70 60 50 40 30 20 10 0
f1 (ppm)

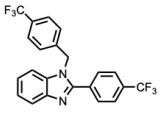

2.8
^{19}F NMR
565 MHz, $CDCl_3$

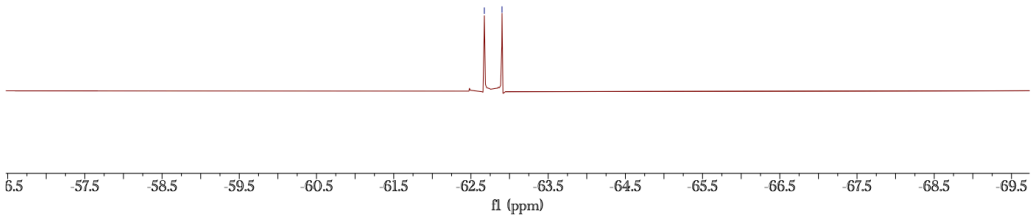

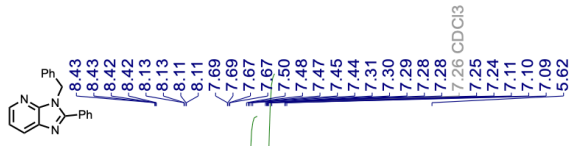

2.9
^{1}H NMR
500 MHz, $CDCl_3$

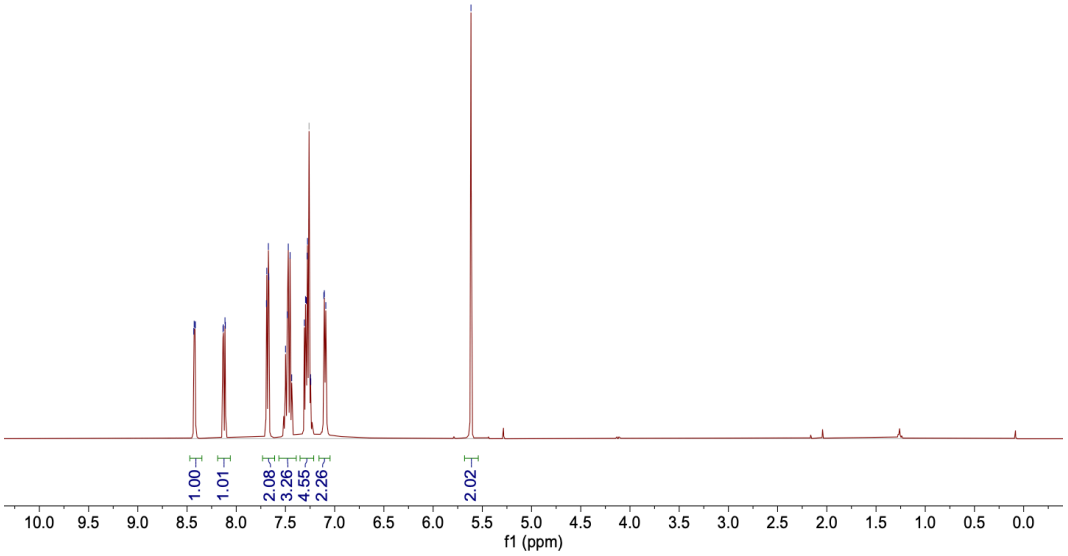

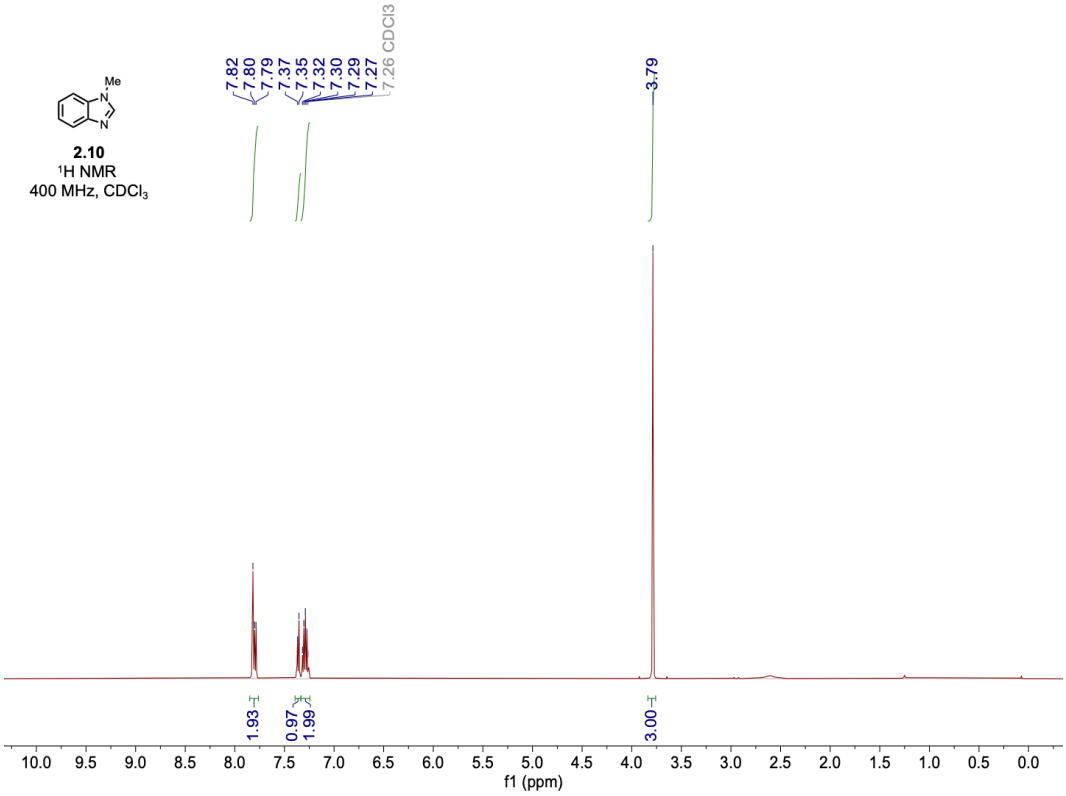
Me
N
N
2.10
1H NMR
400 MHz, CDCl3
7.82
7.80
7.79
7.37
7.35
7.32
7.30
7.29
7.27
7.26 CDCl3
3.79
1.93
0.97
1.99
3.00
10.0 9.5 9.0 8.5 8.0 7.5 7.0 6.5 6.0 5.5 5.0 4.5 4.0 3.5 3.0 2.5 2.0 1.5 1.0 0.5 0.0
f1 (ppm)

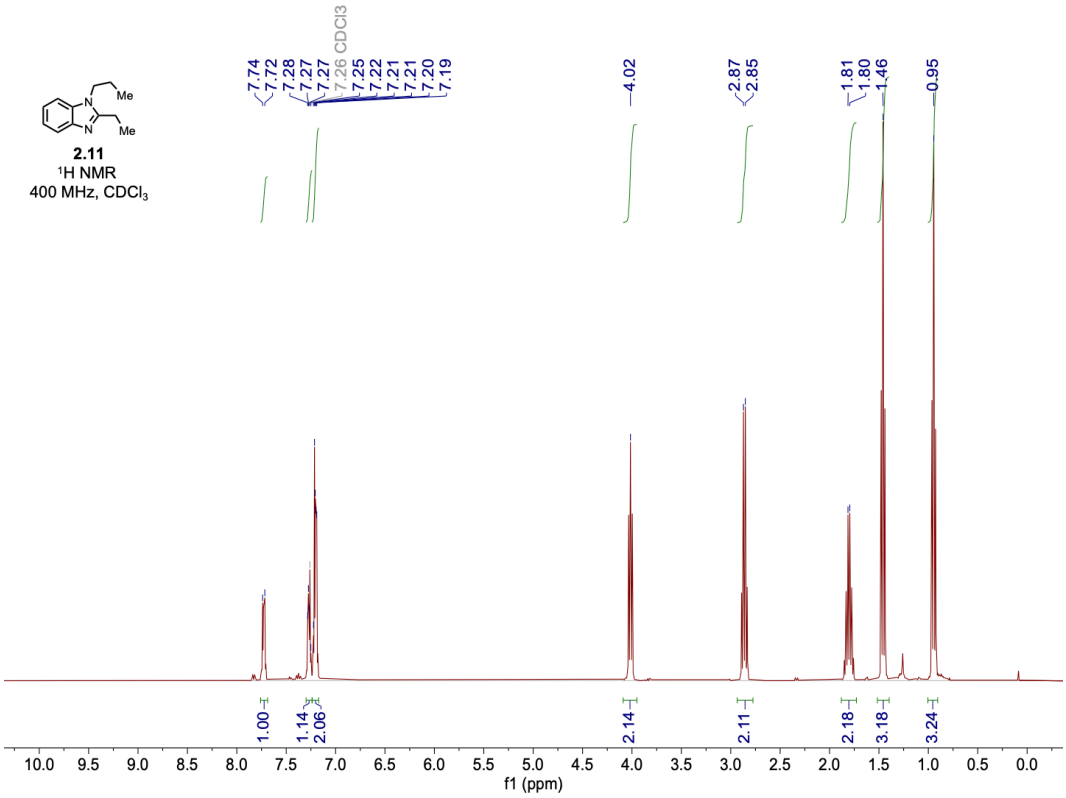
Me
N
N
Me
2.11
1H NMR
400 MHz, CDCl3
7.74
7.72
7.28
7.27
7.27
7.26 CDCl3
7.25
7.22
7.21
7.21
7.20
7.19
4.02
2.87
2.85
1.81
1.80
1.46
0.95
1.00
1.14
2.06
2.14
2.11
2.18
3.18
3.24
10.0 9.5 9.0 8.5 8.0 7.5 7.0 6.5 6.0 5.5 5.0 4.5 4.0 3.5 3.0 2.5 2.0 1.5 1.0 0.5 0.0
f1 (ppm)

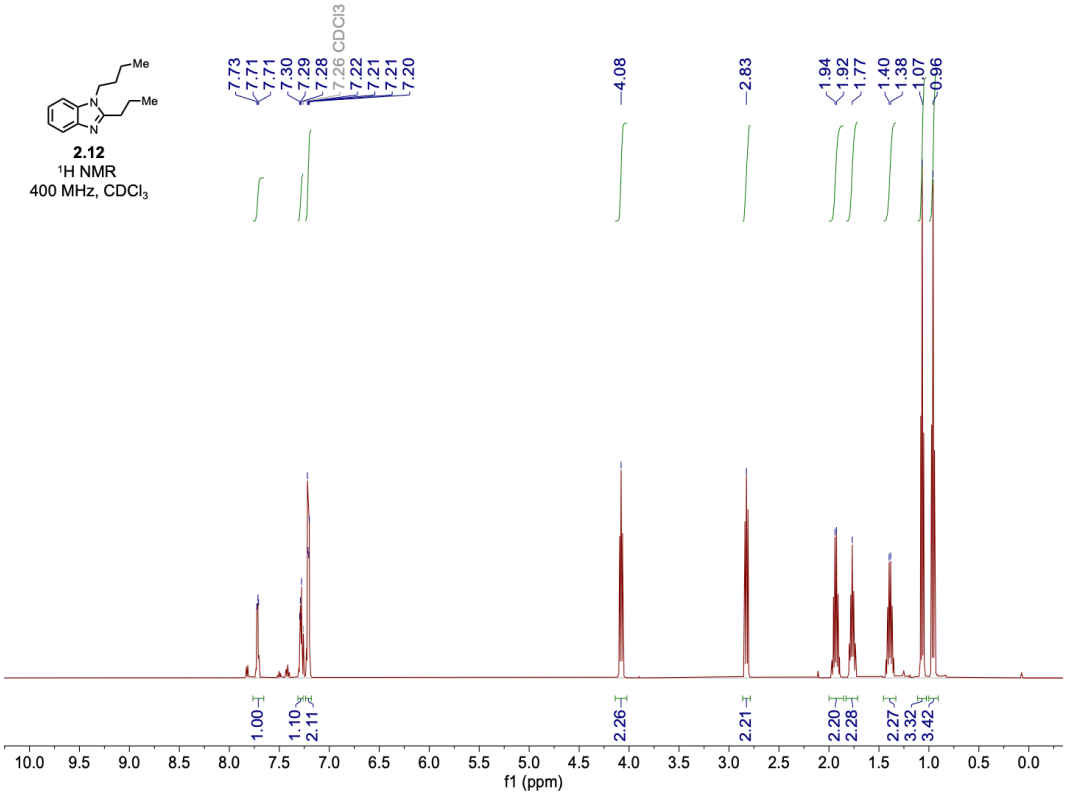

2.12
^{1}H NMR
400 MHz, $CDCl_3$

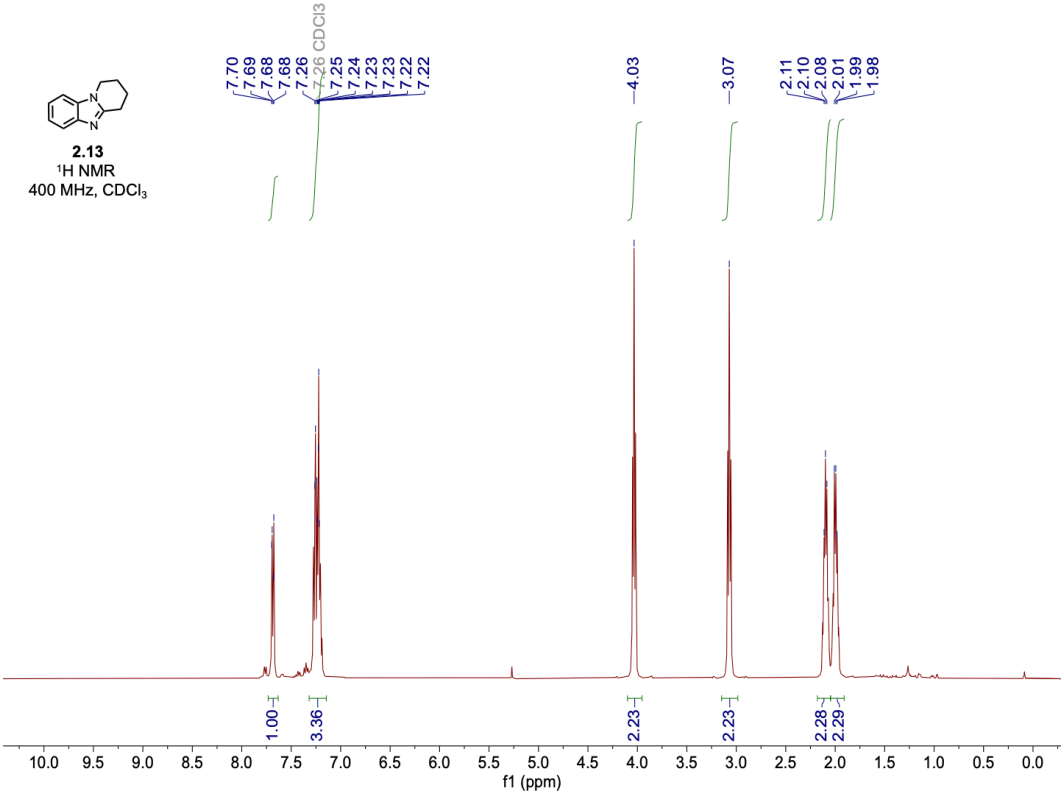

2.13
^{1}H NMR
400 MHz, $CDCl_3$

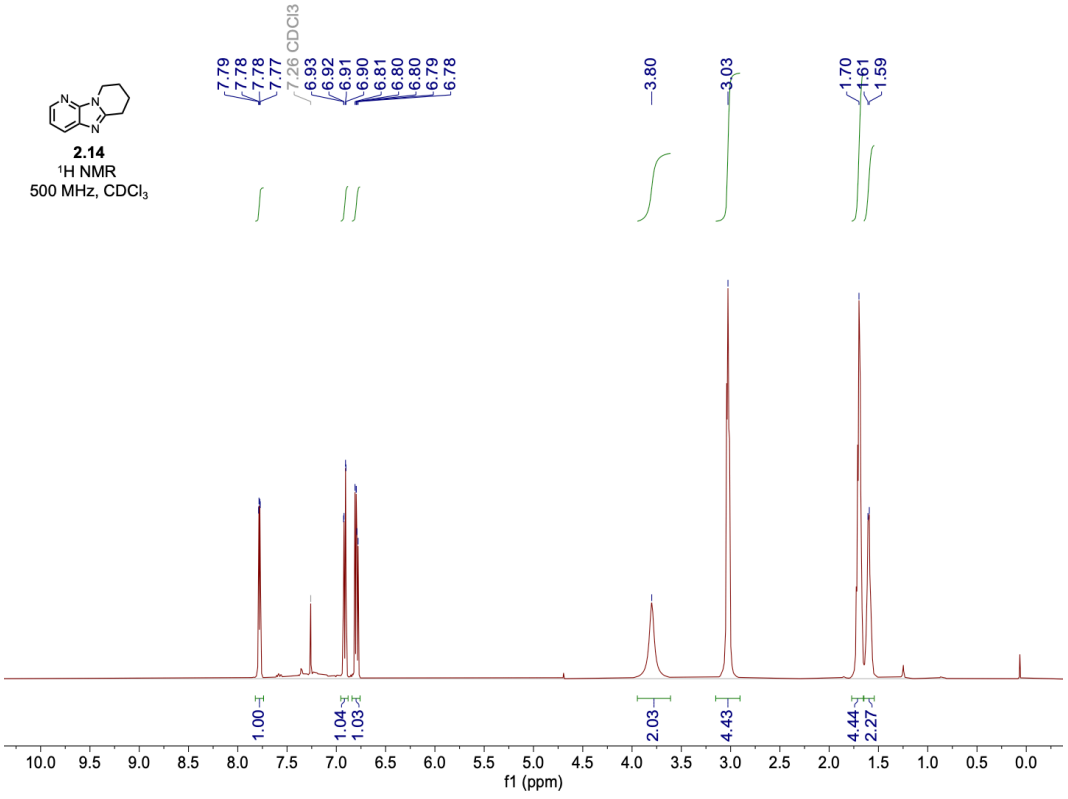
2.14
1H NMR
500 MHz, CDCl3
7.79
7.78
7.78
7.77
7.26 CDCl3
6.93
6.92
6.91
6.90
6.81
6.80
6.80
6.79
6.78
3.80
3.03
1.70
1.61
1.59
1.00
1.04
1.03
2.03
4.43
4.44
2.27
10.0 9.5 9.0 8.5 8.0 7.5 7.0 6.5 6.0 5.5 5.0 4.5 4.0 3.5 3.0 2.5 2.0 1.5 1.0 0.5 0.0
f1 (ppm)

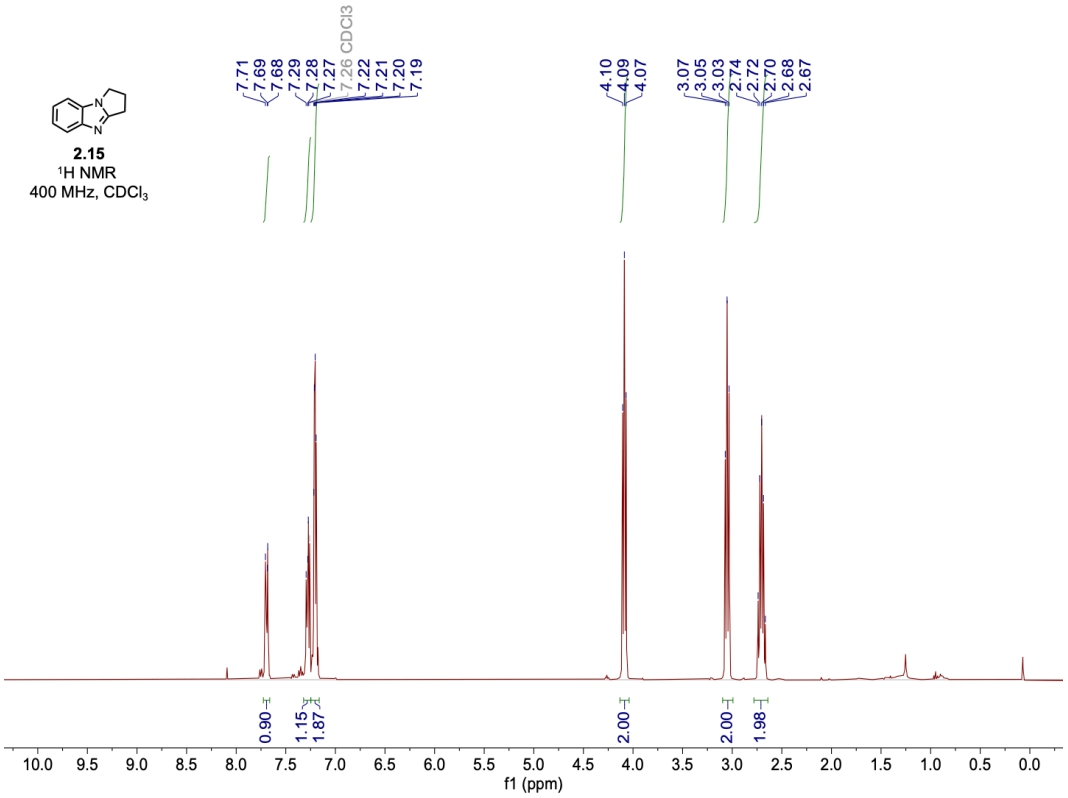
2.15
1H NMR
400 MHz, CDCl3
7.71
7.69
7.68
7.29
7.28
7.27
7.26 CDCl3
7.22
7.21
7.20
7.19
4.10
4.09
4.07
3.07
3.05
3.03
2.74
2.72
2.70
2.68
2.67
0.90
1.15
1.87
2.00
2.00
1.98
10.0 9.5 9.0 8.5 8.0 7.5 7.0 6.5 6.0 5.5 5.0 4.5 4.0 3.5 3.0 2.5 2.0 1.5 1.0 0.5 0.0
f1 (ppm)

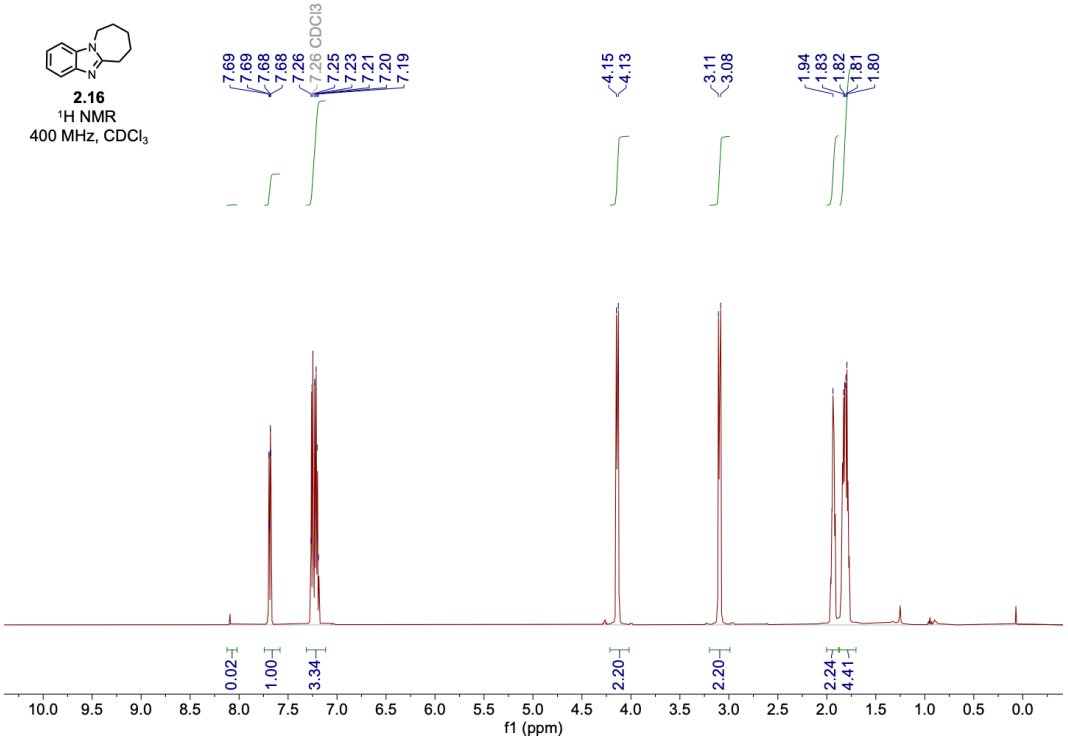
2.16
1H NMR
400 MHz, CDCl3
7.69
7.69
7.68
7.68
7.26
7.26 CDCl3
7.25
7.23
7.21
7.20
7.19
4.15
4.13
3.11
3.08
1.94
1.83
1.82
1.81
1.80
0.02
1.00
3.34
2.20
2.20
2.24
4.41
f1 (ppm)

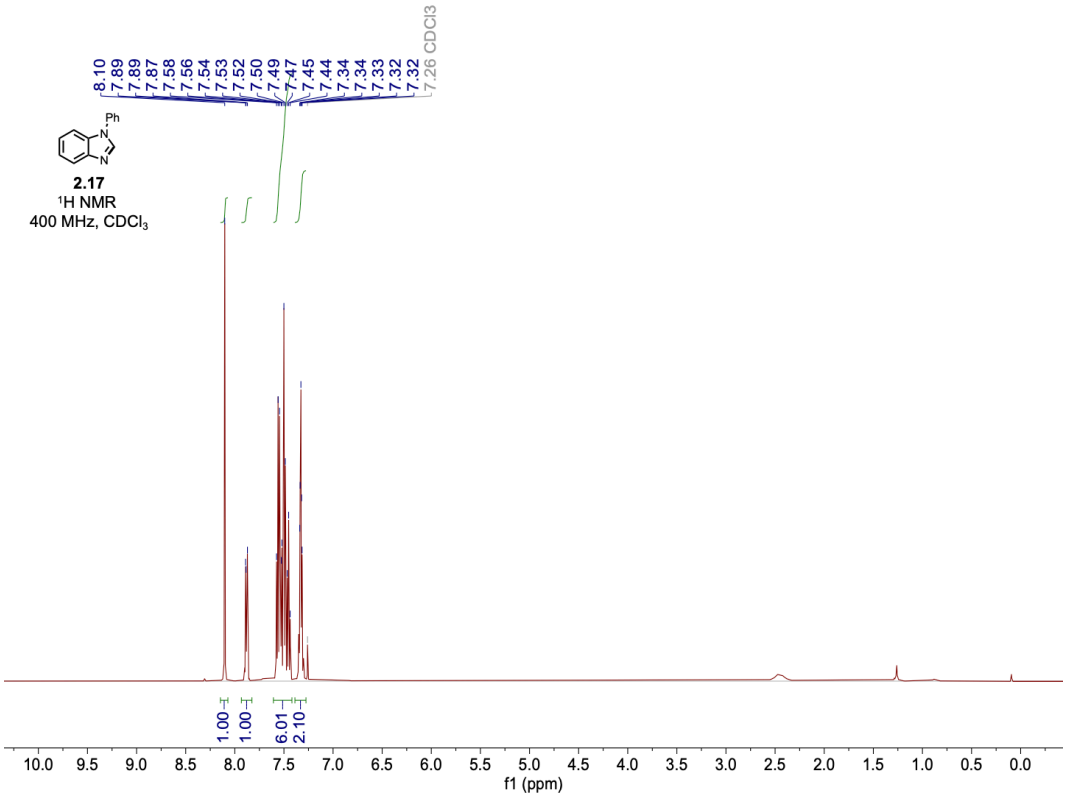
2.17
1H NMR
400 MHz, CDCl3
Ph
8.10
7.89
7.89
7.87
7.58
7.56
7.54
7.53
7.52
7.50
7.49
7.47
7.45
7.44
7.34
7.34
7.33
7.32
7.26 CDCl3
1.00
1.00
6.01
2.10
f1 (ppm)

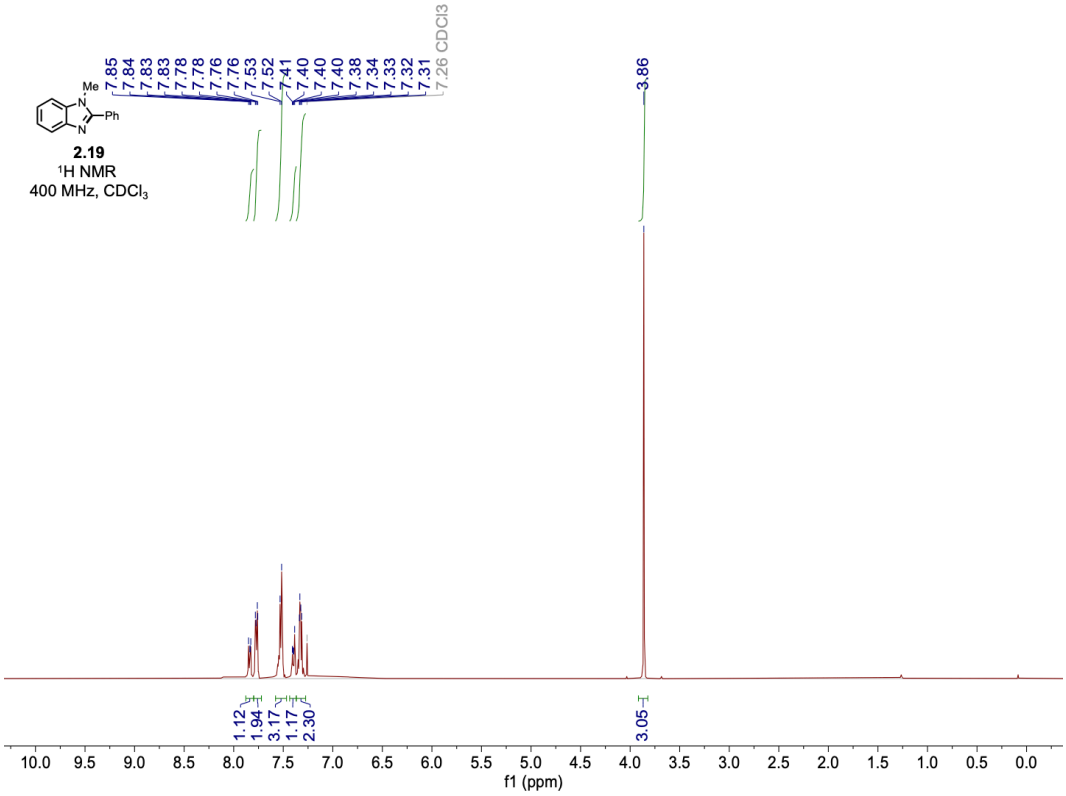
Me
N
N
Ph
2.19
1H NMR
400 MHz, CDCl3
7.85
7.84
7.83
7.83
7.78
7.78
7.76
7.76
7.53
7.52
7.41
7.40
7.40
7.40
7.38
7.34
7.33
7.32
7.31
7.26 CDCl3
3.86
1.12
1.94
3.17
1.17
2.30
3.05
10.0 9.5 9.0 8.5 8.0 7.5 7.0 6.5 6.0 5.5 5.0 4.5 4.0 3.5 3.0 2.5 2.0 1.5 1.0 0.5 0.0
f1 (ppm)

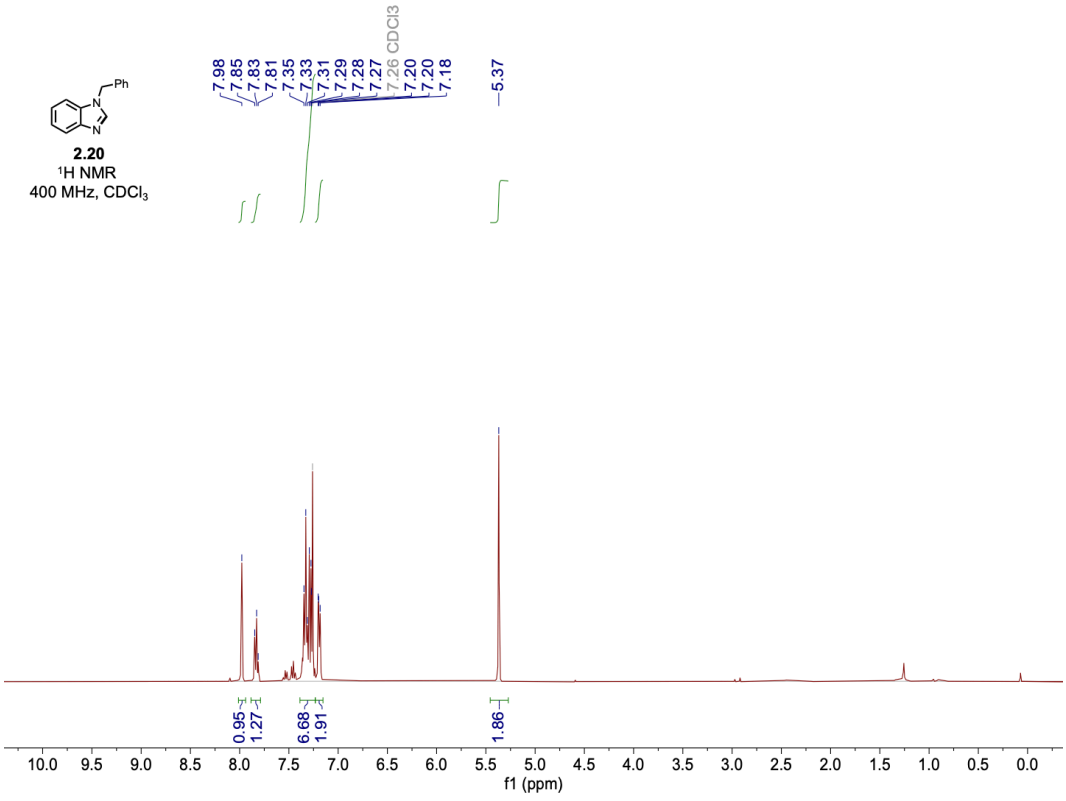
Ph
N
N
2.20
1H NMR
400 MHz, CDCl3
7.98
7.85
7.83
7.81
7.35
7.33
7.31
7.29
7.28
7.27
7.26 CDCl3
7.20
7.20
7.18
5.37
0.95
1.27
6.68
1.91
1.86
10.0 9.5 9.0 8.5 8.0 7.5 7.0 6.5 6.0 5.5 5.0 4.5 4.0 3.5 3.0 2.5 2.0 1.5 1.0 0.5 0.0
f1 (ppm)

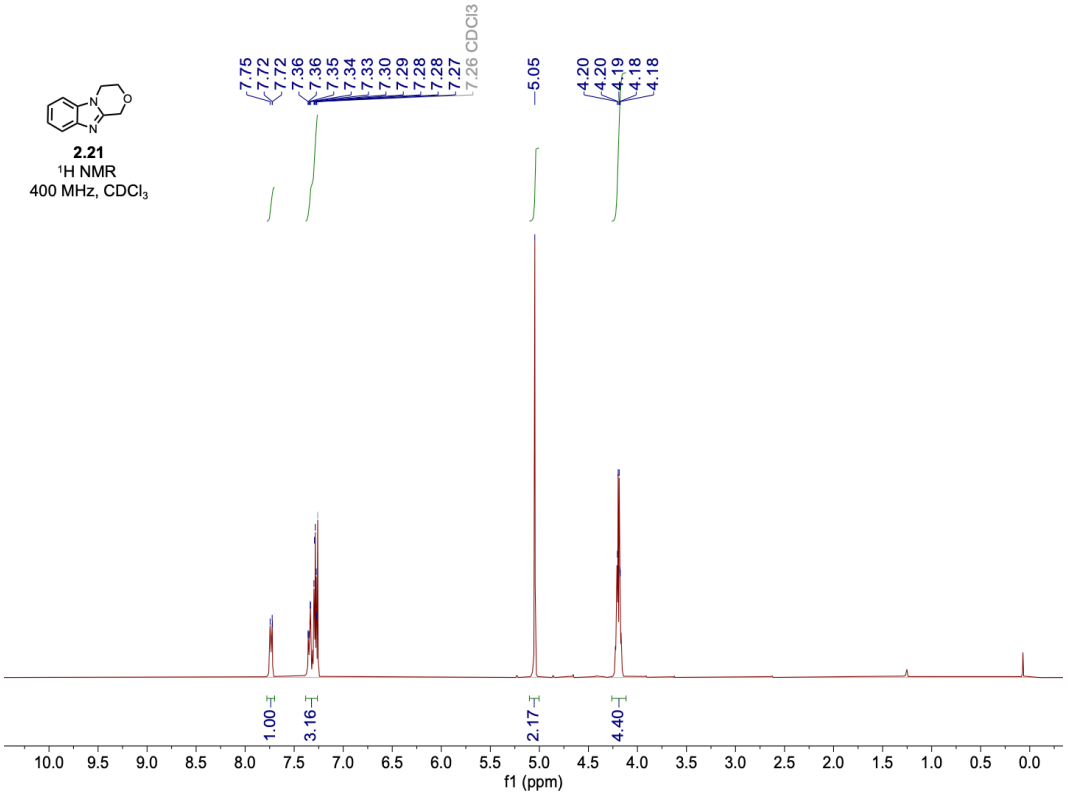
2.21
1H NMR
400 MHz, CDCl3
7.75
7.72
7.72
7.36
7.36
7.35
7.34
7.33
7.30
7.29
7.28
7.28
7.27
7.26 CDCl3
5.05
4.20
4.20
4.19
4.18
4.18
1.00
3.16
2.17
4.40
10.0 9.5 9.0 8.5 8.0 7.5 7.0 6.5 6.0 5.5 5.0 4.5 4.0 3.5 3.0 2.5 2.0 1.5 1.0 0.5 0.0
f1 (ppm)

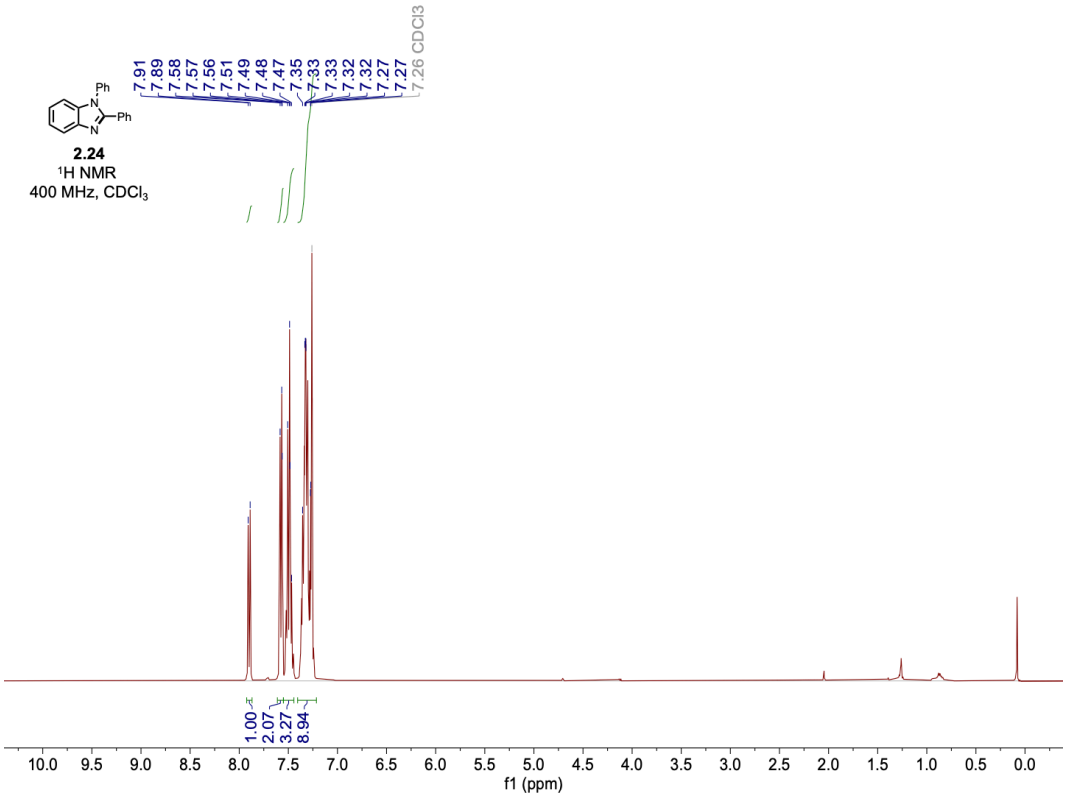
2.24
1H NMR
400 MHz, CDCl3
7.91
7.89
7.58
7.57
7.56
7.51
7.49
7.48
7.47
7.35
7.33
7.33
7.32
7.27
7.27
7.26 CDCl3
1.00
2.07
3.27
8.94
10.0 9.5 9.0 8.5 8.0 7.5 7.0 6.5 6.0 5.5 5.0 4.5 4.0 3.5 3.0 2.5 2.0 1.5 1.0 0.5 0.0
f1 (ppm)

VII. References

[1]Gray, G. A.; Cremer, S. E. "Carbon-13 Nuclear Magnetic Resonance of Organophosphorus Compounds. V. Effect of Changes in Phosphorus Oxidation Statein Four-Membered Phosphorus Heterocycles." *J. Org. Chem.* **1972**, *37*, 3470–3475.

[2]O'Brien, C. J.; Nixon, Z. S.; Holohan, A. J.; Kunkel, S. R.; Tellez, J. L.; Doonan, B. J.; Coyle, E. E.; Lavigne, F.; Kang, L. J.; Przeworski, K. C. "Part I: The Development of the Catalytic Wittig Reaction." *Chem. Eur. J.* **2013**, *19*, 15281–15289.

[3]Ogawa, S.; Tajiri, Y.; Furukawa, N. "Simple Preparation of (2,2′- Formation of Biaryl Biphenylylene)phenylphosphine Oxide and Role of Triphenylphosphine Oxide as a Mediator for Derivatives." *Bull. Chem. Soc. Jpn.* **1991**, *64*, 3182–3184.

[4]Li, A.; Li, C.; Yang, T.; Yang, Z.; Liu, Y.; Li, L.; Zhou, C. Electrochemical Synthesis of Benzo [d] imidazole via Intramolecular C (sp^3)–H Amination. *J. Org. Chem.* **2021**.

[5]Hasuoka, A.; Arikawa, Y. *U.S. Patent Application No. 15/878,087*. **2018**.

[6]Nguyen, T. B.; Ermolenko, L.; Al-Mourabit, A. Formic acid as a sustainable and complementary reductant: An approach to fused benzimidazoles by molecular iodine-catalyzed reductive redox cyclization of o-nitro-t-anilines. *Green Chem.* **2016**, *10*, 2966-2970.

[7]Geng, X.; Liu, S.; Wang, W.; Qu, J.; Wang, B. tert-Amino effect-promoted rearrangement of aryl isothiocyanate: A versatile approach to benzimidazothiazepines and benzimidazothioethers. *J. Org. Chem.* **2020**, *19*, 12635-12643.

[8]Panagopoulos, A. M.; Steinman, D.; Goncharenko, A.; Geary, K.; Schleisman, C.; Spaargaren, E.; Becker, D. P. Apparent alkyl transfer and phenazine formation via an aryne intermediate. *J. Org. Chem.* **2013**, *8*, 3532-3540.

[9]Deng, W.; Wang, Y. F.; Zou, Y.; Liu, L.; Guo, Q. X. Amino acid-mediated Goldberg reactions between amides and aryl iodides. *Tetrahedron Lett*. **2004**, *11*, 2311-2315.

[10]Schmid, S.; Röttgen, M.; Thewalt, U.; Austel, V. Synthesis and conformational properties of 2, 6-bis-anilino-3-nitropyridines. *Org. Biomol. Chem.* **2005**, *18*, 3408-3421.

[11]Frisch, M. J.; Trucks, G. W.; Schlegel, H. B.; Scuseria, G. E.; Robb, M. A.; Cheeseman, J. R.; Scalmani, G.; Barone, V.; Mennucci, B.; Petersson, G. A.; Nakatsuji, H.; Caricato, M.; Li, X.; Hratchian, H. P.; Izmaylov, A. F.; Bloino, J.; Zheng, G.; Sonnenberg, J. L.; Hada, M.; Ehara, M.; Toyota, K.; Fukuda, R.; Hasegawa, J.; Ishida, M.; Nakajima, T.; Honda, Y.; Kitao, O.; Nakai, H.; Vreven, T.; Montgomery, J. A. Jr.; Peralta, J. E.; Ogliaro, F.; Bearpark, M.; Heyd, J. J.; Brothers,

E.; Kudin, K. N.; Staroverov, V. N.; Kobayashi, R.; Normand, J.; Raghavachari, K.; Rendell, A.; Burant, J. C.; Iyengar, S. S.; Tomasi, J.; Cossi, M.; Rega, N.; Millam, M. J.; Klene, M.; Knox, J. E.; Cross, J. B.; Bakken, V.; Adamo, C.; Jaramillo, J.; Gomperts, R.; Stratmann, R. E.; Yazyev, O.; Austin, A. J.; Cammi, R.; Pomelli, C.; Ochterski, J. W.; Martin, R. L.; Morokuma, K.; Zakrzewski, V. G.; Voth, G. A.; Salvador, P.; Dannenberg, J. J.; Dapprich, S.; Daniels, A. D.; Farkas, Ö.; Foresman, J. B.; Ortiz, J. V.; Cioslowski, J.; Fox, D. J. Gaussian 09, revision B.01; Gaussian, Inc.: Wallingford, CT, 2009.

[12](a) Zhao, Y.; Truhlar, D. G. The M06 suite of density functionals for main group thermochemistry, thermochemical kinetics, noncovalent interactions, excited states, and transition elements: two new functionals and systematic testing of four M06-class functionals and 12 other functionals. *Theor. Chem. Acc.* **2008**, *120*, 215. (b) Zhao, Y.; Truhlar, D. G. Density functionals with broad applicability in chemistry. *Acc. Chem. Res.* **2008***, 41*, 157.

[13]Rodríguez-Huerto, P. A.; Peña-Solórzano, D.; Ochoa-Puentes, C. Nitroarenes as versatile building blocks for the synthesis of unsymmetrical urea derivatives and N-Arylmethyl-2-substituted benzimidazoles. *Chem. Pap.* **2021***, 12*, 6275-6283.

[14]Sadig, J. E.; Foster, R.; Wakenhut, F.; Willis, M. C. Palladium-catalyzed synthesis of benzimidazoles and quinazolinones from common precursors. *J. Org. Chem.* **2012**, *21*, 9473–9486.

[15]Li, Y.; Huang, S.; Li, J.; Li, J.; Ji, X.; Liu, J.; Zhang, K. Access to 2-pyridinylamide and imidazopyridine from 2-fluoropyridine and amidine hydrochloride. *Org. Biomol. Chem.* **2020***, 18,* 9292-9299.

[16]Nale, D. B.; Bhanage, B. M. N-substituted formamides as C1-sources for the synthesis of benzimidazole and benzothiazole derivatives by using zinc catalysts. *Synlett* **2015**, *20*, 2835-2842.

[17]Turner, G. L.; Morris, J. A.; Greaney, M. F. Direct arylation of thiazoles on water. *Angew. Chem.* **2007**, *42*, 8142-8146.

[18]Le, Z. G.; Chen, Z. C.; Hu, Y.; Zheng, Q. G. Organic reactions in ionic liquids: N-alkylation of phthalimide and several nitrogen heterocycles. *Synthesis* **2004**, *2*, 208-212.

[19]Laha, J. K.; Tummalapalli, K. S.; Nair, A.; Patel, N. Sulfate Radical Anion (SO_4•–) Mediated C (sp^3)–H Nitrogenation/Oxygenation in N-Aryl Benzylic Amines Expanded the Scope for the Synthesis of Benzamidine/Oxazine Heterocycles. *J. Org. Chem.* **2015**, *22*, 11351–11359.